STRATOSPHERIC TEMPERATURE TRENDS: OBSERVATIONS AND MODEL SIMULATIONS

V. Ramaswamy,[1] M.-L. Chanin,[2] J. Angell,[3] J. Barnett,[4] D. Gaffen,[3] M. Gelman,[5] P. Keckhut,[2] Y. Koshelkov,[2,6] K. Labitzke,[7] J.-J. R. Lin,[5] A. O'Neill,[8] J. Nash,[9] W. Randel,[10] R. Rood,[11] K. Shine,[8] M. Shiotani,[12] and R. Swinbank[9,13]

Abstract. Trends and variations in global stratospheric temperatures are an integral part of the changes occurring in the Earth's climate system. Data sets for analyzing long-term (a decade and more) changes in the stratospheric temperatures consist of radiosonde, satellite, lidar, and rocketsonde measurements; meteorological analyses based on radiosonde and/or satellite data; and products based on assimilating observations using a general circulation model. Each of these contain varying degrees of uncertainties that influence the interpretation and significance of trends. We review the long-term trends from approximately the mid-1960s to the mid-1990s period. The stratosphere has, in general, undergone considerable cooling over the past 3 decades. At northern midlatitudes the lower stratosphere (~16–21 km) cooling over the 1979–1994 period is strikingly coherent among the various data sets with regard to magnitude and statistical significance. A substantial cooling occurs in the polar lower stratosphere during winter-spring; however, there is a large dynamical variability in the northern polar region. The vertical profile of the annual-mean stratospheric temperature change in the northern midlatitudes over the 1979–1994 period is robust among the different data sets, with ~0.75 K/decade cooling in the ~20- to 35-km region and increasing cooling above (e.g., ~2.5 K/decade at 50 km). Model investigations into the cause or causes of the observed temperature trends are also reviewed. Simulations based on the known changes in species' concentrations indicate that the depletion of lower stratospheric ozone is the major radiative factor in accounting for the 1979–1990 cooling trend in the global, annual-mean lower stratosphere (~0.5 to 0.6 K/decade), with a substantially lesser contribution by the well-mixed greenhouse gases. Ozone loss is also an important causal factor in the latitude-month pattern of the lower stratospheric cooling trend. Uncertainties arise due to incomplete knowledge of the vertical profile of ozone loss near the tropopause. In the middle and upper stratosphere, both well-mixed greenhouse gases and ozone changes contribute in an important manner to the cooling, but model simulations underestimate the observed decadal-scale trend. While there is a lack of reliable information on water vapor changes over the 1980s decade, satellite measurements in the early to middle 1990s indicate increases in water vapor that could be a significant contributor to the cooling of the global lower stratosphere.

CONTENTS

1. Introduction 72
2. Observations 73
   2.1. Data 73
   2.2. Summary of Various Radiosonde Trend Investigations 76
   2.3. Zonal, Annual-Mean Trends 77
   2.4. Latitude-Season Trends 83
   2.5. Uncertainties in Trends Estimated From Observations 85
   2.6. Issues Concerning Variability 92
   2.7. Changes in Tropopause Height 96
3. Model Simulations 96
   3.1. Background 96
   3.2. Well-Mixed Greenhouse Gases 98
   3.3. Stratospheric Ozone 100
   3.4. Aerosols 107
   3.5. Water Vapor 108
   3.6. Other (Solar Cycle and QBO) 109
4. Changes in Trace Species and Observed Temperature Trends 110
   4.1. Lower Stratosphere 110
   4.2. Middle and Upper Stratosphere 112
   4.3. Upper Troposphere 112
5. Summary 113
   5.1. Observations 113
   5.2. Model Results and Model-Observation Comparisons 114
6. Future Research 115

[1]NOAA Geophysical Fluid Dynamics Laboratory, Princeton University, Princeton, New Jersey.
[2]Service d'Aéronomie du Centre National de la Recherche Scientifique, Verrières-le-Buisson, France.
[3]NOAA Air Resources Laboratory, Silver Spring, Maryland.
[4]Department of Atmospheric Physics, Oxford University, Oxford, England.
[5]Climate Prediction Center, National Centers for Environmental Prediction, Washington, D. C.
[6]Central Aerological Observatory, Dolgoprudny, Moscow.
[7]Institut für Meteorologie, Frei Universitat, Berlin, Germany.
[8]Department of Meteorology, University of Reading, Reading, England.
[9]U.K. Meteorological Office, Bracknell, England.
[10]National Center for Atmospheric Research, Boulder, Colorado.
[11]NASA Goddard Space Flight Center, Greenbelt, Maryland.
[12]Division of Ocean and Atmospheric Science, Hokkaido University, Sapporo, Japan.
[13]Universities Space Research Association, NASA Goddard Space Flight Center, Greenbelt, Maryland.

Reviews of Geophysics, 39, 1 / *February 2001*
pages 71–122
8755-1209/01/1999RG000065*$15.00*
Paper number 1999RG000065

1. INTRODUCTION

For at least the past decade and a half, the investigation of trends in stratospheric temperatures has been recognized as an essential component of ozone change assessments (e.g., World Meteorological Organization's (WMO) Global Ozone Research and Monitoring Project reports since the early 1980s). For convenience and in terms of the global-mean atmosphere, the region between 100 and 30 hPa (~16–25 km) will be referred to in this study as the lower stratosphere (a subset of this domain is the 100- to 50-hPa (~16–21 km) region), the region between 30 and 3 hPa (~25–40 km) will be referred to as the middle stratosphere, and the region between 3 and 0.7 hPa (~40–50 km) will be referred to as the upper stratosphere. The tropopause separates the stratosphere from the troposphere.

A comprehensive international scientific assessment of stratospheric temperature changes was undertaken by *WMO* [1990a]. Analyses of the then available data sets (rocketsonde, radiosonde, and satellite records) over 1979–1980 to 1985–1986 indicated that the observed temperature trend was inconsistent with the then apparent ozone losses inferred from solar backscatter ultraviolet (SBUV) data but was consistent with Stratospheric Aerosol and Gas Experiment (SAGE) ozone changes. The largest cooling in the observed data sets was in the upper stratosphere, while the lower stratosphere had experienced no significant cooling except in the tropics and Antarctica. It is interesting to note that the period 1979–1986 analyzed by the Temperature Trends Panel [*WMO*, 1990a] was one when severe ozone losses were just beginning to be recognized in the Antarctic springtime lower stratosphere. It was also a period when sunspot maximum reversed to sunspot minimum.

Since the *WMO* [1990a] assessment, there has been an ever-growing impetus for observational and model investigations of the stratospheric temperature trends, as evidenced, for example, in successive WMO assessments. This has occurred owing to the secular increases in greenhouse gases and the now well-documented global and seasonal losses of stratospheric ozone, both of which are estimated to have a substantial impact on the stratospheric climate. The availability of various temperature observations and the ever-increasing length of the data record have also been contributing factors. In addition, models have progressively acquired the capability to perform improved and more realistic simulations of the stratosphere. This has provided a motivation for comparing model results with observations and thereby to search for causal explanations of the observed trends. The developments in modeling have underscored the significance of the interactions between radiation, dynamics, and chemistry in the interpretation of linkages between changes in trace species and temperature trends. Temperature changes have also been identified as affecting the microphysical-chemical processes occurring in the stratosphere [*WMO*, 1999].

The assessment of stratospheric temperature trends is now regarded as a high priority in climate change research inasmuch as it has been shown to be a key entity in the detection and attribution of the observed vertical profile of temperature changes in the Earth's atmosphere [*Hansen et al*., 1995; *Santer et al*., 1996; *Tett et al*., 1996]. Indeed, the subject of trends in the stratospheric temperatures is of crucial importance to the assessment of the *Intergovernmental Panel on Climate Change* (*IPCC*) [1996] and constitutes a significant scientific input into policy decisions.

An excellent perspective on the evolution in the state of the science of the stratospheric temperature trends is given by the WMO in its ozone assessment reports [*WMO*, 1986, 1990a, 1990b, 1992, 1995]. We summarize here the principal results concerning stratospheric temperature trends from these WMO reports. In general, the successive assessments since *WMO* [1986] have traced the evolution of the state of the science on both the observation and model simulation fronts. On the observational side, WMO has reported on available temperature trends from various kinds of instruments: radiosonde, rocketsonde, satellite, and lidar. On the modeling side, since the 1986 report, WMO has reported on model investigations that illustrate the role of greenhouse gases and aerosols in the thermal structure of the stratosphere and the effects due to changes in their concentrations upon stratospheric temperature trends. As was already noted, an important development of *WMO* [1990a] was the synthesis of available observations and theoretical knowledge and the examination of the manner in which radiative, chemical, and dynamical interactions contribute to stratospheric temperature variation and trend. First, *WMO* [1990a] and then *WMO* [1990b] began to recognize, from observational and modeling standpoints, the substantial lower stratospheric cooling that occurred during springtime in the Antarctic as a consequence of the large ozone depletion. The low- and middle-latitude lower stratosphere were inferred to have a cooling of less than 0.4 K/decade over the prior 20 years. The upper stratosphere was estimated to have cooled by 1.5 ± 1 K between 1979–1980 and 1985–1986.

On the basis of radiosonde analyses, a global-mean lower stratospheric cooling of ~0.3 K was estimated to have occurred over the previous 2–3 decades [*WMO*, 1992]. Model calculations indicated that the observed ozone losses had the potential to yield substantial cooling of the global lower stratosphere. At 44°N during summer a cooling of the upper stratosphere (~1 K/decade at ~35 km) and mesosphere (~4 K/decade) was also reported. However, the global stratospheric temperature record and the understanding of temperature changes were found, in general, not to be as sound as those related to ozone changes.

The *WMO* [1995] assessment discussed the observational and modeling efforts through 1994, focusing entirely on trends in lower stratospheric temperatures.

This assessment concluded, on the basis of radiosonde and satellite microwave observations, that there were short-term variations superposed on the long-term trends. A contributing factor to the former was stratospheric aerosol increases following the El Chichon and Pinatubo volcanic eruptions that resulted in an increase of the global stratospheric temperature. These transient warmings posed a complication when analyzing the long-term trends and deducing their attribution. The long-term trends from the radiosonde and Microwave Sounding Unit (MSU) satellite data indicated a cooling of 0.25–0.4 K/decade since the late 1970s, with suggestions of an acceleration of cooling during the 1980s. The global cooling of the lower stratosphere suggested by the observations was reproduced reasonably well by models considering the observed decreases of ozone in the lower stratosphere. For altitudes above the lower stratosphere a clear conclusion concerning the cause of the trends could not be made. The 1992 and 1995 assessments laid the basis for concluding that the observed trends in the lower stratosphere during the 1980s were largely attributable to halocarbon-induced ozone losses.

In addition to the WMO assessment activities during the 1990s, an important development in the mid-1990s was the initiative by the World Climate Research Program's (WCRP) Stratospheric Processes and Their Role in Climate (SPARC) project. SPARC set up a Stratospheric Temperature Trends Assessment (STTA) group to focus on (1) bringing together all available data sets, examining the quality of the data, and intercomparing the resulting global stratospheric temperature trends; and (2) employing model simulations in conjunction with the measurements to search for the causes of the observed trends, with an emphasis on the potential roles of the anthropogenic species.

In this review we discuss the extension of the evaluations of the aforementioned WMO assessments and focus on the decadal-scale lower to upper stratospheric temperature trends arising out of observational (section 2) and model simulation (section 3) analyses. Also, we utilize the results and inferences made available by the SPARC-STTA group. The temperature observations considered span at least 10 years; the period considered for evaluation is typically at least 15 years. The trend estimates discussed here include (1) a long-term period that spans 2 decades or more, (2) the period since 1979 and extending to either 1994 or up to 1998, and (3) the period extending from 1979 to about the early 1990s. The last period mentioned is that for which several model simulations have been compared with observations. In section 4 we use the results from sections 2 and 3 to investigate the extent to which the observed temperature trends can be attributed to changes in the concentrations of radiatively active species, focusing especially on the global mean. Section 5 summarizes the principal conclusions from the observations and observation-model comparisons.

2. OBSERVATIONS

2.1. Data

The types of observational data available for an investigation into stratospheric temperature trends are diverse. They differ in the type of measurement, length of time period, and space-time sampling. There have been several investigations of trends that have considered varying time spans with the different available data sets. In a major intercomparison effort the SPARC-STTA group brought together a variety of data sets (Table 1) and have derived and intercompared global stratospheric temperature trends. STTA selected two different time periods to examine the trends: 1979–1994 and ~1965–1994. The shorter period coincides with the period when severe global ozone losses have been detected; further, satellite observations began in ~1979. The second period is longer for which radiosonde (and a few rocketsonde) data sets are available. Additionally, independent of the STTA activity, some investigations [*Dunkerton et al*., 1998; *Keckhut et al*., 1999; *Komuro*, 1989; *Kokin and Lysenko*, 1994; *Golitsyn et al*., 1996; *Lysenko et al*., 1997] have analyzed trends from rocketsonde observations made at selected geographical locations and over specific time periods (see Table 2). It is convenient to group the currently known data sets as follows: (1) ground-based instruments (radiosonde, rocketsonde, and lidar); (2) satellite instruments (microwave and infrared sounders); and (3) analyses (employing data from one or both of the above instrument types, in conjunction with or without a numerical model).

The data sets indicated in Table 1 are a collection of monthly-mean, zonal-mean temperature time series. The pressure-altitude levels of the data sets vary, but overall they cover the range from 100 to 0.4 hPa (approximately 16–55 km). Most data sets provide temperatures at specific pressure levels, but some provide data as mean temperatures representative of various pressure layers. The instrumental records from radiosondes, rocketsondes, lidar, and satellite (MSU and Stratospheric Sounding Unit (SSU)) are virtually independent of each other. Details concerning the various observational platforms are given by *WMO* [1990a, 1990b]. General characteristics of the different data sets are discussed below.

2.1.1. Radiosonde. Radiosonde data for the stratosphere are available dating back to approximately the early 1940s. Although the sonde data do not cover the entire globe, there have been several well-documented efforts using varied techniques to obtain the temperatures over the entire Northern Hemisphere and the global domain. In the stratosphere the sonde data cover primarily the lower stratospheric region (i.e., pressure levels exceeding 30 hPa). The geographical coverage is reasonable in the Northern Hemisphere (particularly midlatitudes) but is poor in the extremely high latitudes and tropics and is seriously deficient in the Southern Hemisphere [*Oort and Liu*, 1993].

TABLE 1. Zonal-Mean Temperature Time Series Made Available to and Considered by SPARC-STTA

Data Set	*Reference*	*Period*	*Location*	*Monthly*	*Levels, hPa*
Angell	*Angell* [1988]	1958–1994	eight bands	3-monthly	100–50
			four bands	3-monthly	50, 30, 20, 10
Oort	*Oort and Liu* [1993]	1958–1989	85°S–85°N	monthly	100, 50
Russia	*Koshelkov and Zakharov* [1998]	1959–1994	70°N, 80°N	monthly	100
		1961–1994	70°N, 80°N	monthly	50
UK RAOB (or RAOB)	*Parker and Cox* [1995]	1961–1994	87.5°S–87.5°N	monthly	100, 50, 30, 20
Berlin	*Labitzke and van Loon* [1994]	1965–1994	10°–90°N	monthly	100, 50, 30
Lidar	*Hauchecorne et al*. [1991]	1979–1994	44°N, 6°E	monthly	10, 5, 2, 1, 0.4
MSU	*Spencer and Christy* [1993]	1979–1994	85°S–85°N	monthly	90
Nash	*Nash and Forrester* [1986]	1979–1994	75°S–75°N	monthly	50, 20, 15, 6, 5, 2, 1.5, 0.5
CPC	*Gelman et al*. [1994]	1979–1994	85°S–85°N	monthly	70, 50, 30, 10, 5, 2, 1
		1964–1978	20°N–85°N	monthly	50, 30, 10
Reanal	*Kalnay et al*. [1996]	1979–1994	85°S–85°N	monthly	100, 70, 50, 30, 10
GSFC	*Schubert et al*. [1993]	1979–1994	90°S–90°N	monthly	100, 70, 50, 30, 20
UKMO/SSUANAL	*Bailey et al*. [1993]	1979–1994	90°S–90°N	monthly	50, 20, 10, 5, 2, 1

Angell, Oort, Russia, UK RAOB, and Berlin are different radiosonde data sets. MSU and Nash are satellite instruments, while lidar data are from OHP (France). CPC, Reanal, UKMO/SSUANAL, and GSFC are analyzed data sets. For the MSU and Nash satellite data the approximate peak levels "sensed" are listed. References to earlier published versions of the data sets are also listed. See section 2.1 for details.

Two organizations routinely monitor trends and variations in global lower stratospheric temperatures using radiosonde data alone. The "Berlin" group [e.g., *Labitzke and van Loon*, 1995] prepares daily hand-drawn stratospheric maps based on synoptic analyses of radiosonde data at 100, 50, 30, and, in some months, 10 hPa. The Berlin monthly data set examined by SPARC-STTA is derived from these daily analyses. The National Oceanic and Atmospheric Administration (NOAA) Air Resources Laboratory [e.g., *Angell*, 1988] uses daily radiosonde soundings to calculate seasonal layer-mean "virtual temperature" anomalies from long-term means and uses these to determine trends since 1958 in the 850–300, 300–100, and 100–50 hPa (lower stratosphere) layers. ("Virtual temperature" is the temperature of dry air having the same pressure and density as the actual moist air. Virtual temperature always exceeds temperature, but the difference is negligible in the stratosphere [*Elliott et al*., 1994].) The layer-mean virtual temperatures are determined from the geopotential heights of the layer end points. The Berlin analyses are of the Northern Hemisphere stratosphere and troposphere and are based on all available radiosonde data, whereas the Air Resources Laboratory monitors trends at 63 stations, in seven zonal bands covering the globe. Additionally, *Angell* [1991b] also monitors stratospheric temperature, particularly in response to volcanic eruptions, at four levels between 20 km (50 hPa) and 31 km (10 hPa), using a network of 12 stations ranging from 8°S to 55°N.

Extensive analyses of radiosonde temperature data by the NOAA Geophysical Fluid Dynamics Laboratory (GFDL) [*Oort and Liu*, 1993] (labeled "Oort") and the U.K. Meteorological Office's (UKMO) Hadley Centre for Climate Prediction and Research [*Parker et al*., 1997] have also been used for quantifying stratospheric trends. The GFDL database consists of gridded global objective analyses based on monthly means derived from daily soundings (1958–1989) for the tropospheric levels and the 100-, 70-, 50-, and 30-hPa levels in the lower stratosphere. Layer-mean trends for the 100- to 50-hPa layer are based on temperature data at the 100-, 70-, and 50-hPa levels. A subset of this data set is used here.

The UKMO gridded data set (radiosonde observation, or "RAOB," or "UKRAOB" in the context of the U.K. RAOB analyses) for 1958–1996 is based on monthly mean station reports, adjusted (using MSU channel 4 data, discussed below, as a reference) to remove some time-varying biases for stations in Australia and New Zealand and interpolated in some data-void regions. The "Russia" set consists of data from the high northern latitudes (70° and 80°N) [*Koshelkov and Zakharov*, 1998]. Thus the Angell, Berlin, Oort, Russia, and

TABLE 2. Rocketsonde Locations and Periods of Coverage

Station	*Latitude, Longitude*	*Period*
Heiss Island	81°N, 58°E	1964–1994
Volgograd	49°N, 44°E	1965–1994
Balkhash	47°N, 75°E	1973–1992
Ryori	39°N, 141.5°E	1970 to present
Wallops Island	37.5°N, 76°W	1965–1990
Point Mugu	34°N, 119°W	1965–1991
Cape Kennedy	28°N, 80°W	1965–1993
Barking Sands	22°N, 160°W	1969–1991
Antigua	17°N, 61°W	1969–1991
Thumba	08°N, 77°E	1971–1993
Kwajalein	09°N, 167°E	1969–1990
Ascension Island	08°S, 14°W	1965–1993
Molodezhnaya	68°S, 46°E	1969–1994

Data are based on *Dunkerton et al*. [1998], *Golitsyn et al*. [1996], *Keckhut et al*. [1999], *Kokin and Lysenko* [1994], *Lysenko et al*. [1997], and *Komuro* [1989] (updated).

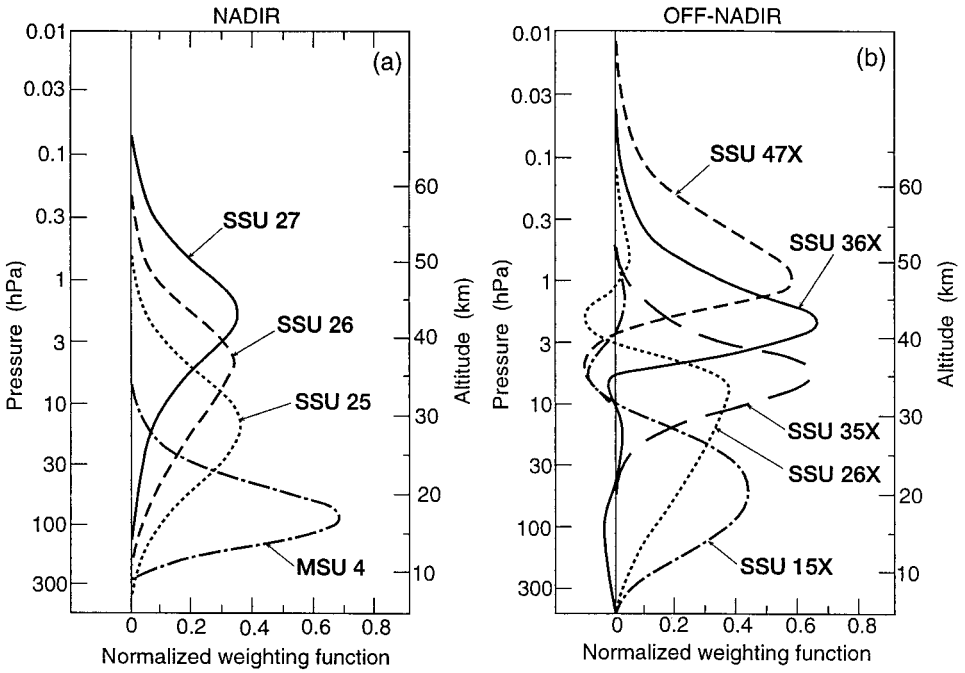

Figure 1. Altitude range of the signals "sensed" by the various thermal infrared channels of the Stratospheric Sounding Unit (SSU) instrument and that sensed by channel 4 of the Microwave Sounding Unit (MSU). Shown are (a) nadir and (b) combination of nadir and off-nadir channel weighting functions.

RAOB data sets used by SPARC-STTA are compilations of data from various radiosonde stations, grouped, interpolated, and/or averaged in various ways to obtain monthly-mean and latitude-mean, pressure-level, or vertical-average temperatures.

2.1.2. Rocket and lidar. Rocket and lidar data cover the altitude range from about the middle to the upper stratosphere and mesosphere. Rocketsonde data are available through the early 1990s from some locations, but the activity now appears to be virtually terminated except in Japan (see Table 2). The lidar measurement, similar to the rocketsondes, has a fine vertical resolution. Since 1979, lidar measurements of stratospheric temperatures are available from the Haute Provence Observatory (OHP) in southern France (Table 1). Specifically, the "lidar" temperatures observed at altitudes of 30–90 km are obtained from two lidar stations, with data interpolated to pressure levels [*Keckhut et al.*, 1995]. Several other lidar sites have initiated operations and could potentially contribute in future temperature trend assessments.

2.1.3. MSU and SSU satellites. Satellite instruments that remotely sense stratospheric temperatures have become available since ~1979 (Table 1). An important attribute of the satellites is their global coverage. The satellite instruments fall into two categories: remotely sensing in the microwave [*Spencer and Christy*, 1993] and thermal infrared [*Nash and Forrester*, 1986] wavelengths. In contrast to the ground-based measurements, for example, the radiosonde, which perform measurements at specific pressure levels, the available satellite sensors sense the signal from a wide range in altitude. The nadir satellite instruments "sense" the emission originating from a layer of the atmosphere typically 10–15 km thick.

The "MSU" channel 4 data set derives from the lower stratosphere channel (~150–50 hPa) of the Microwave Sounding Unit on NOAA polar operational satellites (Figure 1a). The "Nash" data set consists of brightness temperatures from observed (25, 26, and 27) and derived (47X, 36X, 35X, 26X, and 15X) channels of the Stratospheric Sounding Unit (SSU) and High-Resolution Infrared Sounder (HIRS) 2 instruments on these same satellites (Figure 1) [see also *WMO*, 1990a]. Figure 1 also illustrates the weighting function for the MSU and SSU channels analyzed here, illustrating the thick-layer nature of the measurements. For example, the entire atmospheric emission for the microwave MSU channel 4 comes from the ~12- to 22-km layer, while for the thermal infrared SSU channel 15X, it is from the ~12- to 28-km layer. A nominal center pressure of each satellite channel has been designated (Table 1), but note that the preponderance of energy comes from a ~8- to 12-km-thick vertical layer centered around the concerned pressure level (Figure 1).

One complication with satellite data is the discontinuities in the time series owing to the measurements being made by different satellites monitoring the stratosphere since 1979. Adjustments have been made in the Nash channel data to compensate for radiometric differences, tidal differences between spacecraft, long-term drift in the local time of measurements, and spectro-

scopic drift in channels 26 and 27. Adjustments have also been made to MSU data [e.g., *Christy et al*., 1995], and the MSU record is discussed by *Christy* [1995] and *WMO* [1995]. The global-mean anomalies of temperature at various stratospheric altitudes between 1979 and 1995 (deviations with respect to the mean over this period), as derived from the different SSU channels, are illustrated in Figure 2.

2.1.4. Analyzed data sets. There are a number of data sets that involve some kind of analyses of the observations. They employ one or more types of observed data, together with the use of some mathematical technique and/or a general circulation model for data assimilation and analysis, to construct the global time series of the temperatures. They are, in essence, more a derived data set than the satellite- or ground-based sets. The Climate Prediction Center (CPC, formerly the Climate Analyses Center, or CAC) and UKMO/SSUANAL stratospheric analyses (Table 1) do not involve any numerical atmospheric circulation model. The CPC Northern Hemisphere 70-, 50-, 30-, and 10-hPa analyses use radiosonde data. Both the CPC and UKMO/SSUANAL analyses [see also *Bailey et al*., 1993] use TIROS Operational Vertical Sounding (TOVS) temperatures, which incorporate data from the SSU, HIRS-2, and MSU on the NOAA polar orbiting satellites. The UKMO SSUANAL data, which are derived in a fashion somewhat similar to the CPC, use the NOAA satellite radiances to obtain geopotential thickness values at the sounding locations, for the layers formed between the 100-hPa and the 20-, 10-, 5-, 2-, and 1-hPa levels. Those are then interpolated onto a 5° global resolution grid. The thickness fields are then added to a 100-hPa operational height analysis to give height fields up to 1 hPa, from which temperatures and winds are derived. Adjustments based on rocketsonde [*Finger et al*., 1993] have been applied to the CPC 5-, 2-, and 1-hPa temperatures for the SPARC data set. (However, both CPC data above 10-hPa altitude and the UKMO/SSUANAL data sets may be limited in scope for trend studies, as they have not yet been adjusted for some of the known problems associated with SSU satellite retrievals from many different satellites (see section 2.5.2); hence they are not considered in the intercomparisons reported here.)

The "Reanal" (namely, the U.S. National Centers for Environmental Prediction (NCEP) reanalyzed) and the NASA Goddard Space Flight Center (GSFC) data sets are derived using numerical atmospheric general circulation models as part of the respective data assimilation systems. These analysis projects provide synoptic meteorological data extending over many years using an unchanged assimilation system. In general, analyzed data sets are dependent on the quality of the data sources such that a spurious trend in a data source could be inadvertently incorporated in the assimilation. In addition, gaps in the data pose severe constraints, and analyses do not necessarily account for longer-term calibration-related problems. Further, the analyzed data sets may not contain adjustments for satellite data discontinuities [*Santer et al*., 1999]. Analyzed data sets in addition to the above have become available more recently (e.g., European Centre for Medium-Range Weather Forecasts (ECMWF) analyses [*Swinbank and O'Neill*, 1994]) and are likely to be useful in future updates on stratospheric temperature variations and trends.

2.2. Summary of Various Radiosonde Trend Investigations

Analyses with radiosonde data reveal a cooling of the lower stratosphere over the past several decades (Table 3). The data periods and the analyses techniques in the different investigations vary, as do the heights analyzed. No attempt is made here to critically evaluate these diverse estimation techniques. Overall, the trends, based on areal averages and all seasons, are negative and range from zero to several tenths of a degree per decade. The few studies with global coverage show more cooling of the Southern Hemisphere lower stratosphere than the Northern Hemisphere. Large trends evaluated for the decade of the 1980s emphasize the period of ozone loss. Positive trends have been found at a few individual stations in the tropics for the period 1966–1982 [*Reid et al*., 1989], possibly due to the influence of the El Chichon volcanic effects. (It may be noted that *Labitzke and van Loon* [1995] find positive trends (not listed in Table 3) at high and low latitudes for the month of January; see also *Koshelkov and Zakharov* [1998] and Table 3.)

The magnitude of the trend depends on the period of the record considered. This is evident from the time series of global or hemispheric mean lower stratospheric temperature anomalies [*Angell*, 1988; *Oort and Liu*, 1993; *Parker et al*., 1997]. These data (Figure 3a) (*Angell* [1988] updated, and *Halpert and Bell* [1997]) show relatively high temperatures (particularly in the Southern Hemisphere) during the early 1960s, fairly steady temperatures until about 1981, and relatively low temperatures since about 1984, with episodic warmings associated with prominent volcanic eruptions. The evolution of the global temperature anomalies from the MSU satellite record is qualitatively similar to the radiosonde [*Christy*, 1995], including the warming in the wake of the El Chichon and Pinatubo eruptions [*WMO*, 1995], followed by a cooling to somewhat below the preeruption levels (Figure 3b). The long-term cooling tendency of the global stratosphere is discernible in both data sets, although the satellite data exhibit less interhemispheric difference.

The Berlin analysis (Figure 4) shows that the radiosonde temperature time series for the 30-hPa region at the northern pole in July acquires a distinct downward trend when the 1955–1997 period is considered, in contrast to the behavior for the 1955–1977 period. The trend estimates are seen to depend on the end years chosen. The summertime temperature decreases in the high northern latitudes have been more substantial and

significant when the decade of the 1980s and afterward is considered; note that this does not necessarily imply a sharp downward trend for the other months.

A few studies have examined radiosonde observations of extreme temperatures in the lower stratosphere. At Sodankyla, Finland, *Taalas and Kyrö* [1994] found an increase in the frequency of occurrence of temperatures below 195 K at 50 hPa during 1965–1992. At both 50 and 30 hPa, over the Northern Hemisphere (10°–90°N), *Pawson and Naujokat* [1997] found a decrease in the minimum and an increase in the maximum daily wintertime temperatures during 1965–1996. They also found an increase in the area with temperatures less than 195 K and suggested that extremely low temperatures appear to have occurred more frequently over the past 15 years.

2.3. Zonal, Annual-Mean Trends

2.3.1. Trend determination. There is a wide range in the numerical methods reported in the literature to derive trends and their significance. Most studies are based on linear regression analyses, although details of the mathematical models and particularly aspects of the standard error estimates vary. Differences in details of the models include the method of fitting seasonal variability, the number and types of proxies included for atmospheric dynamics, and the method used to account for serial autocorrelation of meteorological data [e.g., *Keckhut et al*., 1995; *Randel and Cobb*, 1994].

The SPARC-STTA group calculated the temperature trends (K/decade) from each of the data sets using autoregressive time series analyses (maximum likelihood estimation method involving monthly-mean anomalies [e.g., *Efron*, 1982]). The methodology consists of fitting the time series of monthly mean values at each latitude with a constant and six variables (annual sine, annual cosine, semiannual sine, semiannual cosine, solar cycle, and linear trend). The derived trend and standard error are the products of this computation. The t test for significance at the 95% confidence level is met if the absolute value of the trend divided by the standard error estimate exceeds 2. The results from the statistical technique used by SPARC-STTA have been intercompared with other methods employed in the literature (A. J. Miller, personal communication, 1998) and found to yield similar trend estimates. It is cautioned, however, that the estimates of the statistical uncertainties could be more sensitive to details of the method than the trend results themselves, especially if the time series has lots of missing data.

An important caveat to the interpretation of the significance of the data sets is that the time series analyzed below, in some instances, is only 15 years long or, in the case of the longer rocketsonde and radiosonde record, up to ~30 years long. In this context it must be noted that the low-frequency variability in the stratosphere, especially at specific locations, is yet to be fully ascertained and, as such, could have a significant bearing on

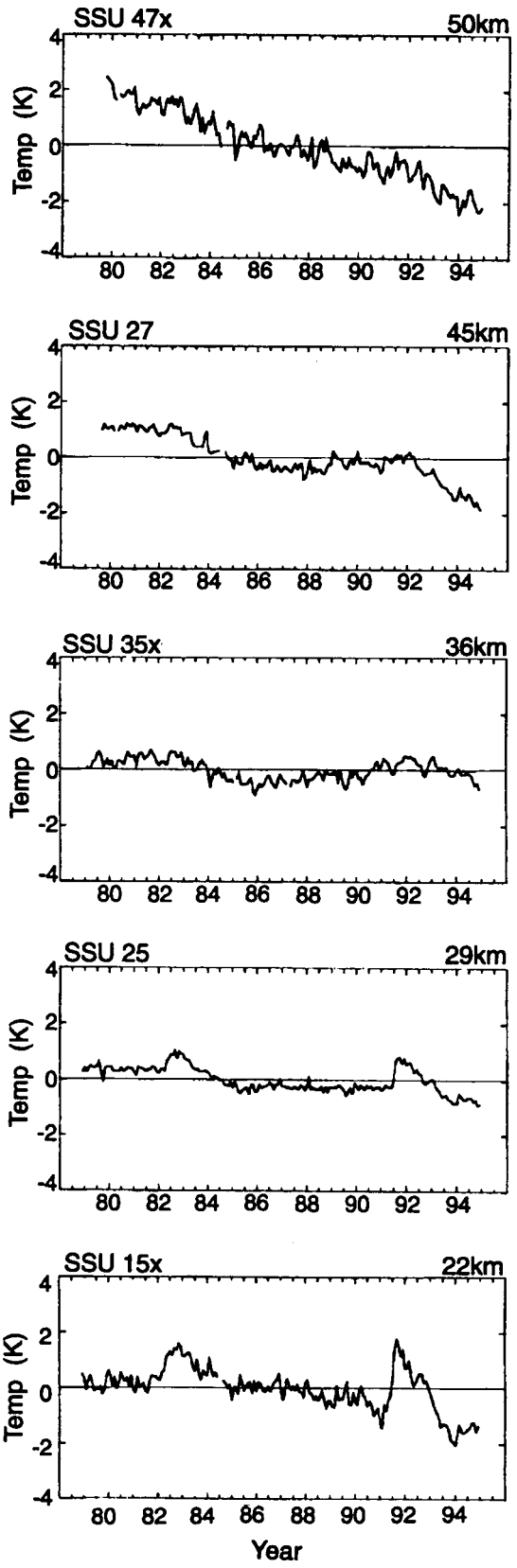

Figure 2. Time series of global temperature anomalies from the overlap-adjusted SSU satellite data for various stratospheric altitudes. These data measure the thermal structure over thick layers (~10–15 km) of the stratosphere. The label on each panel indicates the approximate altitude of the weighting function maximum.

TABLE 3. Lower Stratospheric Temperature Trends From Published Studies of Radiosonde Data

Reference	*Data Period*	*Level or Layer*	*Region*	*Trend, K/Decade*	*Comments*
Angell [1991a]	1972–1989	50 hPa, 20 km	8°S–55°N	−0.5 ± 0.3	12 radiosonde stations; data adjusted for the El Chichon influence; greatest cooling in winter
		30 hPa, 24 km		−0.4 ± 0.3	
		20 hPa, 27 km		−0.3 ± 0.3	
		10 hPa, 31 km		−0.3 ± 0.3	
Angell [1991b]	1970–1988	100- to 50-hPa layer	NH	−0.2	trends reported here based on Angell's presentation of temperature differences between the periods 1980–1988 and 1970–1978
			SH	−0.5	
Koshelkov and Zakharov [1998]	1965–1994	50- and 100-hPa levels	65°N–83°N	0 to −1	significant (95% confidence level) trends only from May to November
	1979–1994	50- and 100-hPa levels	65°N–83°N	2 to −4	significant (95% confidence level) trends only from June to October
Labitzke and van Loon [1995]	1965–1993	100 hPa	NH (10°–90°N)	0 to −0.5	significant (95% confidence level) trends between 60° and 80°N
		50 hPa	NH (10°–90°N)	0 to −0.5	significant (95% confidence level) trends between 20° and 90°N
		30 hPa	NH (10°–90°N)	0 to −0.5	significant (95% confidence level) trends between 30° and 60°N
	1979–1993	100 hPa	NH (10°–90°N)	−0.2 to −0.8	significant (95% confidence level) trends only at about 40°N
		50 hPa	NH (10°–90°N)	0 to −0.9	significant (95% confidence level) trends between 35° and 50°N
		30 hPa	NH (10°–90°N)	0 to −1.0	significant (95% confidence level) trends between 30° and 50°N
Miller et al. [1992]	1964–1986	150- to 30-hPa levels	global (62 stations, as Angell)	−0.2 to −0.4, depending on level	four stations' data adjusted for level shifts
McCormack and Hood [1994]	1979–1990	100 hPa	NH	0 to −4.5	data from the Free University of Berlin analyses; significant trends only in winter at 30°–45°N
Oort and Liu [1993]	1963–1988	100- to 50-hPa layer	NH	−0.38 ± 0.14	
			SH	−0.43 ± 0.16	
			global	−0.40 ± 0.12	
	1959–1988		NH	−0.40 ± 0.10	
Pawson and Naujokat [1997]	1965–1996	50 hPa	NH (10°–90°N)	−1.90 (minimum) +1.67 (maximum)	decrease in daily minimum temperature, increase in daily maximum, for winter season; increase in the area of $T < 195$ K and $T < 192$ K, although the early data for $T < 192$ are questionable
		30 hPa		−1.85 (minimum) +4.07 (maximum)	
Parker et al. [1997]	1965–1996	150- to 30-hPa layer	NH	−0.27	radiosonde data weighted to correspond with MSU4; adjustments made to Australasia data for 1979–1996; trends significant at the 95% confidence level or better
			SH	−0.44	
	1979–1996		NH	−0.63	
			SH	−0.73	
Reid et al. [1989]	1966–1982	100- to 15-hPa levels	tropics	−1.2 to +0.8	five radiosonde stations; trends vary by station and level
Taalas and Kyrö [1992]	1965–1988	50 hPa	Sodankyla, Finland, station	−0.2 ± 1.6 (annual) −1.6 ± 0.08 (January) +1.5 ± 0.05 (April)	100, 70, and 30 hPa showed similar results
Taalas and Kyrö [1994]	1965–1992	50 hPa	Sodankyla, Finland, station	−0.16	increase in the number of observations of $T < 195$ K in winter

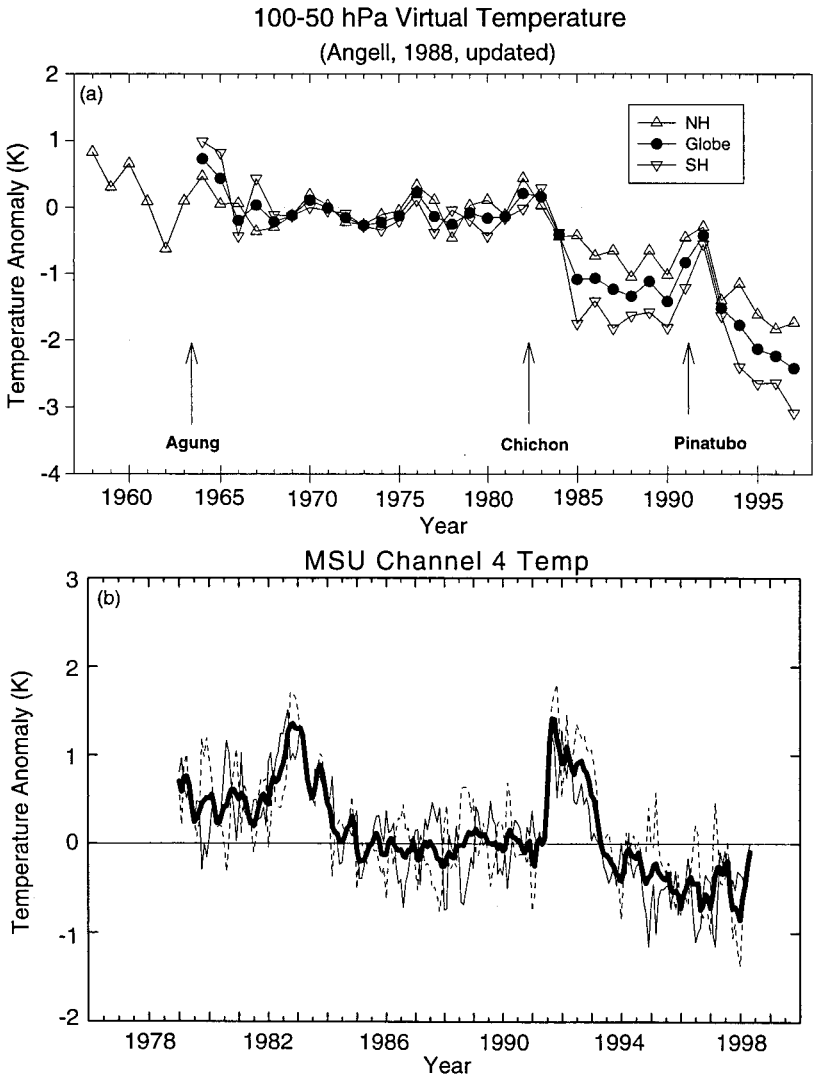

Figure 3. (a) Global and hemispheric averages of annual anomalies of 100- to 50-hPa layer-mean virtual temperature from 63 radiosonde stations (*Angell* [1988], updated; *Halpert and Bell* [1997]). (b) Same as Figure 3a except from MSU channel 4 satellite data (see section 1 for stratospheric altitudes sensed [see also *Spencer and Christy*, 1993; *Christy and Drouilhet*, 1994]). The bold solid curve denotes global mean, the thin solid curve denotes the Northern Hemisphere (NH) mean, and the dashed curve denotes the Southern Hemisphere (SH) mean. Updated from *Randel and Cobb* [1994].

the interpretation of the derived trend values. Another cautionary note concerns the possible misinterpretation of one "natural" signal for another. This possibility arises in the instance of the volcanic signal in the stratosphere being misinterpreted as that due to the solar cycle, since the frequency of large volcanic events over the past 2 decades has approximately corresponded to the period of the solar cycle (see sections 2.6.1 and 2.6.2).

2.3.2. Fifty and 100 hPa. The decadal trends for the different data sets over the 1979–1994 period are compared in Plate 1. The Oort data (Table 1), which have been used widely [e.g., *Hansen et al.*, 1995; *Santer et al.*, 1996], are not included in this plot because it spans a shorter period of time (it terminates in 1989) than the other data sets. All data sets indicate a cooling of the entire Northern Hemisphere and the entire low- and middle-latitude Southern Hemisphere at the 50-hPa level over the period considered. At the 100-hPa level, there is a cooling over most of the northern and southern latitudes. The midlatitude (30°–60°N) trends in the Northern Hemisphere exhibit a statistically significant (Table 4) cooling at both the 50- and 100-hPa levels, with the magnitude in this region being ~0.5–1 K/decade. This feature is found in the satellite data as well. The similarity of the magnitude and significance in the middle Northern Hemisphere latitudes from the different data sets is particularly encouraging and suggests a robust trend result for this time period.

In the case of the MSU and Nash (SSU 15X) satellite data, the trend illustrated is indicative of a response function that spans a wide range in altitude (Figure 1). Because of this, caution must be exercised in comparing them with the magnitude of the nonsatellite data trends. For example, the generally lesser cooling trend seen in the satellite data relative to radiosonde in the tropical regions could be due to the range in altitude "sensed" by the satellites, which includes the upper troposphere. However, this argument is contingent upon the actual trends in the tropical upper troposphere. From an analysis of radiosonde data, *Parker et al.* [1997] find the transition height between tropospheric warming and cooling above to occur at about 200 hPa when comparing the period 1987–1996 with 1965–1974; this indicates

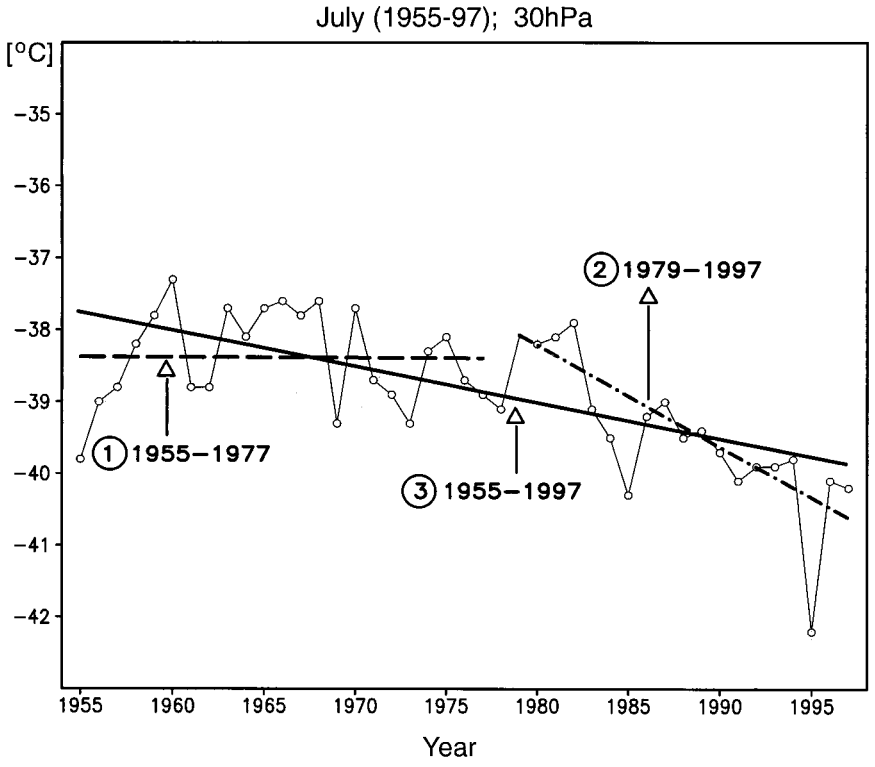

Figure 4. A 1955–1997 time series of July 30-hPa temperatures at high northern latitude (80°N). Trends over the 1955–1977, 1979–1997, and 1955–1997 time periods are −0.01, −1.41, and −0.5 K/decade, respectively. Of these, only the 1979–1997 trend is statistically significant. Updated from *Labitzke and van Loon* [1995].

that part of the MSU weighting function (Figure 1) is likely sampling altitudes at which some warming has occurred. (For a further perspective on trends in the upper troposphere, see *Hansen et al*. [1997b] and *Santer et al*. [1999].) The MSU indicates less cooling than Nash in the tropics. One reason for this could be that the Nash peak signal originates from a slightly higher altitude than MSU; again, though, the extent of the cooling/warming trend in the upper troposphere needs to be considered for a full explanation. The results are statistically insignificant in almost all of the data sets at the low latitudes. This could be due in part to the variable quality of the tropical data. It is conceivable that the radiosonde trends are significant over selected regions where the data are reliable over long time periods but that the significance is eroded when reliable and unreliable data are combined to get a zonal mean estimate.

The trends in the Southern Hemisphere midlatitudes (~15°–45°S) range up to ~0.5–1 K/decade but are generally statistically insignificant over most of the area in almost all data sets, except Reanal. Note that the Southern Hemisphere radiosonde data have more uncertainties owing to fewer observing stations and data homogeneity problems (see section 2.5.1). The nonsatellite data indicate a warming at 50 hPa but a cooling at 100 hPa at the high southern latitudes, while the satellites indicate a cooling trend. Thus, as for the tropical trends, satellite-radiosonde intercomparisons in this region have to consider carefully the variation of the trends with altitude (see section 2.5.3). The lack of statistically significant trends in the southern high latitudes need not imply that significant trends do not occur during particular seasons (e.g., Antarctic springtime; see section 2.4). The high northern latitudes indicate a strong cooling (1 K/decade or more) in the 50-hPa, 100-hPa, and satellite data sets. However, no trends are significant poleward of ~70°N owing to the large interannual variability there. There is a general consistency of the analyzed data sets (CPC, GSFC, and Reanal) with trends derived directly from the instrumental data. Considering all data sets, the global-mean lower stratospheric cooling trend over the 1979–1994 period is estimated to be ~0.6 K/decade. The 50- to 100-hPa cooling is consistent with earlier WMO results based on shorter records [e.g., *WMO*, 1990a, Figure 6.17; 1990b, Figure 2.4-5].

The comparison of the 50-hPa trends over the longer period (1966–1994) with the different data sets (radiosonde only) also reveals a fair degree of consistency (Plate 2). The cooling trends in the northern high latitudes, and in several other latitude belts, are less strong in the radiosonde data sets when the longer period is considered (note that the Berlin radiosonde time series for July at 80°N (Figure 4) exhibits a similar feature). The cooling trend in the 30°–60°N belt is about 0.3 K/decade, and again, the midlatitude regions stand out in terms of the significance of the estimated trends (Table 5). The strong cooling trend in the Oort data in the high southern latitudes is consistent with the *Oort and Liu* [1993], *Parker et al*. [1997], and Angell studies. In the Southern Hemisphere the two global radiosonde data sets indicate a statistically significant (Table 5) cooling over broad belts in the low and middle latitudes, with the Oort data exhibiting this feature at even the higher latitudes. Latitudes as low as 10°–20° exhibit

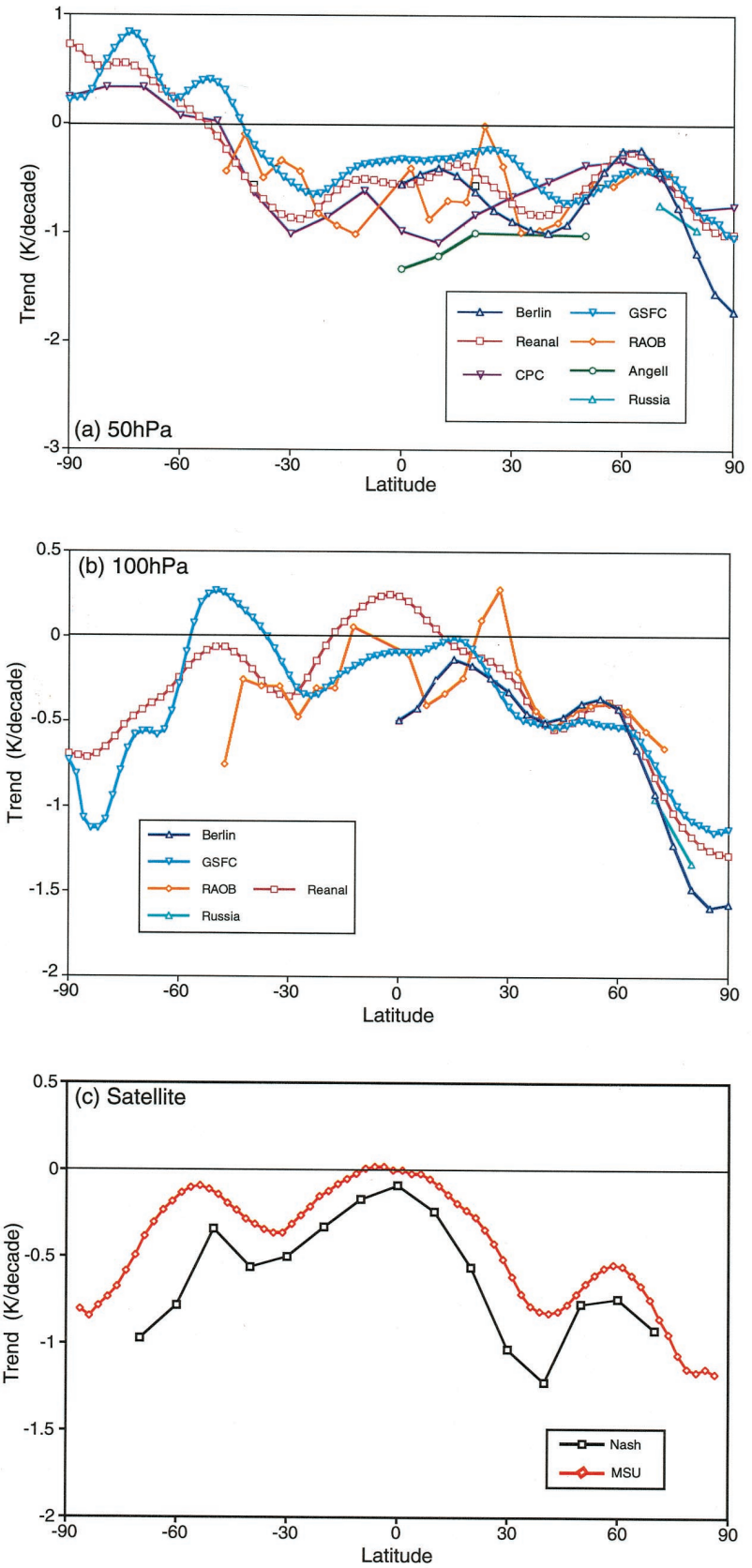

Plate 1. Zonal-mean decadal temperature trends for the 1979–1994 period, as obtained from different data sets. These consist of radiosonde (Angell, Berlin, UK RAOB, and Russia) and satellite observations (MSU and Nash), and analyses data sets (Climate Prediction Center (CPC), Goddard Space Flight Center (GSFC), and Reanal). See Table 1 and sections 2.1 and 2.3.2 for details. Plate 1a denotes 50-hPa trends, Plate 1b denotes 100-hPa trends, and Plate 1c denotes trends observed by the satellites for the altitude range sensed which includes the lower stratosphere (see Figure 1). Latitude bands where the trends are statistically significant at the 2-σ level are listed in Table 4. (Data courtesy of the Stratospheric Processes and Their Role in Climate (SPARC) Stratospheric Temperature Trends Assessment project.)

TABLE 4. Latitude Bands Where the Observed 50- and 100-hPa and Satellite Temperature Trends (1979–1994) From Various Data Sources (See Table 1 and Plate 1) Are Statistically Significant at the 2-σ Level

Data	*Latitude Band*	
	SH	*NH*
	50 hPa	
Berlin	···	30°–55°N
GSFC	···	42°–58°N
Reanal	37.5°–25°S	32.5°–55°N
RAOB	12.5°S	32.5°–62.5°N
CPC	30°S	10°N
Angell	···	50°N
Russia	···	···
	100 hPa	
Berlin	···	0°–5°N; 35°–80°N
GSFC	···	38°–60°N
Reanal	···	37.5°–57.5°N
RAOB	47.5°S	12.5°N; 37.5°–72.5°N
Russia	···	70°N; 80°N
	Satellite	
Nash	···	30°–60°N
MSU	···	28.75°–63.75°N

SH and NH denote Southern and Northern Hemisphere, respectively. No entry denotes either no data or no statistically significant latitude belt in that hemisphere.

significant trends over the longer period. From the Oort and RAOB data sets the global-mean trend is estimated to be about −0.35 K/decade over the 1966–1994 period.

2.3.3. Vertical profile. Analyses of the vertical and latitudinal structure of the zonal, annual-mean temperature trend, as obtained from the SSU and MSU satellite measurements for the 1979–1994 period, demonstrate that the omission of the volcano-induced warming period (particularly that due to Pinatubo near the end of the record) yields an enhanced cooling trend in the lower stratosphere (Figure 5). The vertical profile of the temperature trend in the middle and upper stratosphere between ~60°N and ~60°S shows a strong cooling, particularly in the upper stratosphere (up to 3 K/decade). Cooling at these latitudes in major portions of the middle and upper stratosphere is inferred to be statistically significant.

At 45°N, lidar records from Haute Provence are available, which afford high vertical resolution above 30 km (Figure 6) relative to the other instrumental data available. The annual-mean trend profile for 1979–1998, updated from *Keckhut et al*. [1995], shows a cooling over the entire altitude range 35–70 km of ~1–2 K/decade, but with statistical significance obtained only around 60 km. The vertical gradient in the profile of cooling between 40 and 50 km differs somewhat from the 1979–1990 summer trend reported by *WMO* [1992, Figure 2-20].

Comparing the vertical pattern of temperature trend at 45°N obtained from the different data sets for the 1979–1994 period (Figure 7) suggests that there is broad agreement in the cooling at the lower stratospheric altitudes, reiterating Plate 1. The vertical patterns of the trends from the various data are also in qualitative agreement with one another, except for the lidar data (which, in any case, are not statistically significant over that height range). Note that the lidar trend for the 1979–1998 period at a single location (Figure 6) exhibits better agreement with the satellite trend in Figure 7, indicating a sensitivity of the decadal trend to the end year considered. Generally speaking, there is an approximately uniform cooling of about 0.75 K/decade between ~80 and 5 hPa (~18–35 km), followed by increasing cooling with height (e.g., ~2.5 K/decade at ~0.7 hPa (50 km)). The "analyses" data sets, examined here for $p >$ 10 hPa, are in approximate agreement with the instrument-based data. Table 6 lists the trend estimates and the 1-σ uncertainty at the various altitudes, taking into account the trends and uncertainties of each individual measurement. The vertical profile of cooling, and especially the large upper stratospheric cooling, is consistent with the global plots given by *WMO* [1990a, Figure 6.17; 1990b, Figure 2.4-5] constructed from shorter data records.

2.3.4. Rocket data and trend comparisons. Substantial portions of the three available rocket data sets (comprising U.S., Russian, and Japanese rocketsondes; Table 2) have been either reanalyzed or updated since the review by *Chanin* [1993]. *Golitsyn et al*. [1996] and *Lysenko et al*. [1997] updated the data from five different locations over the period 1964–1990 or 1964–1995. *Golitsyn et al*. [1996] found a statistically significant cooling from 25 to 75 km, except around 45 km (Figure 8a). *Lysenko et al*. [1997] obtain a similar vertical profile of the trend for the individual rocketsonde sites (Figure 8b). They find a significant cooling trend in the mesosphere, particularly at the midlatitude sites (note that the statistical technique employed in the above studies for the rocketsonde data differs from that of the SPARC-STTA analyses).

Out of the 22 stations of the U.S. network, nine provide data for more than 20 years. Some series have noticeable gaps that prevent them from being used for trend determination. Two groups have independently revisited the data: *Keckhut et al*. [1999] selected six low-latitude sites (8°S–28°N), and *Dunkerton et al*. [1998] selected five out of six of the low-latitude sites plus Wallops Islands (37°N). Both accounted for spurious jumps in the data by applying correction techniques.

Keckhut et al. [1999] found a significant cooling between 1969 and 1993 of about 1–3 K/decade between 20 and 60 km (Figure 9a). A similar result is seen in the data available since 1970 from the single, and still operational, Japanese rocket station (Figure 9b, updated from *Komuro* [1989]). *Dunkerton et al*. [1998], using data from 1962 to 1991, infer a downward trend of −1.7 K/decade for the altitude range 29–55 km; they also obtain a solar-induced variation of ~1 K in amplitude. It should be noted that the amplitude of the lower meso-

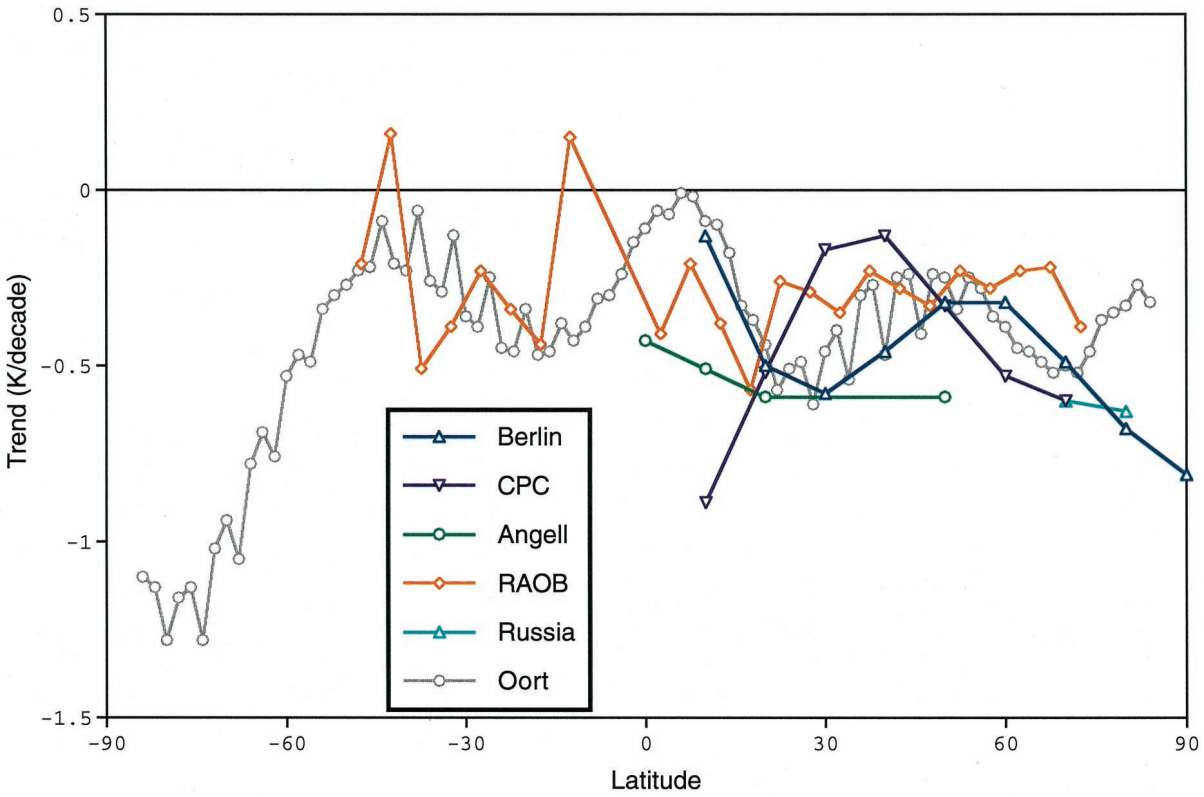

Plate 2. Zonal-mean decadal temperature trends at 50 hPa over the 1966–1994 period from different radiosonde data sets (see Table 1 and sections 2.1 and 2.3.2 for details; note that Oort time series extends only until 1989). Latitude bands where the trends are statistically significant at the 2-σ level are listed in Table 5. (Data courtesy of SPARC Stratospheric Temperature Trends Assessment project.)

sphere cooling observed in the middle and high latitudes from the Russian rockets (between 3 and 10 K/decade) is somewhat larger than from the U.S. data set. Nevertheless, all four rocketsonde analyses shown in Figures 8 and 9, together with the lidar data at 44°N (Figure 6), are consistent in yielding trends of ~1–2 K/decade between about 30 and 50 km. These trends are also consistent with the SSU satellite analyses discussed earlier (in section 2.3.3).

In the latitude band 28°–38°N, just as at 45°N, almost all the data sets, including the rocket stations at 28°N (Cape Kennedy) and 34°N (Point Mugu), agree (see Figure 10) in the sign (though not in the precise magnitude) of temperature change below altitudes of about 20 hPa (~27 km). Above 10 hPa (~30 km), both satellite and rocket trends yield increasing cooling with altitude, with a smaller value at the 28°N rocket site. At 1 hPa, there is considerable divergence in the magnitudes of the two rocket trends. Because the rocket trends are derived from time series at individual locations, this may explain their greater uncertainty relative to the zonal-mean satellite trends. In a general sense, the vertical profile of the trend follows a pattern similar to that at 45°N (Figure 7).

2.4. Latitude-Season Trends

The monthly, zonal-mean trends in the lower stratosphere derived from MSU data over the period January 1979 to May 1998 (Figure 11, updated from *WMO* [1995]) reveal substantial negative values in the midlatitudes of both hemispheres during summer (−0.5 K/decade) and in springtime polar regions (up to −3 to −4 K/decade). There is a broad domain of statistical significance in the cooling at the midlatitudes; in the Northern Hemisphere (NH) this occurs from approximately June through October, while in the Southern Hemisphere (SH) it occurs from about mid-October to April. Little or no cooling is observed in the tropics, although the MSU measurements in the tropics originate from a broad layer (50–150 hPa) and thus include a trend signal from the upper troposphere (the weighting function maximum is near the tropical tropopause; Figure 1). Thus the tropical MSU result is not indicative of a purely lower stratospheric trend (section 2.3.2 and Plate 1). There is some symmetry evident in the observed trends in the two hemispheres, although most of the regions have values not significantly different from zero. Comparison with the MSU trends derived from data over 1979–1991 [*Randel and Cobb*, 1994; *WMO*, 1995, Figure 8-11] shows approximately similar patterns in the SH but substantial differences in the NH. The 1979–1991 NH trends had a peak in winter midlatitudes, while the strong springtime polar cooling was not statistically significant. Addition of data through mid-1998 diminishes the northern midlatitude winter trends and their significance, while increasing the cooling over the pole in

TABLE 5. Latitude Bands Where the 1966–1994 Observed 50-hPa Temperature Trends From Various Data Sources (See Table 1 and Plate 2) Are Statistically Significant at the 2-σ Level

Data	*Latitude Band*	
	SH	*NH*
Berlin	···	20°–70°N
CPC	···	10°–20°N; 50°–60°N
Angell	···	10°, 20°, 50°N
RAOB	37.5°–32.5°S; 22.5°–17.5°S	17.5°N; 32.5°N; 42.5°–72.5°N
Oort	84°–56°S; 30°–28°S 24°–22°S; 18°–16°S	20°–30°N; 34°N; 40°N; 46°N 52°–68°N
Russia	···	70°N; 80°N

spring and making it significant. Thus, owing to a high degree of interannual variability, especially during polar winter/spring, the MSU trend estimates are dependent on the choice of the end year.

The larger springtime polar trends are strongly influenced by the occurrence of several relatively cold years after 1991, as shown in Figure 12a for 80°N using the NCEP reanalyzed data and MSU observations. Note that the NCEP reanalyses data have not been adjusted for the discontinuities arising due to switch-over from a period when there was no satellite data to a period when satellite temperature retrievals became available (1976 for the SH and 1979 for the NH). This leads to a discontinuity in the analyzed temperatures for these years, associated with the model's systematic error. *Naujokat and Pawson* [1996] have also noted the relatively cold 1994–1995 and 1995–1996 northern polar winters. The 1990s-averaged temperature in March is lower than that for the 1980s. *Manney et al.* [1996] suggest that an unusual circulation pattern (low planetary wave forcing and an intense polar vortex) was primarily responsible for this feature. In particular, March 1997 was very cold, about 18 K below the 1980–1989 decadal average. Indeed, the monthly-mean 30-hPa temperature over the pole in March 1997 may have been one of the coldest years since 1966. *Newman et al.* [1997] indicate that this coincided with the occurrence of the lowest total ozone amount in the Northern Hemisphere for this season. The extreme low temperatures in March 1997 appear to be associated with record low planetary wave activity [*Coy et al.*, 1997]. There are suggestions that the observed Arctic polar stratospheric conditions in recent years may be linked to changes in tropospheric circulation [*WMO*, 1999]. It is not certain whether these are secular trends or whether they are the consequence of a decadal-scale variability in the climate system. With regard to the frequency of major sudden stratospheric warmings, *Labitzke and van Loon* [1992] note that before 1992, the largest lapse of time between two major warmings was about 4 years. In comparison, no major warming appears to have occurred between 1991 and 1997, i.e., over seven winters. This is broadly consistent with the cooling trend in the 1990s up to 1997.

In the Antarctic, analysis of long-term records of radiosonde data continues to reveal substantial cooling trends in spring, further confirming the early study of *Newman and Randel* [1988]. This cooling trend is closely linked to springtime ozone depletion [*Angell*, 1986; *Chubachi*, 1986; *Trenberth and Olsen*, 1989; *Jones and Shanklin*, 1995; *Butchart and Austin*, 1996]. This springtime cooling is an obviously large feature of the MSU temperature trends shown in Figure 11. The 100-hPa tem-

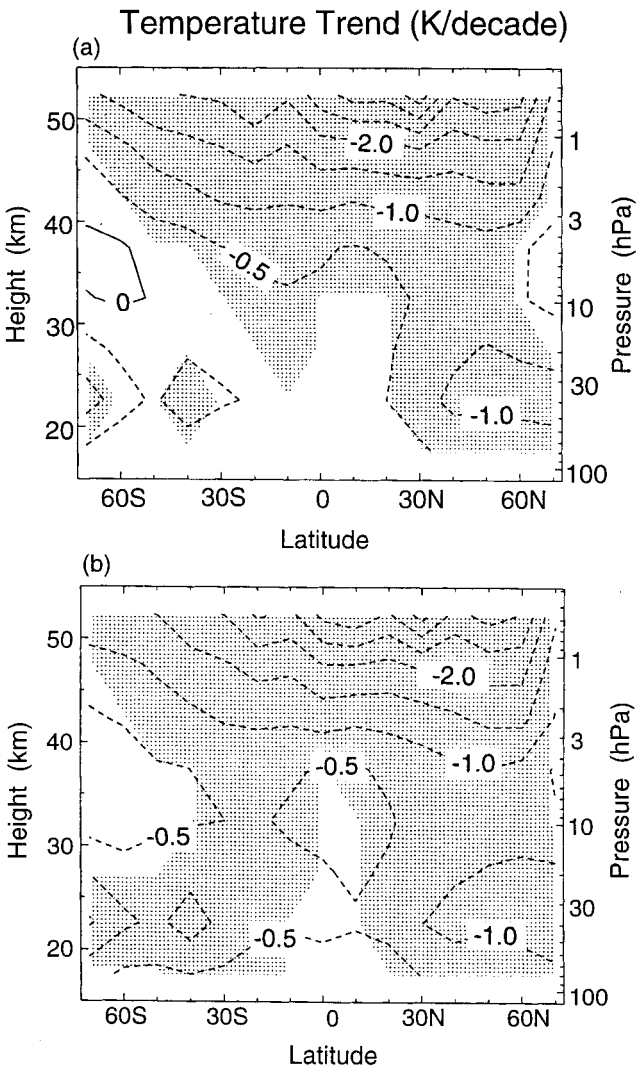

Figure 5. Zonal, annual-mean decadal temperature trends versus altitude for the 1979–1994 period, as obtained from the satellite (using MSU and SSU channels) retrievals (a) with volcanic periods included and (b) with volcanic periods omitted. Contour interval is −0.5 K/decade. The plot is constructed by considering 5-km-thick levels from linear combinations of the weighting functions of the different SSU channels (Figure 1). The "no-volcano" calculations omit 2 years of data following the El Chichon and Pinatubo eruptions. Shaded areas denote significance at the 2-σ level. (Data courtesy of SPARC Stratospheric Temperature Trends Assessment project.)

peratures in November over Halley Bay, derived from radiosonde data, together with time series from NCEP reanalysis interpolated to Halley Bay, reveal a decadal-scale change in temperature beginning in about the early 1980s along with significant year-to-year variability (Figure 12b). The timing of the change in the Antarctic may be compared with that at 80°N (March) around 1990 (Figure 12a). It is notable that temperatures in NH springtime polar regions indicate a strong cooling in recent years and an enhancement above natural variability (also, compare Figure 11 with Figure 8-11 of *WMO* [1995]) that is reminiscent of that observed in the Antarctic about a decade ago.

The structure of the decadal-scale temperature change over Antarctica as a function of altitude and month is calculated as the difference in decadal means (1987–1996 minus 1969–1979) and averaged over seven radiosonde stations [*Randel and Wu*, 1999]. These data (Figure 13) show a significant cooling (of ~6 K) in the lower stratosphere in spring (October–December), persisting through austral summer (March), while no significant temperature changes are found during winter. The data also show a statistically significant warming trend (3 K or more) at the uppermost data level (30 hPa; ~25 km) during spring (Figure 13).

Kokin and Lysenko [1994] have analyzed the seasonal trends in the middle and upper stratosphere from their five rocketsonde station data for the 1972–1990 period. Generally, the cooling is evident almost throughout the year at all sites, but there are exceptions. There is a significant positive trend during springtime above Moldezhnaya (at ~35 km) and during winter above Volgograd and Balkash (at ~40 km) (Figure 14). The warming feature for Moldezhnaya is consistent with the springtime warming inferred for slightly lower altitudes in the Antarctic by *Randel* [1988] and with that shown in Figure 13. The warming is located above the domain of cooling caused by the lower stratospheric ozone depletion. It is interesting that such an effect also takes place during the northern winter over Volgograd and Balkash locations. It may be noted that *Labitzke and van Loon* [1995] also obtain a positive trend in the middle stratosphere (~10 hPa) in winter using radiosonde data (see section 2.2). As will be discussed later (in section 3.3.1), model simulations suggest that this observed warming could be due to the dynamical response occurring as a result of the loss of ozone in the lower stratosphere.

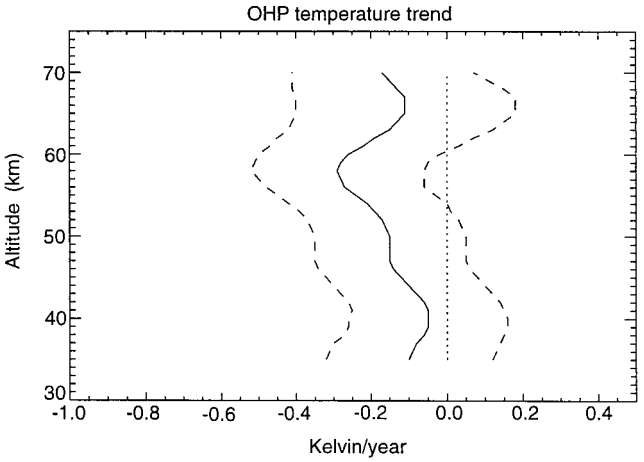

Figure 6. Trend (K/year) from the all-seasons lidar record at Haute Provence, France (44°N, 6°E), over the period 1979–1998. The solid curve denotes the estimated mean, while the dashed curves denote the 2-σ uncertainties. Updated from *Keckhut et al.* [1995].

2.5. Uncertainties in Trends Estimated From Observations

Determining stratospheric temperature trends from long-term observations is complicated by the presence of additional, nontrend variability in the data. Two types of phenomena contribute to the uncertainty in trend estimates. The first is random variability that is internally generated within the atmosphere and that is not trend-like in nature. Major sources of such variability include the periodic and quasi-periodic signals associated with the annual cycle, the quasi-biennial oscillation, the solar cycle, and the El Niño–Southern Oscillation (ENSO). In addition, stratospheric temperatures vary in response to episodic injections of volcanic aerosols. To a first approximation, these atmospheric phenomena have negligible effects on the long-term temperature trend because they are periodic or of relatively short duration. Nevertheless, because current data records are only a few decades long, at most, these phenomena may appear to enhance or reduce an underlying trend. At a minimum, the additional temperature variability associated with these signals reduces the statistical confidence with which long-term trends can be identified. While periodic signals can be removed, the effects of sporadic events are more difficult to model and remove. Furthermore, there may be long-term trends in these cycles and forcings that confound the analysis. A second source of uncertainty is due to spurious signals in the time series that are due to changes in methods of observation rather than to changes in the atmosphere. The problem of detecting temperature trends in the presence of changes in the bias characteristics of the observations is receiving increased attention [*Christy*, 1995; *Santer et al.*, 1999]. It seems likely that over the next few years better methods will be employed to quantify and reduce the uncertainty in stratospheric temperature trend estimates attributable to these spurious signals.

2.5.1. Uncertainties associated with radiosonde data. Although most radiosonde analyses show cooling of the lower stratosphere in recent decades, it is important to recognize that they all rely on subsets of the same basic data set, the global observing system upper air network. This network is fundamentally a meteorological one, not a climate monitoring network, not a reference network for satellite observations, and not a network for detection of stratospheric change. Whatever

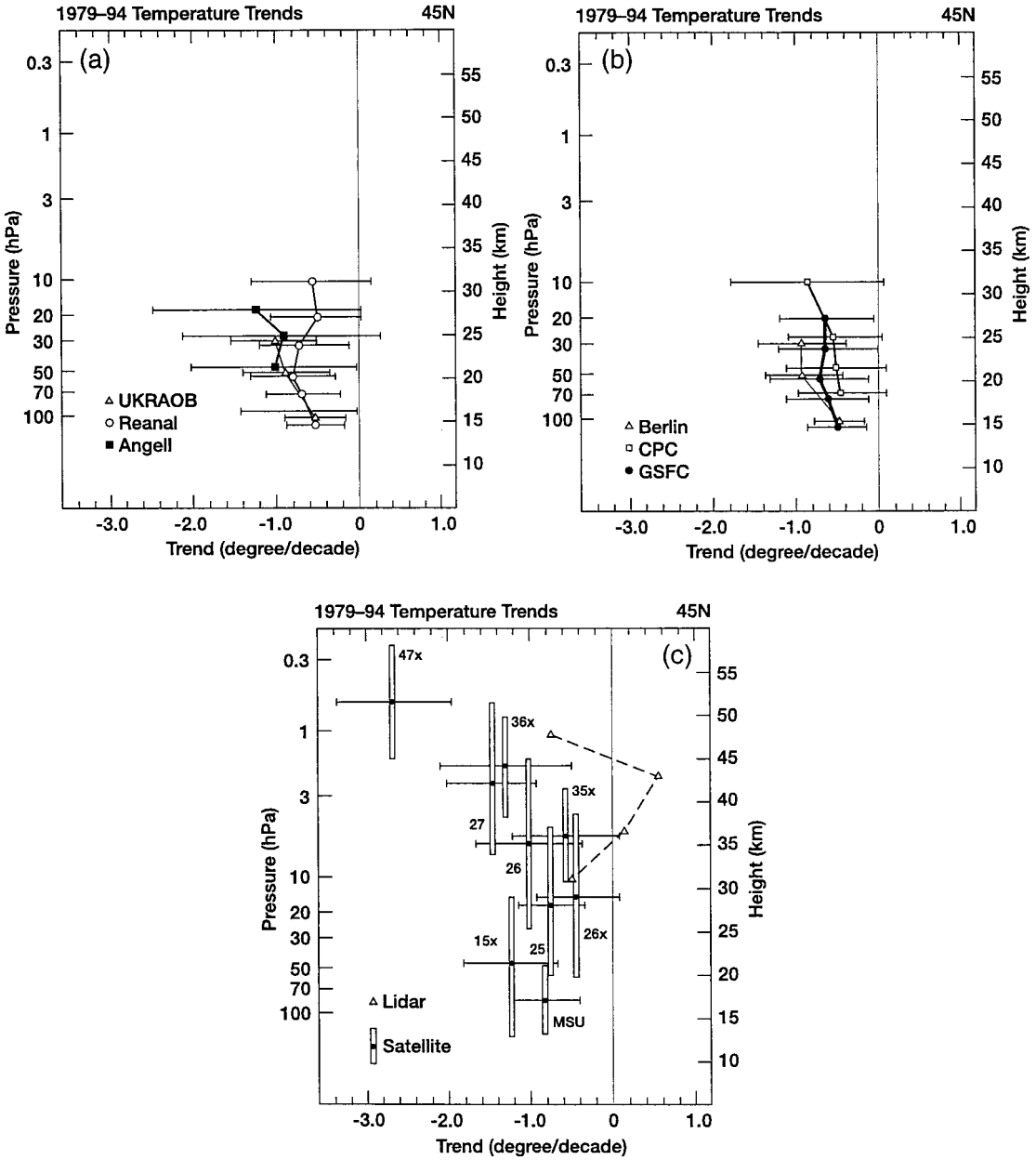

Figure 7. Vertical profile of the zonal, annual-mean decadal stratospheric temperature trend over the 1979–1994 period at 45°N from different data sets (Table 1). Horizontal bars denote the 2-σ level uncertainty, while vertical bars drawn in the case of the satellite data denote the approximate altitude range sensed by the MSU and the different SSU satellite channels, respectively (see Figure 1). The uncertainty in the lidar trend is as large as the plot scale and is not depicted. For the nonsatellite data a line is drawn connecting the mean estimates at the different altitudes. (Data courtesy of SPARC Stratospheric Temperature Trends Assessment project.)

difficulties (described below) plague the radiosonde network when it is employed for temperature trends analysis will affect all analyses that use those data.

Karl et al. [1995] and *Christy* [1995] have reviewed some of the problems associated with using radiosonde data for the detection of atmospheric temperature trends. These fall into two categories: the uneven spatial distribution of the observations and the temporal discontinuities in station records.

The radiosonde network is predominantly a Northern Hemisphere, midlatitude, land network. About half of the stations are in the 30°–60°N latitude band, and less than 20% are in the Southern Hemisphere [*Oort and Liu*, 1993]. Moreover, the uneven distribution of stations is worse for stratospheric data than for the lower troposphere, because low-latitude and Southern Hemisphere soundings have a higher probability of taking only one observation daily (other stations make two, and many

TABLE 6. Weighted Trend Estimates and Uncertainty at the 1-σ Level at 45°N, Computed From the Individual System Estimates Shown in Figure 7

Altitude, km	*Trend, K/decade*	*Uncertainty (1-σ)*
15	−0.49	0.18
20	−0.84	0.18
25	−0.86	0.20
30	−0.80	0.29
35	−0.88	0.30
40	−1.23	0.33
45	−1.81	0.37
50	−2.55	0.40

See also Figure 30, where the trend and the 2-σ level uncertainty are plotted.

formerly made four) and because the soundings more often terminate at lower altitudes [*Oort and Liu*, 1993]. Estimates of layer-mean trends, and comparisons of trends at different levels, are less meaningful when data at the top of the layer are fewer than at the bottom. Additionally, there is an increasing uncertainty with height of the radiosonde trends.

For trend detection the temporal homogeneity of the data is the key. As discussed by *Parker* [1985], *Gaffen* [1994], *Finger et al*. [1993], and *Parker and Cox* [1995], numerous changes in operational methods have led to discontinuities in the bias characteristics of upper air temperature observations, which are particularly severe in the lower stratosphere [*Gaffen*, 1994]. Because radiosondes are essentially expendable probes (although some are recovered and reconditioned), changing methods is much easier than, for example, in the case of surface observations at fixed locations. Effects on data have been shown for changes in instrument manufacturer, replacement of old models with newer ones from the same manufacturer [*Parker*, 1985; *Gaffen*, 1994], changes in time of observation [*Elliott and Gaffen*, 1991; *Zhai and Eskridge*, 1996], changes in the lag characteristics of the temperature sensors [*Parker*, 1985; *Huovila and Tuominen*, 1990], and even changes in the length of the suspension cord connecting the radiosonde balloon with the instrument package [*Suzuki and Asahi*, 1978; *Gaffen*, 1994] and balloon type [*Parker and Cox*, 1995].

Daytime stratospheric temperature data in the early years of radiosonde operations were particularly affected by errors due to solar radiation. Substantial changes in both data correction methods [e.g., *Scrase*, 1956; *Teweles and Finger*, 1960] and instrument design have been made to address the problem. In general, the result has been a reduction in a warm bias over time, leading to an artificial "cooling" in the data [*Gaffen*, 1994]. The example in Figure 15, showing monthly mean 100-hPa temperatures at Tahiti, shows that a 1976 change from one model of the French Mesural radiosonde to another, each with different temperature sensors, was associated with an artificial temperature drop of several degrees. Given estimated temperature trends of the order of tenths of a degree Kelvin per decade, such inhomogeneities introduce substantial uncertainty regarding the magnitude of the trends in the lower stratosphere. Furthermore, *Luers* [1990] has demonstrated that daytime radiosonde temperature errors can exceed 1 K at altitudes above 20 km (~50 hPa) and that the magnitude of the error is a strong function of the temperature and radiative environment. This suggests

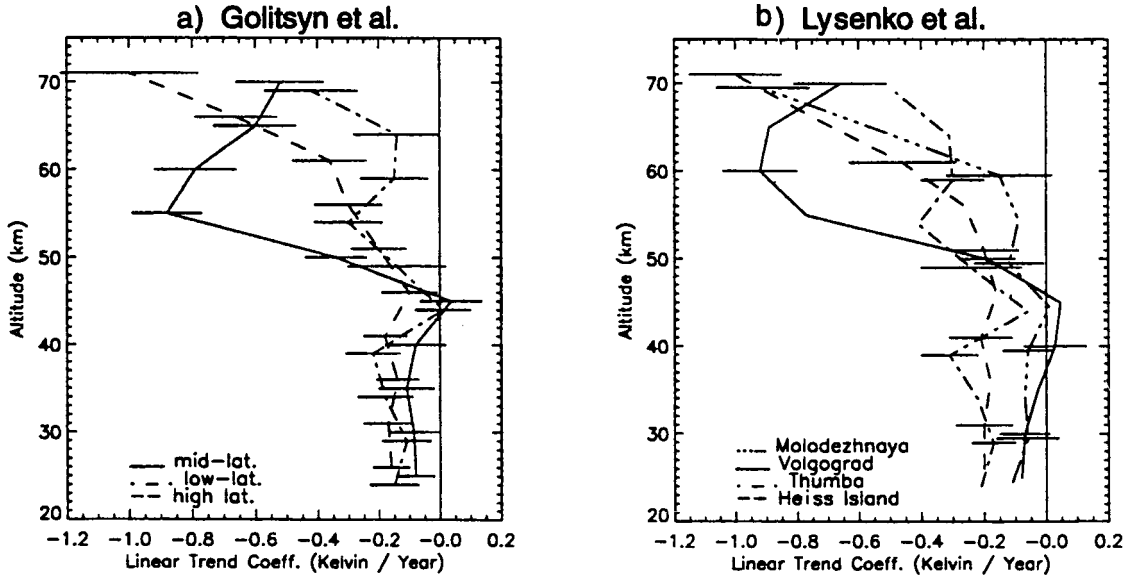

Figure 8. (a) Trends (K/year) based on the former Soviet Union (FSU) rockets (25–70 km) since the mid-1960s. Adapted from *Golitsyn et al*. [1996]. (b) Trends (K/year) based on the same FSU rocket data set. Adapted from *Lysenko et al*. [1997].

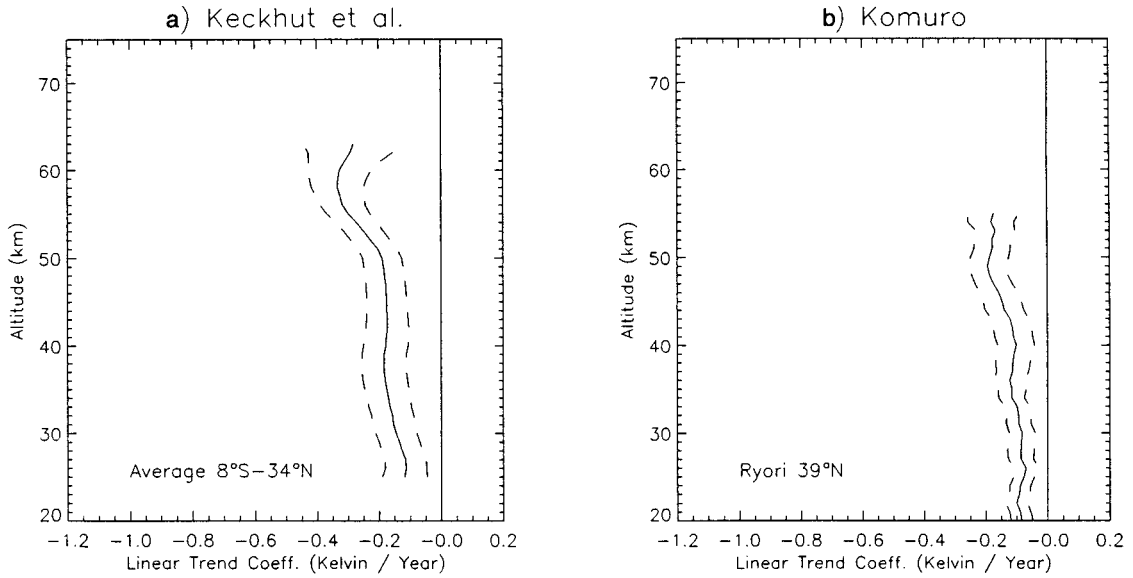

Figure 9. (a) Trend (K/year) compiled from U.S. rocket sites in the 8°S–34°N belt (see Table 2) over 1969–1993 [*Keckhut et al*., 1999]. (b) Trend (K/year) from the Japanese rocket station at Ryori over the period 1970 to present. The solid curves denote the mean estimate, while the dashed curves denote the 2-σ uncertainties. Updated from *Komuro* [1989].

that as the atmosphere undergoes changes owing to natural/anthropogenic causes, so will the quantitative aspects of the measurement errors.

A few investigators have attempted to adjust radiosonde temperature time series to account for "change points," or level shifts like the one illustrated in Figure 15. *Miller et al*. [1992], using data from 1970–1986, made adjustments to lower stratospheric data at four of 62 stations in *Angell*'s [1988] network on the basis of a statistical regression model that includes a level shift term. However, *Gaffen* [1994] concluded that over a longer period, many more of the Angell stations showed data inhomogeneities. *Parker et al*. [1997] have made adjustments to temperature data from Australia and New Zealand for the period 1979–1995 by using MSU data as a reference time series and station histories [*Gaffen*, 1994] to identify potential change points. The adjustments (of earlier data relative to 1995 data) ranged from 0 to −3.3 K and reduced the estimated zonal-mean 30-hPa temperature change between the periods 1987–1996 and 1965–1974 at about 30°S from −2.5 K/decade to about −1.25 K/decade [*Parker et al*., 1997], indicating the potentially large sensitivity of trends to data adjustments. *Gaffen et al*. [2000] found that temperature trends from radiosonde data are highly sensitive to adjustments of step-like changes in mean values, in part because of the difficulty in distinguishing real and artifical changes.

2.5.2. Uncertainties associated with analyses of SSU satellite data. The stratospheric temperature analyses from CPC are an operational product, derived using a combination of satellite and radiosonde temperature measurements. Radiosonde data contribute to the analyses in the NH over the 70- to 10-hPa levels; satellite data alone are used in the tropics and the SH and over the entire globe above 10 hPa [*Gelman et al*., 1986] (see section 2.1). The satellite temperature retrievals are from the TIROS operational vertical sounder (TOVS), which has been operational since late 1978. A series of TOVS instruments (which includes MSU and SSU) have been put into orbit aboard a succession of operational satellites; these instruments do not yield identical radiance measurements for a variety of reasons, and derived temperatures may change substantially when a new instrument is introduced [*Nash and Forrester*, 1986]. *Finger et al*. [1993] have compared the operationally derived temperatures with colocated rocketsonde and lidar observations and find systematic biases of the order of ±3–6 K in the upper stratosphere (due primarily to the low vertical resolution of TOVS). These biases furthermore change with the introduction of new operational satellites, and *Finger et al*. [1993] provide a set of recommended corrections to the temperature data (dependent on the particular satellite instrument for each time period) which have been used by CPC.

In spite of the application of the adjustments recommended by *Finger et al*. [1993], time series of temperature anomalies from the CPC analyses still exhibit significant discontinuity near the times of satellite transitions. Thus, for example, the deseasonalized CPC-analyzed temperature anomaly time series over the equator at 1 hPa and the overlap-adjusted (i.e., accounting for the discontinuity in satellites) SSU channel 27 data (whose weighting function peaks near 1.5 hPa; Figure 1) show quite different characteristics (Figure 16), with apparent "jumps" in the CPC data that are

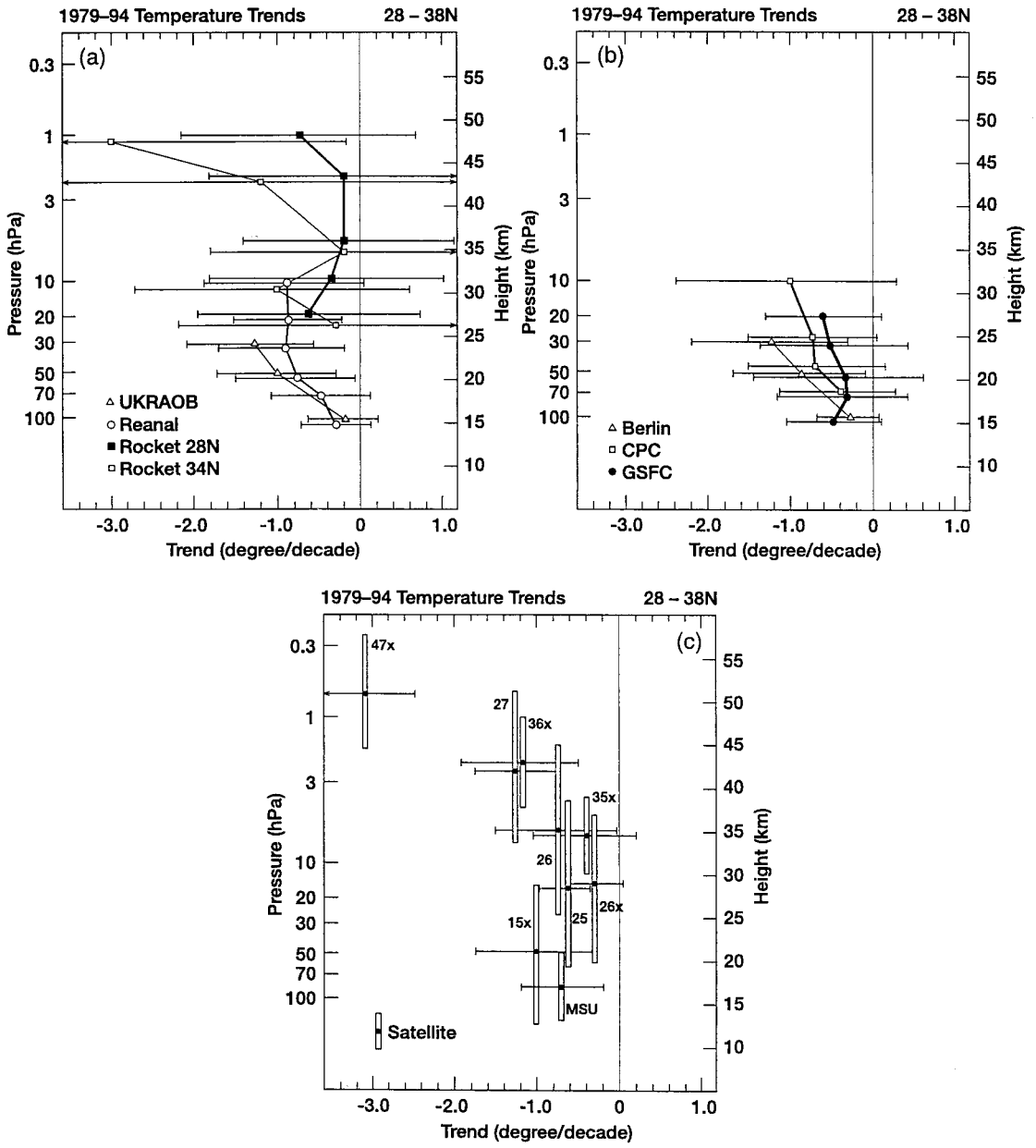

Figure 10. Vertical profile of the zonal, annual-mean decadal stratospheric temperature trend over the 1979–1994 period at 28°–38°N from different data sets (Tables 1 and 2). Horizontal bars denote the 2-σ level uncertainty, while vertical bars denote the approximate altitude range sensed by the MSU and the different SSU satellite channels (see Figure 1). For the nonsatellite data, a line is drawn connecting the mean estimates at the different altitudes. (Data courtesy of SPARC Stratospheric Temperature Trends Assessment project.)

coincident with satellite changes, for example, in mid-1984 and late 1988. Overall, the presence of such discontinuities in the CPC (and also the UKMO/SSU-ANAL) data limits their reliability for robust estimates of upper stratospheric trends (as in, say, Figure 7) and is even problematic for the determination of interannual variability. The overlap-adjusted SSU data (see Figure 2) used in Figures 5, 7, and 10 do not exhibit such obvious problems. While the adjustment process succeeds in resolving one major uncertainty in the satellite data set, there may be residual uncertainties due to other factors that necessitate a continued analysis of this data.

Other uncertainties associated with the satellite data, in general, include the effects due to longitudinal drifts that cause (1) spurious trends as the diurnal cycle is sampled at earlier or later times for a single satellite, and (2) changing solar shadowing effects on the instrument, in turn causing heating or cooling of the radiometer. While estimates for the correction and attempts to remove the biases are made, this factor does introduce a potential uncertainty in the trend determination.

2.5.3. Uncertainties in satellite-radiosonde trend intercomparisons. A distinct advantage of the satellite instruments over in situ ones is their globally extensive

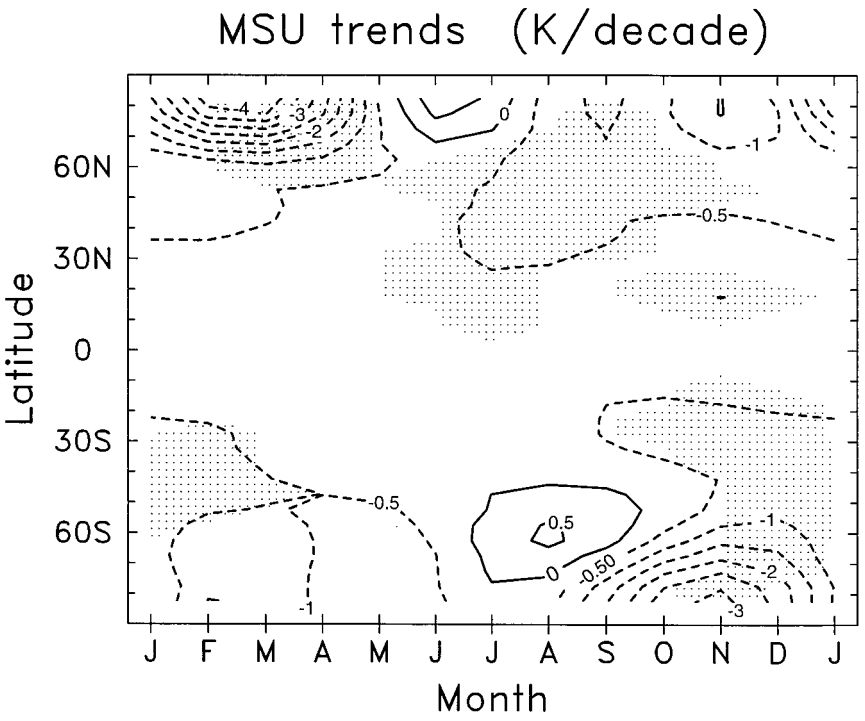

Figure 11. Latitude-month section of trends in MSU channel 4 temperature [*Spencer and Christy*, 1993] over the January 1979 to May 1998 period. Contour interval is 0.5 K/decade, with solid and dashed lines denoting positive and negative values, respectively. Shaded region indicates the trends are significant at the 5% level. Updated from *Randel and Cobb* [1994].

coverage. However, this is tempered by the fact that the signals that they receive originate from a broad range of altitudes (Figure 1). This is in contrast to the specific altitudes of measurements in the case of the ground-based instruments located at specific sites. This feature of the satellite trends complicates the interpretation for any particular vertical region of the atmosphere and more particularly, hampers a rigorous comparison with the radiosonde trends (see section 2.3.2). As an example, consider the lower stratospheric temperature trend. The MSU's channel 4 "senses" the entire extent of the lower part of the stratosphere and even the upper troposphere at low latitudes. This poses problems in the precise intercomparison of presently available satellite-based trends with those from ground-based instruments. In the tropics, approximately a quarter of the signal originates from the upper troposphere, leading to a potential misinterpretation of the actual lower stratospheric temperature trend based on MSU alone. This problem can become acute particularly if the tropical upper troposphere and lower stratosphere have temperature trends of opposite signs (see section 2.3.2). A similar comment also applies to the interpretation of the stratosphere trends from SSU measurements (Figure 1). Further, because of the areal coverage and weight factor of the low latitudes, the global means from satellite data and those from the in situ instruments may be comparable only after appropriate adjustments are made for the differential sampling by the two kinds of instruments. Therefore caution must be exercised in the interpretation of satellite-based trends vis-a-vis radiosonde and other ground-based instruments. Besides, satellite data interpretations also have to cope with problems involving temporal discontinuity, instrument calibration, and orbit drift.

2.5.4. Uncertainties associated with rocket data. The rocket data are very useful, as they were the only observations of the 30- to 80-km region before the lidars started operating. However, determining quantitative trends from rocket data is complicated by both physical and measurement issues. A first difficulty with the rocket data is that there have been instrumental changes and the measurements come from different types of sensors (Arcasonde, datasonde, falling spheres). However, *Dunkerton et al.* [1998] have found that these changes were a less important source of error than previously suggested. The major source of error, and the origin of the observed spurious jumps, seems to be due to the change of corrections made to the data in order to account for aerodynamic heating. Most of the earlier analyses did not take full account of the changes and spurious jumps in the data that ensued from the above mentioned difficulties. These points have been considered in depth by *Keckhut et al.* [1998] and *Dunkerton et al.* [1998]. This has resulted in a very limited number of U.S. stations that can be used for determining trends. Yet another source of uncertainty is due to the different time of measurements, as the amplitude of tidal influence may not be negligible at these altitudes (± 2 K around 40–45 km according to *Gille et al.* [1991] and *Keckhut et al.* [1996]). This may explain the small error bar in the Ryori Japanese measurements (Figure 9b), which are always conducted at the same local time. The factor related to the local measurement time has been accounted for in the analysis of the U.S. rocket data by *Keckhut et al.* [1999]. Since rocket data are available at

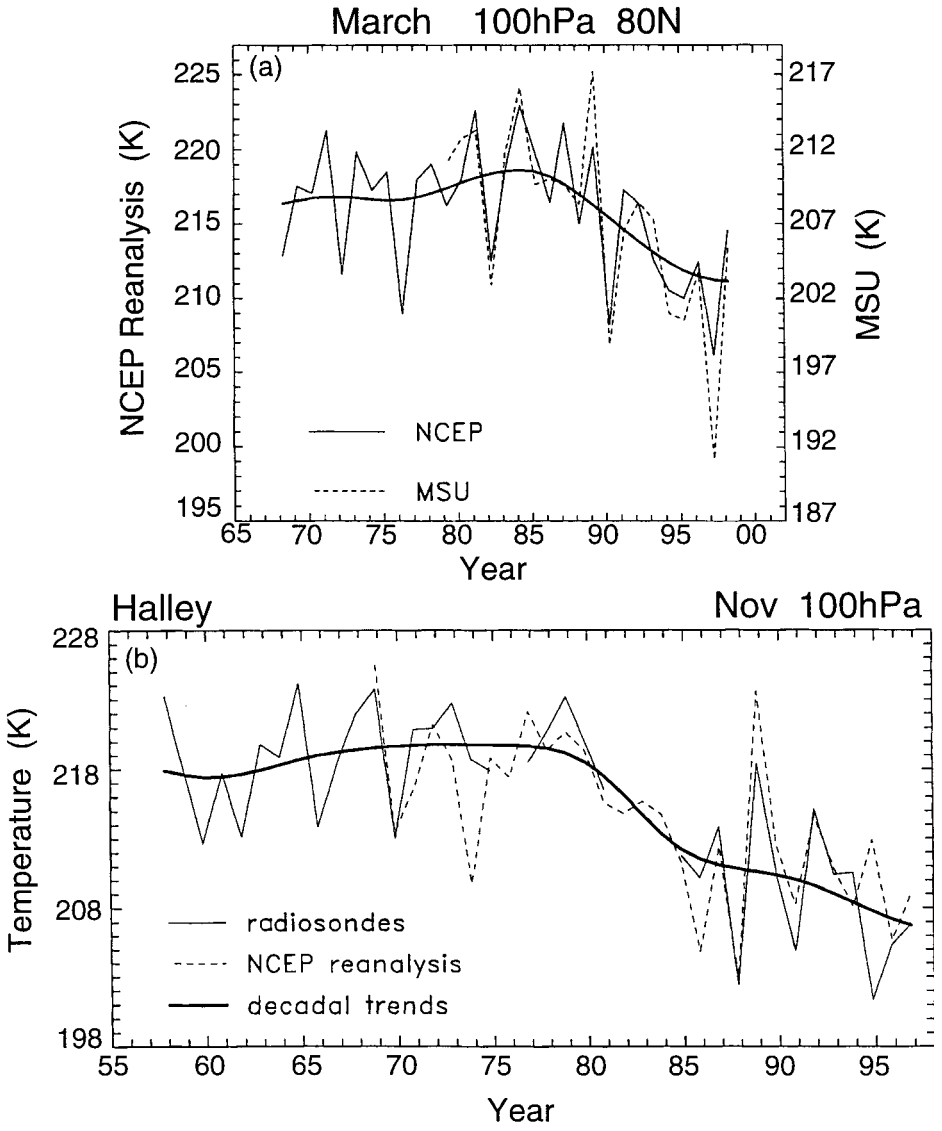

Figure 12. (a) Time series of 100-hPa zonal-mean temperatures at 80°N in March from National Centers for Environmental Prediction (NCEP) reanalyses, together with data from MSU. The smooth curve through the reanalysis data indicates the decadal-scale variation. (b) Time series of 100-hPa temperature in November at Halley Bay, Antarctica, from radiosonde data and NCEP reanalyses. The smooth curve through radiosonde data indicates the decadal-scale variation [*Randel and Wu*, 1999].

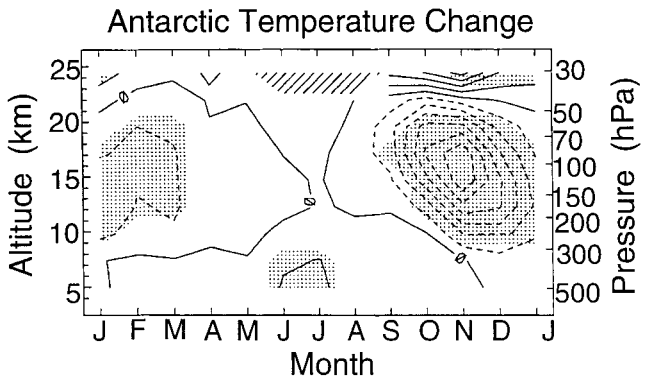

Figure 13. Altitude-month section of temperature differences over Antarctica, 1987–1996 minus 1970–1979, derived from an average of seven radiosonde stations. Dashed lines indicate cooling trends. Contour interval is 1 K. Shading denotes that the temperature differences are significantly different from natural variability [*Randel and Wu*, 1999]. There is a data-void domain at ~25 km during winter.

only a few locations around the globe, there is difficulty in ascertaining the consistency of the trend and its significance when compared against zonal-mean satellite data.

2.5.5. Uncertainties associated with the lidar record. In a pure molecular atmosphere the temperature obtained from a Rayleigh lidar is given in absolute value as a function of altitude, without any need of external calibration. However, Rayleigh lidar measurements are affected by the presence of aerosols. After a major volcanic eruption the stratospheric aerosols can reach altitudes up to nearly 40 km limiting the lower height range where the Rayleigh lidar temperature measurements can accurately be made. An accuracy of 1% is easily attained, with a principal limit for ascertaining the significance of a trend being the length of the available data set. Using the actual measurements at the Haute Provence site, it was found that the establishment of a significance in the trend at the 95% level in the upper

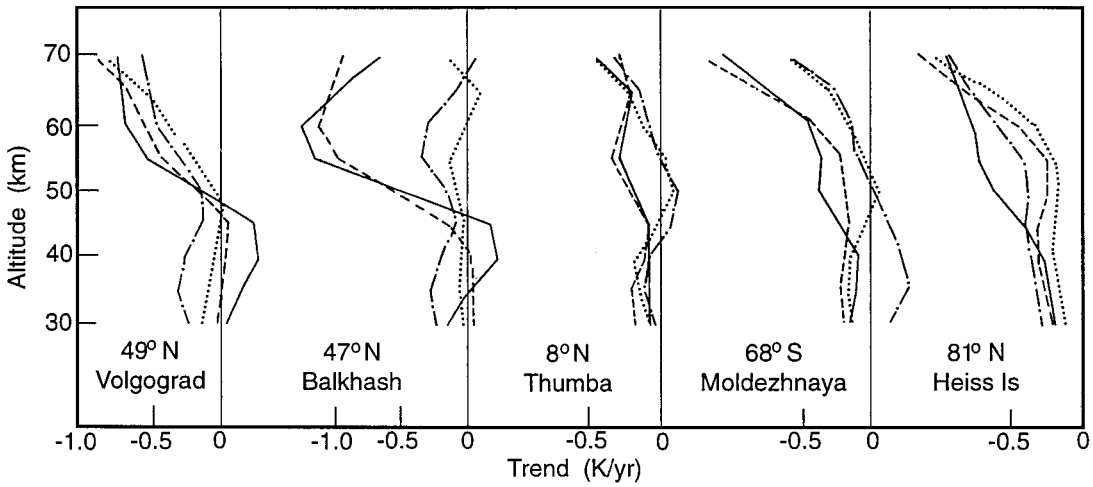

Figure 14. Seasonal rocketsonde trends (K/year) using FSU rocket data from 1972 to 1990 at five sites (see Table 2). Solid curves denote winter, dash-dotted curves denote spring, dotted curves denote summer, and dashed curves denote autumn. Adapted from *Kokin and Lysenko* [1994].

stratosphere required 20.5 years of data for summer trends and 35 years for winter trends. More years are required for the wintertime owing to the increased variability present in that season [*Keckhut et al.*, 1995]. Of course, the length of a period needed to establish statistical significance also depends on the amplitude of the signal. Compared with rocketsonde measurements, which are made at a specific time (even though it may not be the same local time for different sites), the lidar data can be made at any time during the night. This could constitute a potential source of uncertainty owing to tidal effects and may explain, in part, the large error bars observed in Figure 6. The situation can be improved by selecting data corresponding to the same local time.

2.6. Issues Concerning Variability

2.6.1. Volcanic aerosol influences. There are a number of factors that influence temperature trends in the stratosphere. Among the most significant as a short-term phenomenon is the large buildup of stratospheric aerosols following volcanic eruptions [*WMO*, 1990b, 1995]. The SAGE extinction and other satellite data [e.g., *McCormick et al.*, 1995] reveal a notable increase in stratospheric aerosol concentrations for 1–2 years following volcanic eruptions. Over the past 2 decades, such transient enhancements have come about due to eruptions of different intensities. Data from earlier ground-based observations reveal other episodes of volcanic loading of the stratosphere dating back to the 1960s. It is well understood that aerosols injected into the lower stratosphere by major volcanic eruptions result in a warming of this region of the atmosphere owing to enhanced absorption of solar radiation and the upwelling terrestrial infrared radiation [*Pollack and Ackerman*, 1983; *WMO*, 1990a; *Labitzke and McCormick*, 1992].

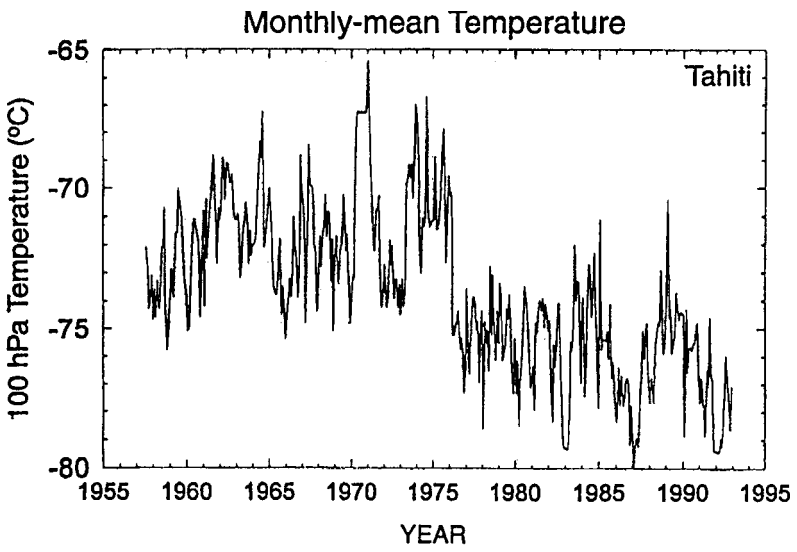

Figure 15. Monthly-mean 100-hPa raw temperatures (°C) measured by radiosondes at Tahiti. Several instrument changes occurred during this data period, but the 1976 change from Mesural 1943B with a bimetal temperature sensor, to Mesural 1944C with a thermistor, had the most obvious effect on the time series [*Gaffen*, 1996; see also *Gaffen*, 1994]. The transient in 1976 is thus inferred to be an instrumental artifact.

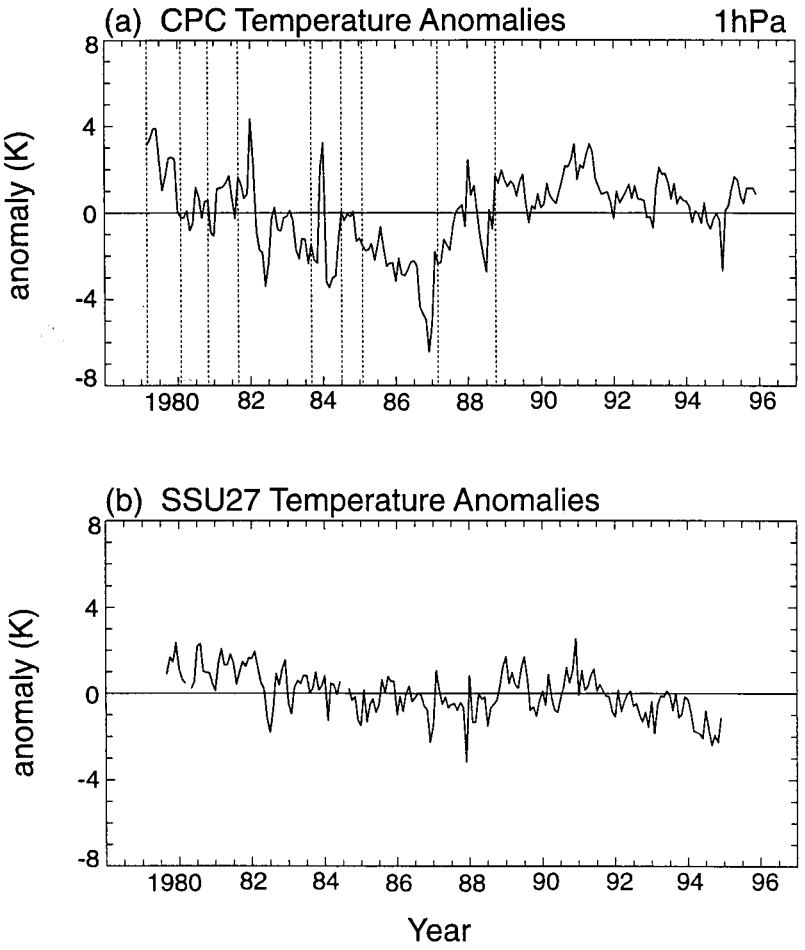

Figure 16. Time series of deseasonalized temperature anomalies at the equator for (a) CPC data at 1 hPa and (b) SSU 27 data. Vertical dashed lines in Figure 16a indicate time of changes in the operational satellites. Refer to Figures 1 and 2 concerning SSU 27.

Since the 1960s, the period when widespread and routine radiosonde observations began, three volcanos are of particular importance for climate variations: Agung (Bali, Indonesia, 1963), El Chichon (Mexico, 1982), and Mount Pinatubo (Philippines, 1991). In each one of these three cases, well-documented instrumental records indicate that the temperatures in the stratosphere increased and stayed elevated until the aerosol concentrations were depleted [*WMO*, 1990a, 1995]. All three eruptions produced somewhat similar warming characteristics [*Angell*, 1993], namely, a warming of the lower stratosphere (~15–25 km) centered in the tropics (~30°N–30°S), with a magnitude of 1–2 K (up to 3 K for Pinatubo). The warming diminishes in time, but the anomalies are observed for approximately 2 years following each eruption (Figures 2 (SSU 15X) and 3). Because the volcanic effects are episodic and clearly identifiable, their direct effect on calculation of trends is not large (the volcanic time periods simply need to be omitted prior to trend calculation, e.g., Figure 5), except as they possibly overlap with other potentially causal phenomena such as the solar cycle.

The magnitude and evolution of the transient warming agree reasonably well between the radiosonde and satellite data sets [*Labitzke and McCormick*, 1992; *Christy and Drouilhet*, 1994; *Randel and Cobb*, 1994] (Figures 3a and 3b). Relative to the analyses of *WMO* [1995], the temperature of the global-mean lower stratosphere has become progressively colder in both the radiosonde and satellite time series (Figure 2, bottom panel, and Figure 3).

In the upper stratosphere and mesospheric regions an indirect effect could be expected from the change of circulation and/or the upwelling flux arising from the lower stratospheric heating. Such an indirect effect appears to have been observed after the Pinatubo eruption in the OHP lidar data. A cooling of 1.5 K in the upper stratosphere and a warming of 5 K at 60–80 km were detected [*Keckhut et al.*, 1995]. Thus a trend analysis for these regions also requires the omission or correction of postvolcanic eruption data (e.g., such a correction was applied to the data plotted in Figure 6 by adding a term proportional to the aerosol optical thickness in the analysis technique).

2.6.2. Solar cycle. The 11-year modulation of the now well-documented UV solar flux is expected, through photochemistry, to influence stratospheric ozone and therefore stratospheric temperature. A number of investigators have attempted to identify a signature of the 11-year solar cycle in the temperature data set. The solar proxy used in most studies is the 10.7-cm radio flux which spans the longest period, even though more real-

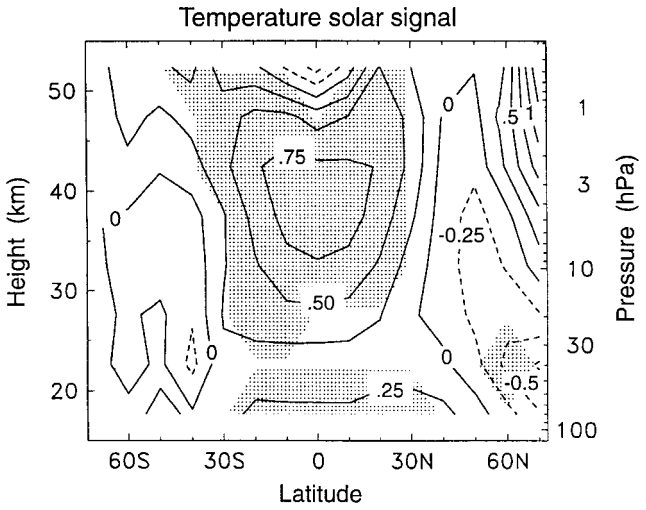

Figure 17. Latitude-altitude structure of the amplitude of the solar signal in the satellite data set, derived from regression analyses. Contour interval is 0.25 K/decade, with solid and dashed lines denoting positive and negative values, respectively. Shaded areas show 95% confidence intervals for the regression estimates. (Data courtesy of SPARC Stratospheric Temperature Trends Assessment project.)

istic proxies would be the He I line, Mg II line, or UV irradiance. However, several analyses using these different proxies justify the choice of the 10.7-cm flux [*Donnelly et al*., 1986; *Keckhut et al*., 1995].

Satellite data provide a global view of the signature due to solar variations, but the time series is relatively short. The overlap-adjusted SSU plus MSU data sets (spanning 1979–1995) exhibit a coherent temperature variation approximately in phase with the solar cycle. Figure 17 shows the vertical-latitudinal structure of the solar signal (derived via regression onto the 10.7-cm solar flux time series) using the overlap-adjusted MSU and SSU data. Even though the data set is limited to 17 years, this shows a statistically significant solar component of the order of 0.5–1.0 K throughout most of the low-latitude (30°N–30°S) stratosphere, with a maximum near 40 km. The spatial patterns show maxima in the tropics, with an approximate symmetry about the equator. A small solar response is observed in these data at the high latitudes. The 0.5- to 1-K solar signal seen in the Nash data is in reasonable agreement with results from the longer records of radiosondes or rocketsondes discussed below. At northern midlatitudes, the satellite-derived signature, which is not statistically significant, goes from slightly positive at ~17 km to slightly negative at ~25 km, with a null value at 45–50 km. This is similar to the OHP lidar record [*Keckhut et al*., 1995] and to the Volgograd rocket record [*Kokin et al*., 1990]. This alternation in the sign of the solar signature is likely due to dynamical effects [*Balachandran and Rind*, 1995]. At high latitudes, although the satellite data uncertainty is large, there is a hint of a large positive response in the mesosphere, as is observed in the Heiss Island rocket data [*Kokin et al*., 1990].

The longest time series is provided by radiosondes and rockets; even then, they barely cover at best four solar cycles. Thus, in general, there is some difficulty in establishing a firm relationship with the 11-year solar cycle. *Labitzke and van Loon* [1989] and *van Loon and Labitzke* [1990] use the Berlin meteorological analyses, beginning in 1964 and spanning the NH lower stratosphere, to isolate coherent temperature cycles in the subtropics in phase with the solar cycle. *Labitzke and van Loon* [1997] update their previous analysis and find a correlation of 0.7 with the 30-hPa geopotential height (which can be taken to imply a similar correlation with layer-mean temperature below this level). The maximum correlation occurs from North America across the Pacific to China. Using the NCEP reanalyzed global data set, *van Loon and Labitzke* [1998] show a similar solar signal manifest in the Southern Hemisphere, with higher correlations in the tropical regions.

Angell [1991b] has used radiosonde and rocketsonde data to deduce tropical and NH midlatitude solar cycle variations of approximately 0.2–0.8 K from the lower to the upper stratosphere, respectively (changes per 100 units of 10.7-cm solar flux, or approximately solar maximum minus solar minimum values). *Dunkerton and Baldwin* [1992] isolate a weak solar cycle in CPC temperatures in the NH winter lower stratosphere, using data from 1964–1991 (these analyses are based primarily on radiosonde data). Isolation of a solar cycle signal in CPC upper stratospheric temperature data beginning in 1979 is somewhat problematic, due to the spurious discontinuities introduced by satellite changes (see Figure 16, section 2.5.2). This suggests that the solar cycle variations derived from these data [e.g., *Kodera and Yamazaki*, 1990; *Hood et al*., 1993] should be treated with caution.

In their rocket data analysis, *Dunkerton et al*. [1998] found a 1.1-K response to the solar cycle for the integrated altitude range of 29–55 km (Figure 18). *Kokin et al*. [1990], *Angell* [1991b], and *Mohanakumar* [1995], using rocket data, and *Keckhut et al*. [1995], using lidar data, infer a clear solar signature in the mesosphere of +4 to 10 K per 100 units of 10.7-cm flux. On the other hand, the results obtained in the upper stratosphere and around the stratopause are different in both amplitude and sign for the different sites and are also variable with season.

From the records it thus appears that the solar cycle signature in stratospheric temperatures need not be uniform and identical all over the globe and at all altitudes. This has been manifest the work by *Labitzke and van Loon* [1997] on the horizontal scale, as well as on the vertical scale in the work by *Chanin and Keckhut* [1991], and may be attributable to the role of planetary waves (see section 3.6). An additional point to note is that the solar-induced temperature changes need not occur at the same latitudes as changes in ozone.

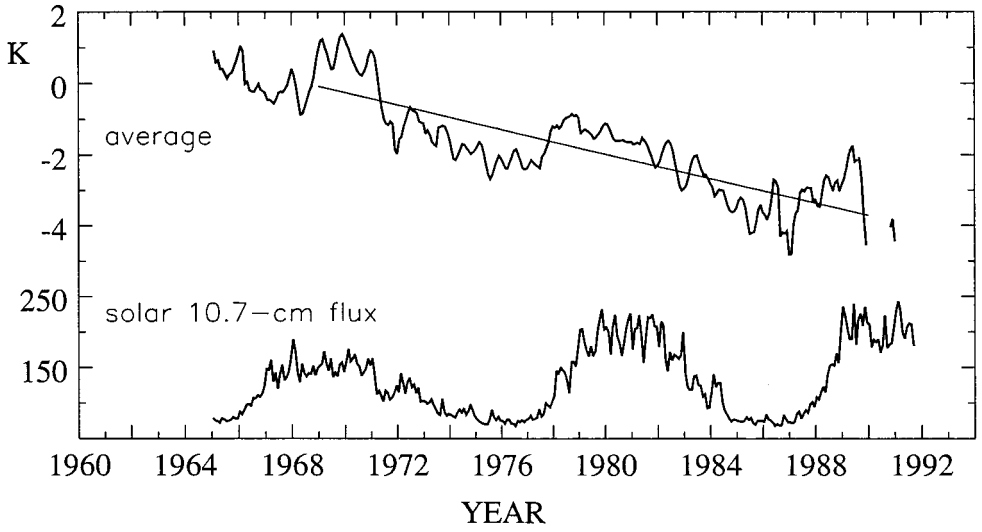

Figure 18. The top curve represents the time evolution of the mean temperature (in kelvins) for six U.S. rocket stations from 1965 to 1990, with the solid line denoting the linear trend. The bottom curve shows the solar flux at 10.7 cm [*Dunkerton et al*., 1998]. The temperature time series is suggestive of a modulation in phase with the solar cycle.

In the lower stratosphere the effect of solar variations is found to have a relatively small effect on trend calculations for time series longer than 15 years, such as those analyzed here. Regression estimates of trends neglecting a solar cycle term change by only ~10% (this sensitivity was determined by testing several of the time series analyzed here). Elsewhere in the stratosphere, the amplitude of the solar cycle signature has the potential to introduce a bias in trend estimates (especially if the number of cycles involved in the time series is small).

The determination of the amplitude and structure of the solar cycle effect may become subject to considerable uncertainty owing to the influence of volcanic events. For example, the major stratospheric warming due to volcanic aerosols (see section 2.6.1) over the past 2 decades has consisted of the El Chichon and Pinatubo eruptions, spaced coincidentally 9 years apart and thus approximately in phase with the solar cycle. Because of the possible convolution of the effects from these two independent phenomena, the trends analyses could misinterpret the volcanic signal as a solar cycle effect.

2.6.3. QBO temperature variations. Interannual variability of zonal winds and temperature in the tropical stratosphere is dominated by an approximate 2-year periodicity: the quasi-biennial oscillation (QBO). The QBO is most often characterized by downward propagating zonal wind reversals in the tropics [e.g., *Naujokat*, 1986; *Reid*, 1994], but the QBO is also prevalent in tropical temperatures (which are in thermal wind balance with the zonal winds). Aspects of the QBO in global stratospheric temperatures have been derived from radiosonde observations [*Dunkerton and Delisi*, 1985; *Labitzke and van Loon*, 1988; *Angell*, 1997] and satellite-derived data sets [*Lait et al*., 1989; *Randel and Cobb*, 1994; *Christy and Drouilhet*, 1994]. *Randel et al*. [1999] have used UKMO assimilated wind and temperature fields [*Swinbank and O'Neill*, 1994], together with overlap-adjusted SSU data, to isolate global patterns of the QBO. The results of these studies produce the following picture of the QBO in temperature:

1. Tropical QBO temperature anomalies maximize in the lower stratosphere (~20–27 km) over 10°N–10°S, with an amplitude of ±2–4 K. There is a secondary maximum in the tropical upper stratosphere (~35–45 km) of similar magnitude, approximately out of phase with the lower stratosphere maxima. The structure in temperature is qualitatively similar to the two-cell structure observed in ozone [see also *WMO*, 1999, chapter 4].

2. There is a substantial midlatitude component of the QBO in temperature, maximizing over ~20°–50° latitude and approximately out of phase with the tropical anomalies. The midlatitude patterns also exhibit maxima in the lower and upper stratosphere, which are vertically out of phase. An intriguing aspect of the midlatitude QBO is that it is seasonally synchronized, largely restricted to winter-spring of the respective hemispheres; this produces a highly asymmetric temperature pattern at any given time.

3. There is also evidence for a coupling of the QBO with the lower stratosphere polar vortex in late winter-spring of each hemisphere [*Holton and Tan*, 1980, 1982; *Lait et al*., 1989]. The polar QBO temperatures are out of phase with those in the tropics. Observational evidence for the polar QBO is less statistically significant than that in the tropics or midlatitudes, at least partly because of the high level of "natural" interannual variability in polar vortex structure. Evidence of a quasi-biennial modulation of the Southern Hemisphere stratospheric polar vortex has been presented by *Baldwin and Dunkerton* [1998b]. An interesting question arising from

recent studies [*Salby et al*., 1997; *Baldwin and Dunkerton*, 1998a] is whether the interactions between the QBO and a so-called biennial oscillation could be a factor in the observed signature of the solar cycle. It may be noted that earlier results of *Labitzke and van Loon* [1988] showed evidence of a solar signature in stratospheric temperature when the data are sorted according to the phase of the QBO. However, no physical mechanism has as yet successfully explained these results.

Because the available satellite and radiosonde data records span many observed QBO cycles, it is possible to empirically model and isolate QBO variations in temperature with a good degree of confidence. The QBO has little effect on calculated trends, although trend significance levels are increased by accurate characterization of QBO variability.

2.6.4. Planetary wave effects. The trend, solar cycle, volcanic, and QBO variations account for the majority of observed interannual temperature variability in the tropics and low latitudes. Over middle and high latitudes, there is a substantial amount of residual interannual variance, particularly during winter [e.g., *Dunkerton and Baldwin*, 1992]. This additional variance is due to natural meteorological fluctuations, in particular the presence or absence of stratospheric warming (or planetary wave) events during a particular month (a large wave event corresponds to a warm month, and vice versa). This relatively high level of natural variability of the polar vortex means that statistical significance may be possible only for somewhat larger natural or anthropogenic signals (e.g., trends due to changes in radiative species, solar, or QBO variations).

2.6.5. ENSO. El Niño–Southern Oscillation (ENSO) events are known to have a major impact on lower stratospheric temperature anomalies in the tropics, with a warming of the sea surface temperature (SST) and the increase in moist convection being accompanied by a cooling of the lower stratosphere [*Pan and Oort*, 1983; *Reid*, 1994]. This inverse relationship between tropical surface and lower stratosphere temperatures is also manifest in the long-term record [*Sun and Oort*, 1995]. Since tropical SSTs are known to have been increasing in recent decades [e.g., *Graham*, 1995], this suggests a potential contribution toward a tropical lower stratospheric cooling trend. It remains to be determined how the secular trends in the upper troposphere and lower stratosphere are quantitatively related to SST variations and trends, both in the tropical and extratropical latitudes. The ENSO phenomenon has also been linked to features in the polar stratosphere. *Hamilton* [1993] and *Baldwin and O'Sullivan* [1995] find a modest correlation between NH polar stratospheric circulation and ENSO.

2.7. Changes in Tropopause Height

Temperature changes in the upper troposphere and lower stratosphere may induce a change in the tropopause height [see *Sinha and Shine*, 1994], which may complicate the determination of temperature trends in the tropopause region. This has been suggested by *Fortuin and Kelder* [1996] in the context of radiative cooling caused by the trends in ozone and other greenhouse gases. To date, most models are unable to represent such changes, as they are much smaller than the typical vertical spacing in models. Therefore inferences have to rely entirely on the review of the available observations. Several results obtained at northern midlatitudes provide some indication of such changes, even though there is a lack of agreement on the amplitude of the effect.

An increase of the tropopause height by 150 ± 70 m (2-σ) has been found at Hohenpeissenberg over the last 30 years [*Steinbrecht et al*., 1998]. This increase is correlated with the decrease in the ozone mixing ratio in the lower stratosphere and with a tropospheric warming at 5 km of 0.7 ± 0.3 K (2-σ) since 1967 (Figure 19). Further, the tropopause height over central Europe appears to have increased by about 300 m over the last 20 years [*Bojkov and Fioletov*, 1997]. For the tropics a preliminary analysis of data from Truk (7.5°N, 151.8°E) for the period 1965–1994 (G. Reid, personal communication, 1998) finds no detectable change in the temperature but a significant change in height, consistent with a warming of the troposphere (7.7 m/yr, or 230 m in 30 years). These results have yet to be extended to include other stations and have not yet accounted for ENSO and volcanic influences. On a global scale, on the basis of a study of the tropopause surfaces in the European Centre for Medium-Range Weather Forecasting reanalyses data, *Hoinka* [1998] infers that the sign of the trend could vary depending on the latitude and longitude. Clearly, this subject warrants a full scrutiny on all spatial scales in order to quantify rigorously the increase in the tropopause height over the past decades.

3. MODEL SIMULATIONS

3.1. Background

In this section we discuss results from model investigations that have analyzed the effects upon stratospheric temperature trends and variations due to various natural and anthropogenic factors. We focus on the changes in the lower stratospheric region and also discuss the vertical profile of the modeled trends from the lower to upper stratosphere. Where possible and relevant, we compare available model results with observations.

Numerical models based on a fundamental understanding of radiative, dynamical, and chemical processes constitute essential tools for understanding the effects of different mechanisms on temperature trends and variability in the stratosphere and for interpreting observed temperature changes in terms of specific processes. The numerical models used thus far have attempted to include, to varying degrees, the relevant components of the climate system that could influence stratospheric temperatures. The models also attempt to capture the

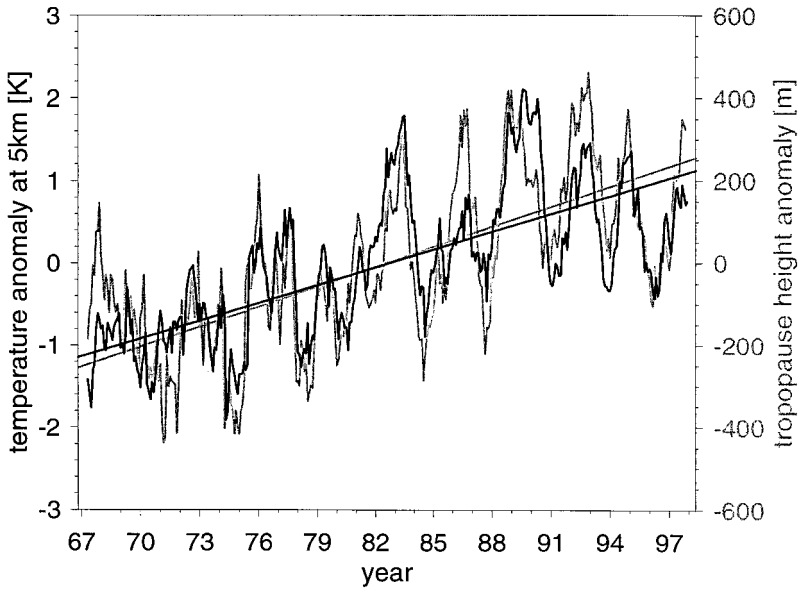

Figure 19. Change in tropopause height compared with the change in the 5-km temperature at Hohenpeissenberg. The 5-km temperature (solid curve) shows a trend of 0.7 K/decade, while the tropopause height (shaded curve) shows a trend of 150 m/decade [*Steinbrecht et al.*, 1998]. The linear trends are indicated by the appropriate lines drawn through the two time series.

important links between the stratosphere, the troposphere, and the mesosphere.

It is well recognized that the global, annual-mean thermal profile in the stratosphere represents a balance between solar radiative heating and longwave radiative heating and cooling, involving the effects of mainly ozone, carbon dioxide, water vapor, methane, nitrous oxide, halocarbons, and aerosols [see *Goody and Yung*, 1989, chapter 9, and references therein]. In the context of the general global stratosphere, dynamical effects also become a factor in determining the thermal profile. Since the late 1950s, with increasing knowledge of trace species' concentration changes and their optical properties, numerical models have played a significant role in highlighting the potential roles of various constituents and the different mechanisms operating in the stratosphere. For example, *WMO* [1986, 1990a] concluded that changes in the concentrations of trace gases and aerosols could substantially perturb the radiative balance of the contemporary stratosphere and thereby affect its thermal state.

Early numerical models were developed as one-dimensional ones on the basis that the global, annual-mean stratosphere is in radiative equilibrium. Together with the assumption of a radiative-convective equilibrium in the troposphere, this led to the so-called one-dimensional radiative-convective models (1-D RCMs), which have been widely employed to study effects due to trace gas perturbations [*WMO*, 1986]. The RCMs represent the atmosphere as a single global-mean vertical column [*Manabe and Wetherald*, 1967; *Ramanathan*, 1981]. The temperatures at the surface and in the troposphere are determined by radiation and by some representation of the processes that determine the vertical advection of heat by fluid motions (normally via a convection scheme). In the stratosphere the thermal state determined is a balance between absorbed solar radiation and absorbed and emitted thermal infrared radiation. Radiative-convective models can also include chemical processes to represent feedbacks between temperature and chemical constituents [e.g., *Bruhl and Crutzen*, 1988].

A variation of the RCMs is the "fixed dynamical heating," or FDH, model [*Fels and Kaplan*, 1975; *Ramanathan and Dickinson*, 1979; *Fels et al.*, 1980]. The FDH models [e.g., *WMO*, 1992] hold the tropospheric temperature, humidity, and cloud fields fixed and allow for changes in the stratospheric temperature in response to changes in radiatively active species. In the unperturbed state the radiative heating is exactly balanced by the dynamical heating at each height and latitude. If the concentration of a radiatively active constituent is altered, then the radiative heating field is altered. It is assumed that the dynamical heating remains unchanged and that the temperature field adjusts in response to the perturbation. In turn, this alters the radiative heating field such that it again exactly balances the dynamical field. The timescale for adjustment to a specific perturbation typically varies of the order of a few months in the lower stratosphere to a few days in the upper stratosphere.

The application of the RCM and FDH model concepts for understanding stratospheric temperature changes has evolved with time [see *WMO*, 1990a, 1992, 1995]. Both types of models have been extensively used for gaining perspectives into the thermal effects due to the observed and projected changes in radiatively active trace gases. These simple models have important limitations. In particular, the FDH models can only predict temperature changes at any location due to constituent changes occurring there; that is, the response is entirely localized within that particular stratospheric column. As will be seen later, changes in the circulation as a consequence of a radiative perturbation at any latitude can

influence temperature changes at other latitudes. Hence it should not be expected that FDH models can realistically simulate features such as the latitudinal and monthly variation of trends. Nonetheless, these simple models remain useful in revealing reasonable, first-order solutions of the problem.

There has been a steady progression from the simple RCMs and FDH models to the three-dimensional general circulation model (GCM) (see *WMO* [1986] for an early discussion of models used for studying the stratosphere), which seeks to represent the radiative-dynamical (and even chemical in some instances) interactions in their entirety. Such models have representations of radiative processes that may be less complete and accurate than in the 1-D models but provide the best means of mimicking the real atmosphere. One useful aspect of the FDH simulations is that their comparison vis-a-vis a GCM simulation enables a quantitative distinction to be made between the radiative and radiative-dynamical responses of the stratosphere to a specific perturbation.

The perturbations introduced by the changes in the radiative constituents lead, in general, to an alteration of the stratospheric circulation. The resulting radiative-dynamical response involves characteristic changes in the meridional gradient of the stratospheric temperatures. An important role in determining the latitudinal structure of stratospheric temperatures is played by planetary waves. The potential response to different types of meridional radiative heating perturbations (discussed below) can be viewed from a simple, quasi-geostrophic standpoint [e.g., *Rind et al*., 1992; *Balachandran and Rind*, 1995; *Kodera and Yamazaki*, 1994; *Kodera*, 1994]. Especially in the Northern Hemisphere and in a general qualitative sense, an increase in the equator-to-pole temperature gradient caused by a radiative perturbation tends to be associated with a strengthening of the polar jet. With planetary waves being refracted equatorward, a convergence of this planetary wave energy occurs at lower latitudes, causing a degree of positive feedback that tends to make the polar regions even colder and the jet stronger. Although model simulations of the stratospheric dynamical processes have advanced considerably over the past 2 decades, quantitative aspects, in particular the temperature behavior at the high latitudes and the polar response to radiative perturbations, require substantial progress. In general, the simulated temperature changes at the different latitudes, and their statistical significance, depend on the type and magnitude of perturbation and the natural dynamical variability of the model, in addition to being critically dependent on model parameterizations.

3.2. Well-Mixed Greenhouse Gases

While increases in well-mixed greenhouse gases (carbon dioxide, methane, nitrous oxide, halocarbons) warm the surface, their effects on the lower stratospheric temperature vary, primarily because of the location of the absorption bands of each of the species and the radiative characteristics of the atmosphere in those bands. The essential radiative processes are that, first, an increase in greenhouse gas concentration enhances the thermal infrared emissivity of a layer in the stratosphere; hence, if the radiation absorbed by this layer remains fixed and other factors remain the same, then, to achieve equilibrium, the same amount of energy has to be emitted at a lower temperature, and the layer cools. Second, an increase in emissivity due to increased concentration also implies an increase in the thermal infrared absorptivity; a larger amount of the radiation emitted by the troposphere will be absorbed in the stratosphere, leading to a warming tendency. Note that the upwelling/downwelling radiation reaching the lower stratosphere is itself dependent on the infrared opacity and the thermal state of the troposphere or middle and upper stratosphere. The net result is a balance involving these processes [*Ramanathan et al*., 1985; *Ramaswamy and Bowen*, 1994; *Pinnock et al*., 1995].

For carbon dioxide the main 15-μm band is saturated over quite short distances. Hence the upwelling radiation reaching the lower stratosphere originates from the cold upper troposphere. When the CO_2 concentration is increased, the increase in absorbed radiation is quite small and the effect of the increased emission dominates, leading to a cooling at all heights in the stratosphere. For gases such as the CFCs, their absorption bands are generally in the 8- to 13-μm "atmospheric window" [*WMO*, 1986], and much of the upwelling radiation originates from the warm lower troposphere. In this case the increase in the absorbed energy is generally greater than the increase in emitted energy, and a warming of the lower stratosphere results (although there are exceptions to this case if the halocarbon absorption is in a region of already large atmospheric absorption [see *Pinnock et al*., 1995]). Methane and nitrous oxide are midway between these two regimes so that an increase in concentration has little effect on the lower stratospheric temperature, as the increased absorption and increased emission almost balance. In the upper stratosphere, increases in all well-mixed gases lead to a cooling because the increased emission effect becomes greater than that due to the increased absorption.

One significant consequence of this differing behavior concerns the common use of "equivalent CO_2" in climate simulations. Equivalent CO_2 is the amount of CO_2 used in a model calculation that results in the same radiative forcing of the surface-troposphere system as a mixture of greenhouse gases [see, e.g., *IPCC*, 1995]. Although the equivalence concept works reasonably well for tropospheric climate change [*IPCC*, 1995], it does not work well for stratospheric temperature changes because increases in different greenhouse gases cause different stratospheric temperature responses, thus requiring the consideration of each gas explicitly. In fact, some trace gases warm, not cool, like CO_2, the lower stratospheric region near the tropopause [*WMO*, 1986]. Even if all gases were to cause an effect of the same sign

in the stratosphere, an equivalence with respect to CO_2 that holds for the troposphere need not be true for the stratosphere. In general, the use of an equivalent CO_2 concentration overestimates the actual stratospheric cooling by the non-CO_2 well-mixed greenhouse gases. For realistic mixtures of greenhouse gases, the stratospheric cooling is approximately half of that calculated using equivalent CO_2 [*Wang et al*., 1991; *Shine*, 1993].

The mechanism by which temperatures change in the stratosphere as a result of constituent changes is twofold. First, the change in the constituent leads to a change in the radiative heating field, even if all other conditions remain fixed. The timescale for the adjustment of stratospheric temperatures is less than about 100 days, which is much faster than the decadal (or multidecadal) timescale response of surface and lower tropospheric temperatures. This "fast" process of stratospheric temperature change is then modified by a second process as the troposphere comes into a new equilibrium. Thus, for example, an increase in CO_2 leads to an initial cooling of the stratosphere. As the surface and troposphere warm due to CO_2 increase, the increased emission from the surface-troposphere system contributes a warming tendency in the lower stratosphere. *Forster et al*. [1997] have shown that this second process leads to a significant reduction of the initial cooling in the lowest portion of the stratosphere for CO_2, whereas in the case of CFCs, it leads to significant heating. When increases in all of the well-mixed gases over the last century are considered in a 1-D RCM, the overall result for the lower stratosphere is one of an initial radiative cooling, arising due to an increase in tropospheric opacity that reduces the upwelling longwave flux reaching the stratosphere and its absorption there; there is also an increased emission from the stratosphere. The equilibrium result is a decrease in lower stratospheric temperatures, with an increased flux divergence of the downward longwave beam in the now colder lower stratosphere balancing the increase in the flux convergence of the upward beam due to tropospheric warming [*Ramaswamy and Bowen*, 1994]. Thus the actual temperature change in the lower stratosphere depends on the degree to which the surface-troposphere system equilibrates in response to the changes in the radiative constituents.

GCMs have been used to determine the changes in stratospheric climate due to changes in the well-mixed greenhouse gases. *Fels et al*. [1980] obtained a cooling of ~10 K at 50 km for a doubling of CO_2. They also found that FDH results for CO_2 doubling agreed reasonably well with the GCM simulations. Subsequently, other GCM experiments of a similar nature have also computed a substantial cooling of the stratosphere [e.g., *Kiehl and Boville*, 1988; *Rind et al*., 1990; *Wang et al*., 1991]. However, the degree of cooling, especially in the polar stratospheres, is model-dependent because of differences in how physical processes are parameterized in the models [*Mahlman*, 1992; *Shindell et al*., 1998]. GCMs that are used to determine changes in surface and tropospheric climates also simulate the stratospheric changes (e.g., those discussed in chapter 8 of *IPCC* [1996]). However, several such models have a coarse vertical resolution in the stratosphere that inhibits performing a reliable trends assessment using their results at those altitudes. Nonetheless, all models predict a general cooling of the stratosphere due to CO_2 increases. *WMO* [1990a] estimated a cooling of 0.2–0.3 K at 2 hPa and 0.15 K at 10 hPa between 1979–1980 and 1985–1986 due to CO_2 increases alone.

A number of 1-D radiative-photochemical model predictions of cooling due to increased concentrations of greenhouse gases (CO_2, N_2O, CH_4, and the CFCs) were reviewed by *WMO* [1990a]. These models included the temperature feedbacks due to the increased trace gas concentrations upon ozone concentration. Our understanding of chemistry at that time was such that the important feedbacks were deemed to occur in the upper stratosphere. Briefly, the features of these calculations were that peak coolings were estimated to occur between 40 and 50 km. Simulations indicate that the mean cooling rate was about 1.5 K/decade for the period since 1960, about 1 K/decade for the period since 1940, and about 0.4 K/decade for the period from 1850. There was more spread in model results at 24 km ranging from almost zero to −0.3 K/decade for the period since 1960.

Both 1-D RCMs [e.g., *Ramanathan et al*., 1985] and 3-D GCMs [e.g., *Wang et al*., 1991] indicate that the presence of the well-mixed non-CO_2 trace gases can be expected to yield a slight warming of the lower stratosphere. *Ramaswamy et al*. [1996] have compared the 50- to 100-hPa temperature change for different time periods for CO_2 alone and for a realistic mixture of gases (Figure 20) using a 1-D RCM. For the period 1765–1990 the temperature change due to all gases is less than 50% of the effect due to CO_2 alone. For more recent periods, for example, since ~1960, when the relative importance of other gases, and in particular that of the CFCs, has grown [*Ramanathan et al*., 1985], the temperature change due to all well-mixed greenhouse gases not only is less than that due to CO_2 alone, but also becomes quite small in absolute value. The overall cooling effect in the lower stratosphere due to increases in the well-mixed greenhouse gases is to be contrasted with their warming effect on the surface [*IPCC*, 1996].

The vertical profile of temperature change in the stratosphere due to recent changes in the well-mixed gases suggests that there is a general increase of the cooling with height [see *WMO*, 1992, Figure 7-7]. This is further exemplified by *Forster and Shine* [1997], who show that the FDH-computed increases in the well-mixed greenhouse gases over the decade of the 1980s would yield an increasing cooling with height at 40°N (~0.7 K/decade at 35 km; Figure 21). The FDH model of *Ramaswamy et al*. [1992] considered the well-mixed greenhouse gas increases over the 1979–1990 period and yields an annual-mean cooling that increases with height between ~20 and 50 km and that is fairly uniform

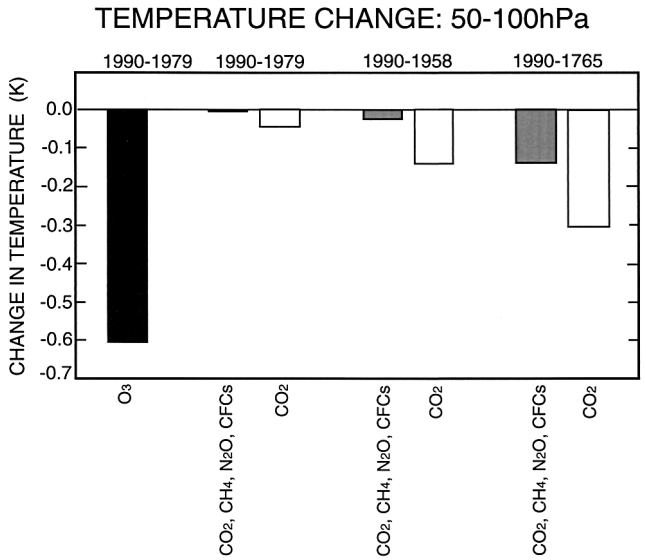

Figure 20. Computed global- and annual-mean temperature changes in the ~50- to 100-hPa (~16–21 km) lower stratospheric region due to various gases. The result for the ozone depletion corresponds to the 1979–1990 losses and is computed using a general circulation model (GCM). The results for CO_2 alone, and for all the well-mixed greenhouse gases together (namely, CO_2, CH_4, N_2O, and CFCs) are computed using a one-dimensional radiative connective model for three different periods. Reprinted from *Ramaswamy et al*. [1996] with permission from *Nature*. Copyright 1996 Macmillan Magazines Ltd.

throughout the globe (Figure 22), with a peak cooling of ~1 K/decade occurring in the tropics at ~50 km. The combined well-mixed greenhouse gases' effect yields a slight but characteristic warming near the tropopause, notably in the tropical regions (Figure 22). The recent GCM simulation of *Forster and Shine* [1999] substantiates the features emerging from the FDH calculations.

3.3. Stratospheric Ozone

3.3.1. Lower stratosphere. Over the past decade or more, much of the work on stratospheric temperature trends has focused on the effects due to lower stratospheric ozone change, following the realization of the large ozone loss trends in this region, as well as the accumulating evidence for substantial temperature changes in this region [*WMO*, 1990b, 1992, 1995]. In particular, the large Antarctic springtime ozone losses were the first to be examined for their potential temperature effects. Subsequently, investigations have been extended to examine the changes initiated by ozone depletion in the global lower stratosphere.

As a general demonstration of the sensitivity of the global lower stratosphere to changes in ozone, the change in lower stratospheric temperatures when the entire ozone in the 70- to 250-hPa region is removed results in temperature decreases of up to about 4 K (Figure 23). The region in the vicinity of the tropopause is most substantially affected, consistent with the known radiative sensitivity and large radiative damping time of this region [*Fels*, 1982; *Kiehl and Solomon*, 1986]. Although this GCM had a low vertical resolution, other models with improved vertical resolution also yield a cooling, albeit with a larger magnitude [e.g., *Rind and Lonergan*, 1995].

With regard to actual decadal trends, *Miller et al*. [1992] estimated a cooling of the global lower stratosphere of about 0.3 K/decade over the 1970–1986 period based on radiosonde observations. By performing a calculation of temperature changes using observed ozone trends, they inferred a substantial role due to ozone losses in the observed temperature trend. Since ozone changes vary greatly with latitude, there is a need to proceed beyond global means and perform model calculations which resolve the latitudinal variations. Locally, the stratosphere is not in radiative equilibrium, and the temperature is determined by both radiative and dynamical processes. However, by considering the stratosphere to be in a local radiative-dynamical equilibrium, with the dynamical heating rates fixed over some specific timescale (e.g., season), the FDH concept in effect can be extended to derive the local columnar temperature changes [see *Ramanathan and Dickinson*, 1979]. *Shine* [1986] demonstrated that a large cooling would occur in the Antarctic winter/spring lower stratosphere owing to the "ozone hole."

McCormack and Hood [1994] presented the first attempt to match the observed seasonal and latitudinal variation of lower stratospheric temperature with that predicted by an FDH model using imposed ozone changes based on observations. The resemblance between the size and pattern of the model temperature changes, with peak changes in the winter/spring of northern midlatitudes and the spring of southern high latitudes, and MSU satellite observations [*Christy and Drouilhet*, 1994; *Randel and Cobb*, 1994] was encouraging. As will be discussed below, this work has been taken further by using GCMs, which strengthens the model-observation comparisons.

One particular item of interest in the case of FDH calculations [e.g., *McCormack and Hood*, 1994] is that the peak cooling in the Antarctic springtime tends to occur about 1 month earlier than in the observations. This occurs because the standard FDH approximation does not account for the time duration over which the perturbation in the constituent (in this case ozone) persists. In the Antarctic springtime, typical radiative timescales are in excess of a month and yet the timescale of the most marked ozone change is only about a month. Hence the atmosphere does not have time to fully equilibrate to the ozone-induced radiative perturbation [*Shine*, 1986]; the standard FDH approximation does not account for this and assumes that the temperature adjustment occurs essentially instantaneously. A modified FDH approach (termed the seasonally evolving FDH, or

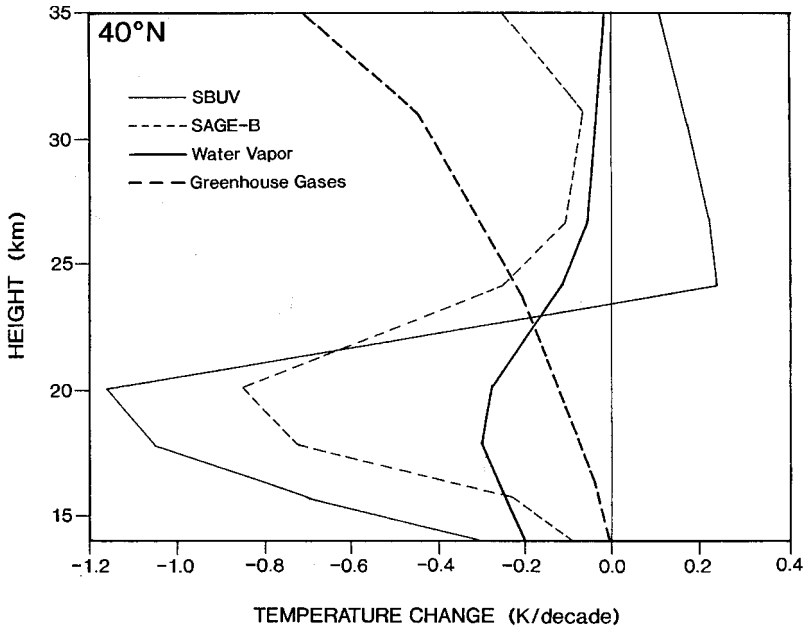

Figure 21. Vertical profile (~15–35 km) of the fixed dynamical heating (FDH) computed annual-mean temperature change during the 1980s (normalized to indicate a decadal change) at 40°N due to changes in the concentrations of various stratospheric species. "Greenhouse gases" denotes well-mixed greenhouse gases; "SBUV" refers to calculation which considers the ozone column loss using solar backscattered ultraviolet satellite trends; the "SAGE-B" calculation uses the vertical profile of ozone change observed by the Stratospheric Aerosol and Gas Experiment satellite; "water vapor" refers to the decadal change in water vapor reported by *Oltmans and Hoffman* [1995] at a single location. Adapted from *Forster and Shine* [1997].

SEFDH) has been formulated by *Forster et al.* [1997] which accounts for the time duration of the perturbation. The SEFDH result is obtained by time-marching the radiation calculations through the seasons. Using seasonally varying ozone changes and comparing the effects due to the FDH and SEFDH methods, *Forster et al.* [1997] find that the maximum cooling in the FDH occurs earlier in the austral spring and is significantly larger than the SEFDH-derived maximum cooling (Figure 24). The FDH model does not retain a "memory" of perturbations during other times of year; thus an ozone loss occurring in October has no effect on temperatures at other times of year. In contrast, the SEFDH model retains a memory of the radiative perturbations, with an increased cooling persisting from late spring to late summer, owing to the model temperatures not yet having recovered from the large springtime ozone loss.

Early GCM works investigating the effects of ozone depletion did so assuming uniform stratospheric ozone losses, with a view toward diagnosing the first-order radiative-dynamical response of the stratosphere [*Fels et al.*, 1980; *Kiehl and Boville*, 1988]. Although the depletion profiles employed were idealized and do not exactly represent those observed subsequently in the lower stratosphere, these studies have been illustrative in highlighting the manner of the stratospheric dynamical response to ozone losses. *Christiansen et al.* [1997] have further examined the nature of the stratospheric response and climate sensitivity to idealized ozone perturbations.

With the steady buildup of knowledge since the early to middle 1980s of the spatial and temporal distribution of ozone losses in the lower stratosphere, GCM experiments of two types have been carried out to determine

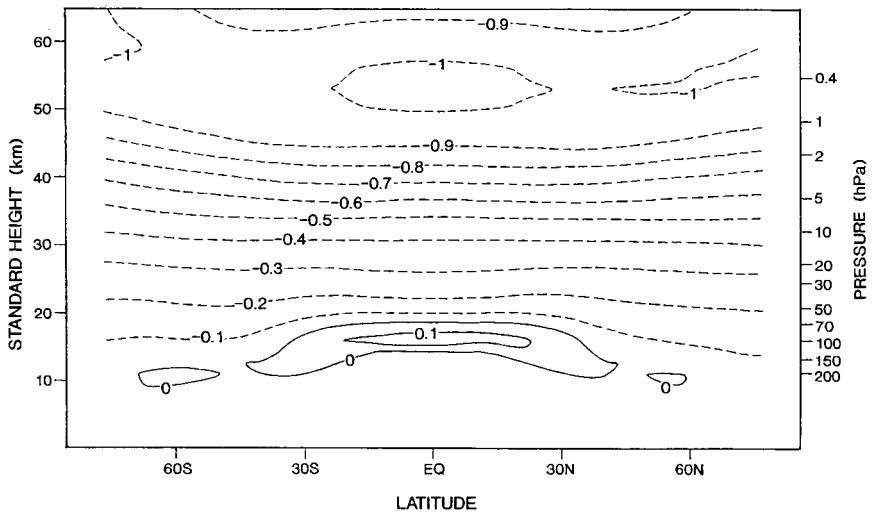

Figure 22. Vertical profile of the zonally and annually averaged temperature change (in kelvins) from the lower to upper stratosphere due to the 1979–1990 changes in the well-mixed greenhouse gases. Solid and dashed lines denote positive and negative values, respectively. (The results are from the FDH model used by *Ramaswamy et al.* [1992].)

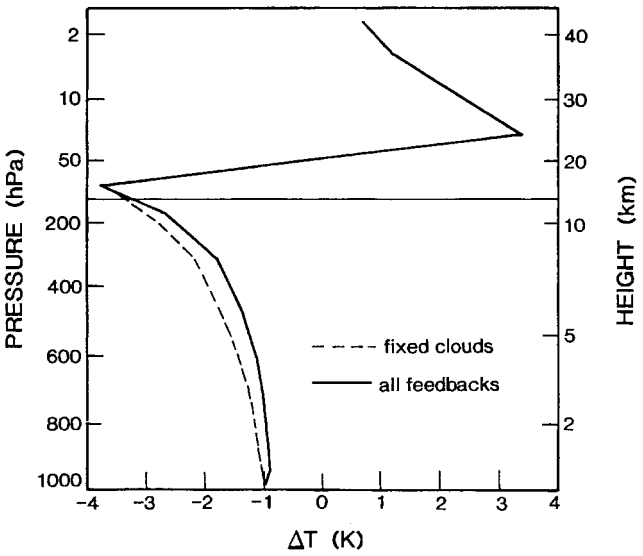

Figure 23. GCM-computed, global- and annual-mean temperature change in the atmosphere due to a complete loss of ozone between 70 and 250 hPa. Results are shown without consideration (dashed curve) and with consideration (solid curve) of cloud feedbacks. The horizontal line denotes the location of the model's tropopause. Adapted from *Hansen et al*. [1997a].

the resulting temperature changes in the stratosphere. One type of investigation concerns attempts to simulate the interactive radiative-chemistry-dynamical changes due to ozone losses in the Antarctic polar region during springtime. *Cariolle et al*. [1990] and *Prather et al*. [1990] found a substantial lower stratospheric cooling during the duration of the ozone hole. From multiple-year GCM integrations, *Mahlman et al*. [1994] found a statistically significant cooling in the Antarctic spring due to the ozone loss. They also found a significant warming of the altitude region above the altitudes of ozone loss, consistent with the observations [*Randel*, 1988] (Figures 13 and 14). Recent studies have extended the interactive simulations to the Arctic region as well. The stratosphere can be expected to be cooler owing to both long-term CO_2 increases and ozone decreases [*Austin et al*., 1992; *WMO*, 1999]. This raises the possibility of a strong positive feedback effect involving ozone depletion and colder stratospheric temperatures in the Arctic in the future. The GCM results of *Shindell et al*. [1998] demonstrate the sensitivity of the polar springtime temperatures to greenhouse gas increases and the feedback effect caused by ozone losses. The magnitude and statistical significance of the effects in the winter/spring polar stratosphere are subject to details of model representations of various physical processes and the internal dynamical variability of the climate system.

Another type of GCM investigation consists of imposing the observed ozone losses and then determining the GCM response, without any considerations of the chemical and dynamical processes affecting ozone distributions. Early studies began with investigations of the Antarctic springtime lower stratosphere owing to the large observed losses. A substantial lead-in to the 3-D aspects was provided by the 2-D study of *Chipperfield and Pyle* [1988]. They found a large cooling (>9 K) at ~70 hPa during October, similar to the FDH result [*Shine*, 1986]. In addition, they found a warming (up to ~6 K) in the upper stratosphere. The GCM simulation of *Kiehl et al*. [1988] yielded a large cooling (~5 K) by October's end, which further substantiated the FDH inference. This GCM study also found a warming in the upper stratosphere (up to ~4 K at 10 hPa).

Employing the observed global lower stratospheric ozone depletion, *Hansen et al*. [1997b, 1998] demonstrate a good agreement in the magnitude of the GCM-simulated cooling of the global, annual-mean lower stratosphere with the observed MSU satellite and radiosonde temperature trends (Figure 25). This study along with others also indicates that the cooling due to ozone loss overwhelms the temperature change resulting from changes in concentration of the well-mixed greenhouse

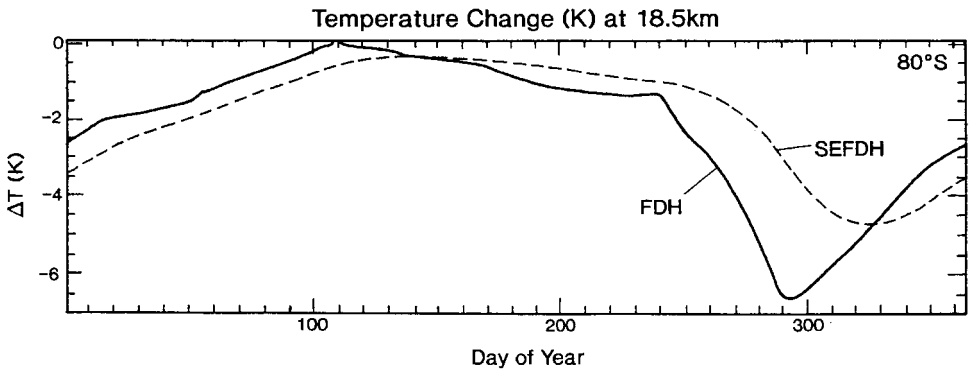

Figure 24. Modeled evolution of temperature changes in the lower stratosphere (80°S) using two different assumptions. FDH denotes fixed dynamical heating, while SEFDH denotes seasonally evolving fixed dynamical heating calculations. Note the shift in the temperature change to a later time in the year in the case of SEFDH. Adapted from *Forster et al*. [1997].

gases in the 50- to 100-hPa (~16–21 km) region (see Figures 20, 21, and 25).

The differences between FDH and GCM simulations of the effects of ozone losses have been investigated by *Fels et al*. [1980] and *Kiehl and Boville* [1988] using idealized stratospheric ozone perturbations. For annual-mean model simulations, *Fels et al*. [1980] concluded that the FDH response to uniform percentage reductions tended to be comparable to the GCM solutions, except at the tropical tropopause and in the tropical mesosphere. For "perpetual January" simulations, *Kiehl and Boville* [1988] found that the uniform reduction experiments were not well represented by the FDH calculations. However, more realistic ozone scenarios in which the losses increase from the equator to the poles yielded FDH results comparable to the GCM. This point is substantiated by the perpetual January simulations of *Christiansen et al*. [1997], who performed uniform ozone reduction and large lower stratospheric depletion experiments. The main dynamical effect in their perturbation experiments was a weakening of the diabatic meridional circulation accompanied by a general latitudinal smoothing of the stratospheric temperature response. However, for an "ozone hole" type perturbation, the latitudinally uniform temperature response occurs only in the lower stratosphere. In another model study of the impacts of a global ozone depletion between 200 and 50 hPa, *Rind and Lonergan* [1995] note that because the latitudinal temperature gradient changes sign with altitude in the stratosphere, so does the planetary wave refraction and hence the residual circulation intensity. Since the latitudinal gradient decreases in the lower stratosphere, poleward refraction leads to an increased residual circulation; by the middle stratosphere the latitudinal gradient increases, and equatorward propagation leads to a decrease in the residual circulation. Thus, in this study, the residual circulation change serves to exaggerate the latitudinal gradient response.

Using the satellite-observed global lower stratospheric ozone losses over the ~1979–1990 period (i.e., just prior to the Pinatubo volcanic eruption), a comparison of the resulting radiative and radiative-dynamical solutions for the stratospheric temperature changes can be obtained. This is illustrated by comparing the results of the FDH and GCM simulations performed by *Ramaswamy et al*. [1992] and *Ramaswamy et al*. [1996], respectively, using an identical model framework (Figure 26). This comparison delineates the role of dynamical influences on the temperature changes caused by the observed ozone depletion. The GCM result, like the FDH, indicates a cooling of the lower stratosphere. However, there are distinct differences due to dynamical changes. In the middle to high southern latitudes, there is less cooling in the GCM. In the Northern Hemisphere the midlatitudes are less cold in the GCM, but the high latitudes are more so relative to the FDH result, a consequence of the dynamical changes in the model. In the GCM, there is a cooling even in those regions where there are no ozone losses imposed, for example, in the lower stratosphere equatorward of 15° [see also *Forster and Shine*, 1999]. A warming occurs above the region of cooling, particularly noticeable in the Southern Hemisphere, similar to the results obtained by other GCM studies [*Kiehl et al*., 1988; *Mahlman et al*., 1994; *Shindell et al*., 1998; *Forster and Shine*, 1999]. The dynamical changes [see also *Mahlman et al*., 1994] consist of an induced net rising motion in the tropics and a compressional heating of the middle stratosphere at the higher latitudes. The annual-mean response is statistically significant between ~13 and 21 km in the ~20° to 50° latitude belt [*Ramaswamy et al*., 1996]. The changes at high latitudes (>60°) fail the significance test because of large interannual variability in those regions. The warming above the lower stratospheric regions in both hemispheres is reasonably similar to observations [*Randel*, 1988] (Figures 13 and 14). On the basis of the GCM-observation comparisons, a principal factor for the observed warming is the radiative-dynamical feedback associated with the ozone depletion in the lower stratosphere.

The zonal-mean patterns of GCM-simulated lower stratospheric temperature change due to imposed ozone losses correspond well with observed changes [*Hansen et al*., 1993]. In a study analogous to the FDH model-observation comparison discussed earlier, *Ramaswamy et al*. [1996] have compared the latitude-month trend pattern of the decadal (~1979–1990 period) temperature change and its statistical significance, as simulated by a GCM (Figure 27a) in the altitude region of the observed lower stratospheric ozone change (tropopause to ~7 km above), with that derived from MSU satellite [*Spencer and Christy*, 1993] observations (Figure 27b) of the lower stratosphere for the same period [*Randel and Cobb*, 1994]. The match of the latitudinal-month pattern of cooling with observations bears a fair resemblance to the FDH-based study of *McCormack and Hood* [1994]. This inference is further substantiated by another GCM study [*Forster and Shine*, 1999]. In the midlatitudes, both Figures 29a and 29b illustrate a cooling from approximately January to October in the Northern Hemisphere and from approximately September to July in the Southern Hemisphere. The cooling in the midlatitudes of the Northern Hemisphere from approximately December to July, and in the Southern Hemisphere from approximately December to May, are statistically significant in both model and observation. Comparing with Figure 11, it is apparent that the observed space-time domain of statistically significant cooling is also dependent on the end year chosen for the analysis. Near the poles, both the simulation and observation exhibit a relatively large magnitude of cooling during winter and spring. The simulated cooling in the Antarctic is highly significant during the austral spring (the period of the ozone hole), consistent with observations. The springtime cooling in the Arctic does not show a high significance, owing to a large degree of dynamical variability. The simulated

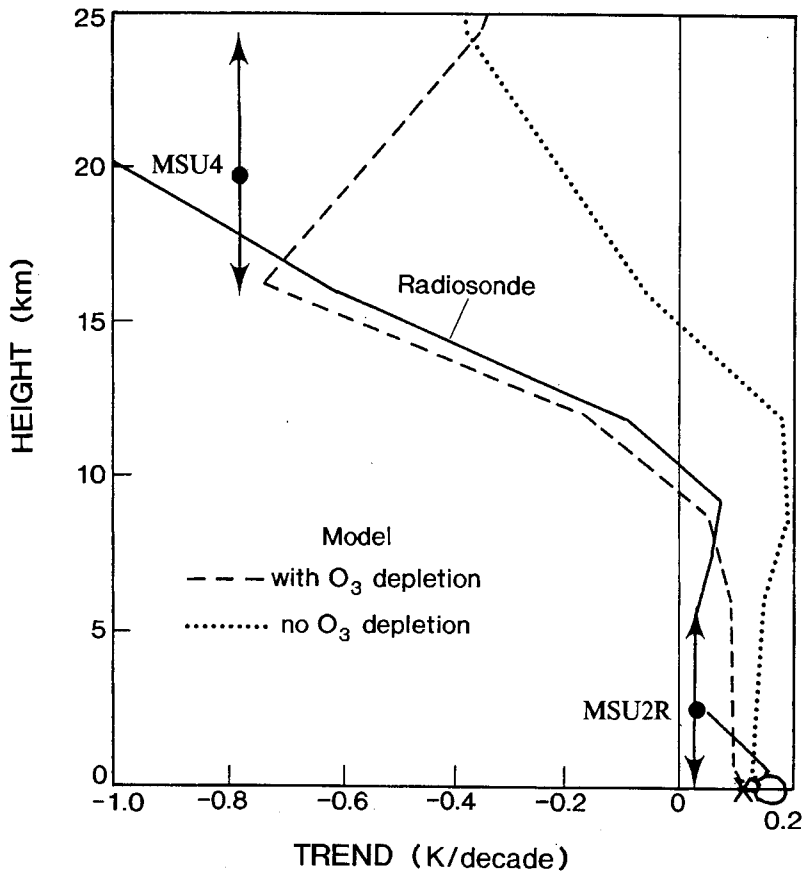

Figure 25. Comparison of GCM-simulated vertical profile of global- and annual-mean temperature trend over the 1979–1990 period with radiosonde and MSU satellite observations. The simulations are performed considering the well-mixed greenhouse gas increases and with or without consideration of the lower stratospheric ozone depletion over the time period. The vertical range sensed by the MSU lower stratospheric and lower tropospheric channels is indicated. The circle and cross denote the surface temperature changes from the *Jones* [1994] and *Hansen and Wilson* [1993] observational data sets, respectively. Adapted from *Hansen et al.* [1995] with kind permission from Kluwer Academic Publishers.

cooling in the tropics, which arises as a result of changes in circulation and is absent in FDH, is not significant for most of the year, owing to small temperature changes there. There exist quantitative differences between the simulated and observed trends, and there is less variability in the model compared with observations. In the global and annual mean, the GCM-simulated lower stratospheric temperature changes over the 1980s decade are approximately 0.5–0.6 K/decade (Figures 25 and 26).

In general, the observed ozone losses introduce a nonuniform space-time cooling. This is in contrast to well-mixed greenhouse gas effects, which tend to yield a more uniform lower stratospheric cooling with season (not shown). Thus the observed seasonal trend (Figure 27b) [see also *Forster and Shine*, 1999], which exhibits a spatial dependence, is unlikely to be due to increases solely in well-mixed greenhouse gases. Note that in the context of the GCM results, care should be taken in associating the specific seasonal cooling at any location with the corresponding seasonal ozone loss, especially in a quantitative sense.

Some models that have been principally used to study tropospheric climate changes due to greenhouse gases [e.g., *IPCC*, 1996] have also considered the lower stratospheric ozone depletion. However, several of these climate models have poor vertical resolution in the stratosphere, which affects the accuracy of the calculated temperature changes. Nevertheless, the cooling predicted by these models using observed ozone loss in the lower stratosphere is generally consistent with the observed global-mean cooling trend, typically 0.5 K/decade.

In addition to lower stratospheric ozone, model calculations illustrate that tropospheric ozone change could also have a smaller but nonnegligible cooling effect on stratospheric temperatures [*Ramaswamy and Bowen*, 1994]. Since preindustrial times, tropospheric ozone may have increased by ~50% or more in some regions in the Northern Hemisphere [*IPCC*, 1995]. *Berntsen et al.* [1997] found that the cooling of the lower stratosphere due to this effect exceeded 0.5 K in low latitudes for the period since preindustrial times. In recent decades the cooling may have been of the order of 0.05 K/decade from this source, indicating a contribution of about 10% of the observed trend. As a result, tropospheric ozone increases may have contributed to a nonnegligible cooling tendency in the lower stratosphere in specific regions. However, there is considerable uncertainty in modeling the trends in tropospheric ozone.

In a diagnostic study, *Fortuin and Kelder* [1996] discuss relationships between ozone and temperature changes by analyzing concurrent measurements of these two quantities made at eight stations over the past 2 decades. They find that both vertical displacement and the computed radiative adjustment to trace gas concen-

trations need to be considered in order to explain the observed ozone and temperature variations at the various locations.

3.3.2. Sensitivities related to ozone change. One of the most important factors affecting the quantitative estimate of modeled temperature change is the precise vertical profile of the ozone change in the region near the tropopause, a problem that has been reiterated for a number of years [*WMO*, 1986, 1992, 1995]. Additionally, there are some uncertainties about the middle and upper stratospheric ozone changes that also impact in a nonnegligible manner upon the temperature changes at those altitude regions.

The temperature change to two somewhat different vertical profiles of ozone change, namely, those based on SBUV column and SAGE vertical profile trends in the 1980s, suggests that the cooling in the lower stratosphere (see Figure 28) is strong irrespective of the assumption [*Forster and Shine*, 1997] and that it outweighs the contributions estimated due to other possible species' changes (see Figure 21). Although the general vertical profile of the ozone-induced coolings remains the same, peaking at ~1 K/decade in some regions, the latitudinal variation is quite different. The SBUV trends give only small ozone changes in low latitudes, and the cooling is concentrated in the extratropical lower stratosphere. The SAGE trends show large changes in the tropical lower stratosphere (despite modest total column changes there), and these result in the peak cooling in the tropics. According to the SPARC Ozone Trends Panel and *Cunnold et al*. [1996a, 1996b], the large trends of SAGE I and II in the 15- to 20-km region are likely unrealistic, with the data being most reliable above 20 km.

Using the simplified ozone change profile, there is a heating at ~30 km (middle stratosphere), most marked in southern high latitudes (Figure 28a), where the increase in the upwelling thermal infrared radiation, as a result of the removal of ozone in the lower stratosphere, leads to an increase in the absorbed radiation. Using the SAGE vertical profiles, which are probably more reliable at these heights, there is cooling at almost all latitudes, reaching 0.4 K/decade (Figure 28b). Hence while the ozone loss is probably most important in the lower stratosphere, the losses at these stratospheric altitudes (~30 km) remain substantial and could lead to trends that are approximately of the same magnitude as the temperature trends, over the same period, due to increases in well-mixed greenhouse gases (see Figure 22).

The sensitivity of the lower stratospheric temperature changes due to ozone depletion has been examined by conducting various GCM experiments with varying profiles and amounts of ozone losses [*Hansen et al*., 1997a] (their result for the specific case when depletion of ozone occurs over the 70- to 250-hPa region is illustrated in Figure 23). They find the magnitude of temperature change near the tropopause to be strongly governed by the assumed vertical profile of the ozone loss there.

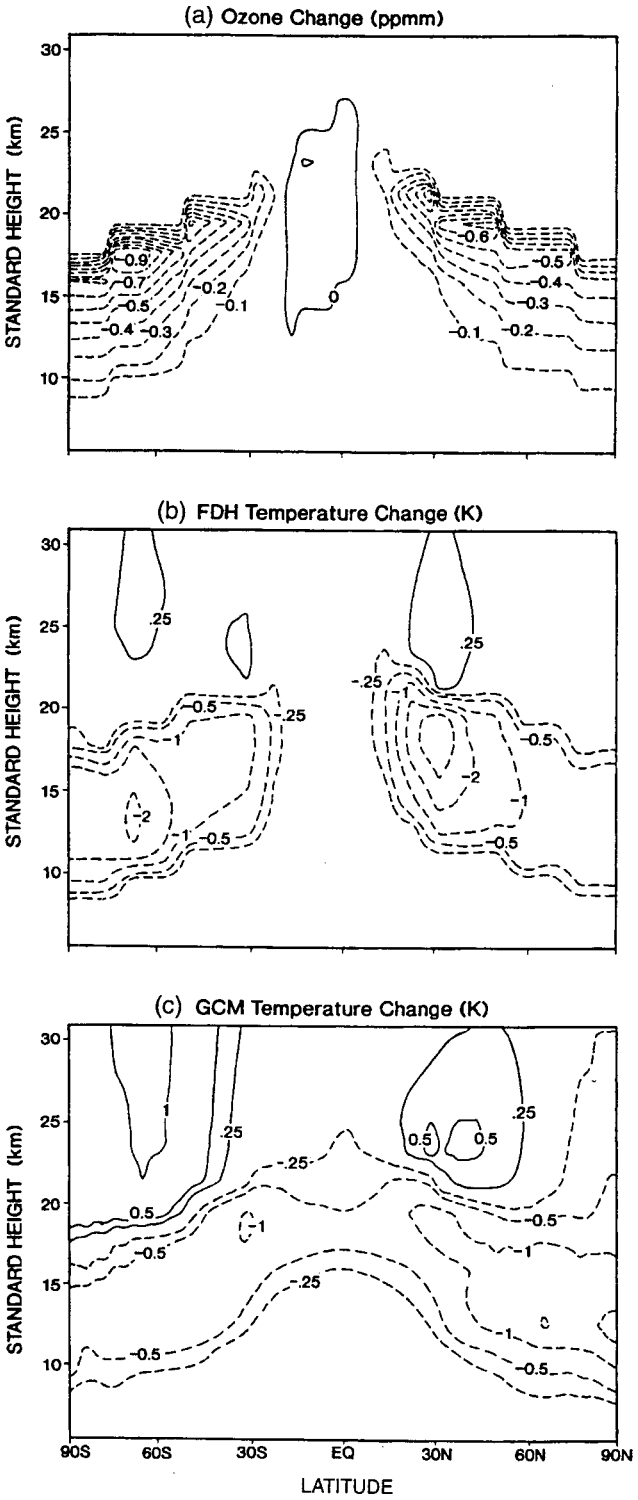

Figure 26. Zonal- and annual-mean stratospheric ozone loss profile (Figure 26a) and the corresponding temperature changes, as obtained using an FDH model (Figure 28b) and GCM (Figure 26c). Adapted from the model simulations of *Ramaswamy et al*. [1992, 1996].

The GCM sensitivity experiments [*Hansen et al*., 1997b] also demonstrate that the observed ozone losses not only cool the lower stratosphere but also affect the vertical profile of temperature change below the region

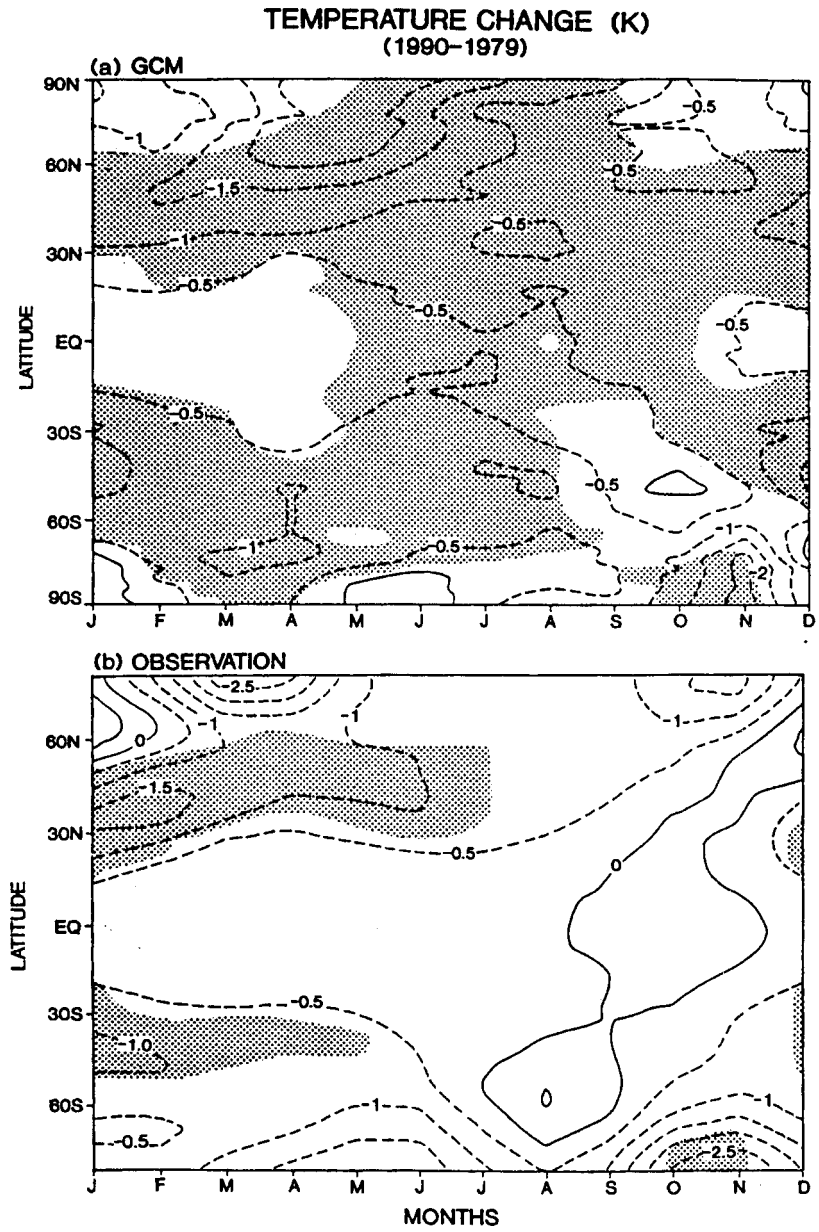

Figure 27. Zonally and monthly averaged lower stratospheric temperature change over the 1979–1990 period: (a) as simulated by the general circulation model (90°S–90°N) due to the observed global ozone depletion (see Figure 26), and (b) as inferred [*Randel and Cobb*, 1994] from satellite observations (82.5°S–82.5°N). Shaded areas show statistical significance at the 95% confidence level. Reprinted from *Ramaswamy et al.* [1996] with permission from *Nature*. Copyright 1996 Macmillan Magazines Ltd.

of ozone losses. The crossover of temperature change from a warming in the troposphere to a cooling in the stratosphere occurs at a lower altitude when stratospheric ozone depletion is considered, in contrast to when only the changes in the well-mixed gases are considered. The inclusion of the ozone loss in the lower stratosphere not only alters the modeled vertical profile of the simulated atmospheric temperature change due to anthropogenic species, but also is a critical element in the attribution of the observed temperature profile change to human activity [*Santer et al.*, 1996; *Tett et al.*, 1996; *Folland et al.*, 1998].

Ozone changes also affect higher regions of the stratosphere. *Fels et al.* [1980] and *Rind et al.* [1990, 1998] point out that while the stratosphere generally cools in response to the carbon dioxide increases, the cooling in the middle and upper stratosphere is reduced (by ~10% at 50 km) when ozone is allowed to respond photochemically. FDH estimates using the SAGE vertical profile of temperature change indicate that the positive (or negative) temperature change generally follows the positive (or negative) changes in ozone. Thus the result from the calculations performed by *Schwarzkopf and Ramaswamy* [1993] suggests that ozone losses over the 1980–1990 period would cause a cooling of ~0.3 K/decade at ~40 km. This is to be contrasted with the well-mixed greenhouse gas–induced cooling of about 0.8 K/decade at these altitudes (Figures 21 and 22).

Shindell et al. [1998] simulate the changes in the stratosphere due to secular trends in greenhouse gases and ozone changes using an interactive radiative-dynamical-chemical GCM [see also *WMO*, 1999]. Their results indicate that the cooling of the entire stratosphere due to the trace gas changes leads to a significant expansion

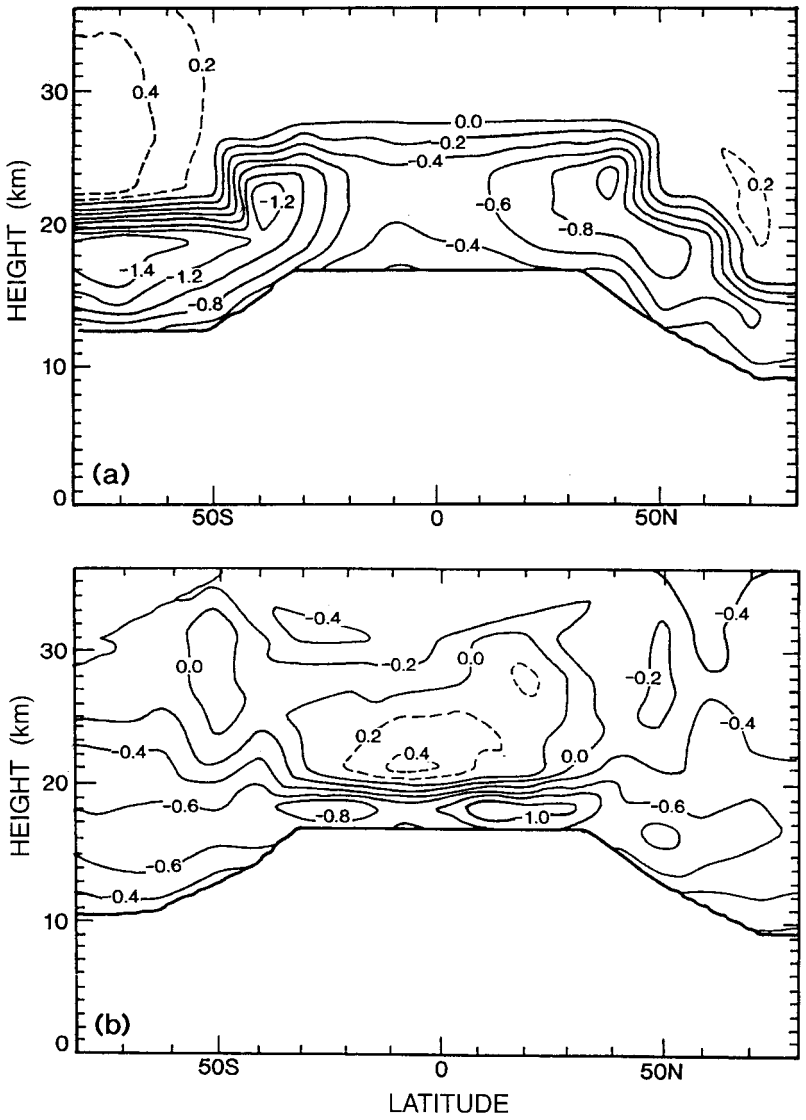

Figure 28. FDH-computed, annual-mean global stratospheric temperature change (in kelvins) during the 1980s due to (a) SBUV-based column depletion [*WMO*, 1995] and adopting a simplified profile, with the ozone loss assumed to be a constant percentage between the local tropopause and 7 km above it, and (b) assumption of the SAGE vertical profile. Adapted from *Forster and Shine* [1997].

of the area of ozone loss in the polar regions. Besides the expansion of the Antarctic polar ozone loss area, there also occurs a pronounced depletion of the Arctic springtime ozone. The rather dramatic simulated cooling is attributed to changes in the planetary wave characteristics in their model.

The altitude and latitudinal distribution of ozone depletion impacts the dynamical response in the global stratosphere and is a major factor in determining the meridional distribution of temperature changes. If the ozone changes are uniform with latitude (a hypothetical but nevertheless illustrative example), there would be a radiatively induced cooling of the lower stratosphere, maximized in the tropics, with a warming higher up. *Rind and Lonergan* [1995] suggest that in the middle stratosphere, there would be an increased meridional temperature gradient, with stronger west winds, equatorward planetary wave refraction, and colder polar temperatures. They further argue that if the ozone depletion is maximized in the lower stratosphere of the higher latitudes (as has been the case during the 1980s and 1990s), then the circulation changes act to enhance the cooling of the polar stratosphere.

3.4. Aerosols

Major volcanic eruptions result in temporary increases in stratospheric aerosol concentrations, which, in turn, cause transient warmings of the lower stratosphere [*WMO*, 1990a, 1992]. One-dimensional radiative-convective, two-dimensional, and three-dimensional models all have been used to estimate the effects on stratospheric temperatures [e.g., *Hansen et al*., 1978; *Harshvardhan*, 1979; *Pitari et al*., 1987; *Hansen et al*., 1997b]. An important research outcome has been the fact that simulations of the climatic effect of the Pinatubo eruption [*Hansen et al*., 1993, 1997b] reproduce the observed lower stratospheric warming (refer to section 2.6.1, *Christy* [1995], *Randel et al*. [1995], and *Angell* [1997]; also see Figure 2, bottom panel, and Figure 3), both the peak and its duration, remarkably well [*IPCC*, 1995]. Although tem-

porary, the volcanic aerosol–induced lower stratospheric warming is opposite to the cooling due to ozone depletion, and the cooling due to the combined well-mixed greenhouse gas increases (Figures 21, 22, and 25).

GCM experiments show that in response to the volcanic injections, the lower stratospheric warms and the upper stratosphere cools, while the mesosphere warms at middle and high latitudes [*Rind et al*., 1992]. These responses bear a qualitative resemblance to the OHP lidar observations. However, there are problems in establishing the statistical significance of the observed and simulated signals. The occurrence of mesospheric warming is indirectly supported by a decrease in the occurrence of noctilucent clouds in the summer of 1992 [*Zalcik*, 1993]. Model simulations indicate that the volcanic aerosol–induced warming of the tropical lower stratosphere produces an enhanced meridional temperature gradient that strengthens the west winds, producing equatorward wave refraction and colder conditions at high latitudes [*Rind et al*., 1992; see also *Kodera*, 1994]. Qualitatively similar features of the meridional temperature response are obtained by *Graf et al*. [1993] and *Kirchner et al*. [1999] for the specific instance of the Pinatubo volcanic eruption. Again, however, the significance of the response at higher latitudes is constrained by the large dynamical variability there.

Several 2-D radiative-dynamical-photochemical models [*Brasseur and Granier*, 1992; *Tie et al*., 1994; *Rosenfield et al*., 1997], with different degrees of complexity in the representation of physical and chemical processes, have been deployed to study the temperature, circulation, and ozone changes due to the increase in stratospheric aerosol concentrations following the Mount Pinatubo volcanic eruption. Additionally, *Eluszkiewicz et al*. [1997] have used the UARS measurements to investigate the stratospheric heating rate sensitivity and the resulting residual circulation. These studies indicate a warming of the tropical lower stratosphere that is approximately consistent with observations. This heating is found to be sensitive to the presence of tropospheric clouds and to the aerosol vertical extinction profiles, which corroborates the sensitivity results of *WMO* [1990a]. The perturbed heating in the tropics results in an upwelling and an altered circulation, a feature seen in model simulations and diagnosed from observations. Thus the transient volcanic aerosol–induced warming has the potential to alter atmospheric dynamics and could thereby affect the surface-troposphere system [*Hansen et al*., 1997b]. Ozone depletions are obtained by the 2-D model as a result of the heterogeneous processes involving aerosols, changes in photolysis rates, and changes in the meridional circulation [*Tie et al*., 1994]. The ozone loss at the high latitudes yields a cooling there [*Rosenfield et al*., 1997] that could have contributed to the prolonged duration of the colder-than-normal temperatures in the Arctic region (see section 2.4, Figure 4, and Figure 12a).

Although both the El Chichon and Pinatubo eruptions have resulted in large transient warmings, these are estimated to have only a small direct effect on the decadal temperature trends in the lower stratosphere, with even smaller effects higher up. However, an indirect effect through aerosol-induced, chemically catalyzed ozone loss (e.g., in midlatitudes) and the subsequent ozone radiative feedback can yield a global cooling contribution [*Solomon et al*., 1996]. It is of interest to note that the global-mean lower stratospheric temperatures were colder (Figure 2, bottom panel, and Figure 3) in the post-Pinatubo phase after the aerosols had decayed (~1994 onward) than in the pre-Pinatubo period [see also *WMO*, 1999]. Thus the volcanic events have had an important bearing on the lower stratospheric temperature trend observed over the decade of the 1980s and early 1990s.

Changes in tropospheric aerosols can also affect lower stratospheric temperatures [*Ramaswamy and Bowen*, 1994]. While the tropospheric aerosols assumed in that study acted to oppose the greenhouse warming in the troposphere, they enhanced the cooling in the stratosphere by reducing the upwelling thermal infrared radiation coming from a cooler troposphere. However, there is considerable uncertainty in the distribution and optical properties of aerosols. In addition, the aerosols may have a substantial effect on the optical properties of clouds [*IPCC*, 1995, 1996], which would also affect the upwelling longwave flux from the troposphere. Overall, it is not yet possible to quantify the present-day effect of tropospheric aerosol on stratospheric temperatures.

3.5. Water Vapor

Stratospheric water vapor is an important radiatively active constituent, and it is expected to generally increase in concentration due to increased methane oxidation [*WMO*, 1995], although the rate of change could be subject to influences by other physical factors such as changes in tropospheric water vapor concentrations, changes in tropopause temperatures, and changes in the transport of water vapor across the tropopause. *Oltmans and Hoffmann* [1995] reported significant positive trends of 0.5%/year in water vapor over Boulder, Colorado, from balloonsonde observations between 1981 and 1994. It is not clear whether these changes are occurring at other locations and, more important, on a global scale. Using an FDH model to calculate the impact of these changes, at 40°N and between 15 and 20 km, *Forster and Shine* [1997] find that the cooling due to water vapor changes exceeds 0.2 K/decade (Figure 21). This is much larger than the effect of changes in the well-mixed greenhouse gases at the same altitude (typically 0.1 K/decade; see Figures 21 and 22). Depending on the vertical profile of ozone loss adopted, the water vapor change causes a cooling of around 20–30% of the effect of the ozone change. Recent observational analyses [*Nedoluha et al*., 1998] suggest an increase in H_2O of 1–2% or more per year (between 1991 and 1996) in the middle and upper stratosphere and mesosphere. If sustained for a decade,

the heating rate change would be about 0.05 K/day. Combining this with a radiative damping time of ~10 days [*Fels*, 1982; *Kiehl and Solomon*, 1986] would yield a cooling of 0.5 K/decade at 50 km. This value would be about half of that for the well-mixed greenhouse gases (see section 3.2 and Figure 22) and could exceed that due to ozone change at that altitude (see section 3.3.2).

A GCM study [*Rind and Lonergan*, 1995] finds an increase of water vapor of 7% to yield a stratospheric cooling of a few tenths of a kelvin overall, while a doubling of the stratospheric water vapor from present concentrations yields a temperature change 10 times larger (~2–3 K). The temperature changes scale approximately linearly with respect to water vapor changes of this magnitude. Overall, for a 5%/decade water vapor increase, these GCM results would suggest a cooling of ~0.2 K/decade, a result that corroborates the FDH result above. A recent GCM simulation [*Forster and Shine*, 1999], using the Boulder measurements together with the satellite data from the early to middle 1990s period, demonstrates that the effect of water vapor increases on the stratospheric temperatures, if sustained for a decade or more, could be comparable to the decadal temperature trends due to ozone changes. This is true of both the global- and zonal-mean contexts, including as a function of latitude and month (in a manner similar to Figure 27).

There are substantial problems in the quantitative assessment of the global changes and decadal trends in stratospheric water vapor, including consistency in the sign and magnitude among the different observational platforms over the different time periods, and the profile of change in the lower stratospheric region. The evidence for sustained global increases over the past decades in stratospheric water vapor remains quite weak, but it is clear that plausible changes in it could make a significant contribution to the temperature trend.

3.6. Other Factors (Solar Cycle and QBO)

All the above variations in constituent changes take place in the stratosphere itself. External changes, such as variations in the incoming solar radiation, in reflected solar radiation from the troposphere, and in the emitted thermal infrared radiation, can also impact stratospheric temperatures.

Changes in the output of the Sun can clearly influence the amount of UV and visible radiation absorbed by the stratosphere. In the absence of changes in ozone, *WMO* [1990a] radiative-convective model calculations showed that over the course of a solar cycle, the temperature at the stratopause can vary by about 1 K, but by 20 km the changes are less than 0.1 K. If, as is suggested by observations, there are interactions between planetary wave propagation and solar cycle influences [see *Chanin and Keckhut*, 1991; *Hauchecorne et al*., 1991], for example, changes in meridional heating inducing changes in the refraction of the planetary waves and the subsequent impacts on winds and temperature structure in the polar stratosphere (see section 3.1), then model simulations need to adequately account for these processes. Several numerical model simulations [*Garcia et al*., 1984; *Brasseur*, 1993; *Fleming et al*., 1995; *McCormack and Hood*, 1996; *Shindell et al*., 1999b] indicate that the maximum of solar effect, allowing for ozone changes, should be situated at the stratopause at all latitudes, with a value of around 1.5–2 K/cycle in the tropics. The models yield amplitudes of ~2 K at the tropical stratopause (Figure 29). The modeled temperature change is roughly consistent with observations (Figure 17), but substantial differences remain. The same models, in general, are less successful when compared with observations at middle and high latitudes. In fact, the latest interactive radiative-chemical-dynamical model simulations, while beginning to capture some of the sense of the observed solar cycle signature (see section 2.6.2), have to make further progress.

Model simulations [*Balachandran and Rind*, 1995; *Shindell et al*., 1999b] reveal insights into the temperature changes and mechanisms associated with the transition from a solar maximum to a solar minimum time period. There is a warming of the tropical upper stratosphere. This strengthens the meridional temperature gradient and, through the thermal wind relationship, strengthens zonal winds in the upper stratosphere. It leads to planetary wave refraction equatorward, leading to an enhanced stratospheric polar vortex and warm subtropical ridges, as have been observed [e.g., *Labitzke and van Loon*, 1997]. There is then less northward heat transport by the planetary waves and less driving of the residual circulation to high latitudes and hence less subsidence in the polar regions.

Balachandran and Rind [1995] found that changes in UV tended to alter the radiative heating with an accompanying influence on the planetary wave activity, high-latitude response, and winter polar jet. The influence of solar change on the temperature yielded changes of opposite sign at the stratopause between latitudes above and below 60°N. Such changes are quite similar to those seen in the overall stratosphere from the SSU satellite analyses (Figure 17). In the same study the QBO was found to exert a modulating effect on the planetary waves and the changes at the high latitudes. The west minus east QBO is associated with warmer lower latitudes, which increases the latitudinal temperature gradient. This strengthens the west winds, leading to relative equatorward propagation of planetary wave energy and thereby to colder conditions at the polar latitudes.

Haigh [1996] has simulated the possible effect of solar-induced stratospheric ozone and temperature variations on the tropospheric Hadley circulation and jet streams using a GCM. The results suggest that changes in stratospheric ozone may provide a mechanism whereby small changes in solar irradiance can cause a measurable impact on climate. It has been proposed that changes in the thermal structure of the lower stratosphere could cause a strengthening of the low-latitude

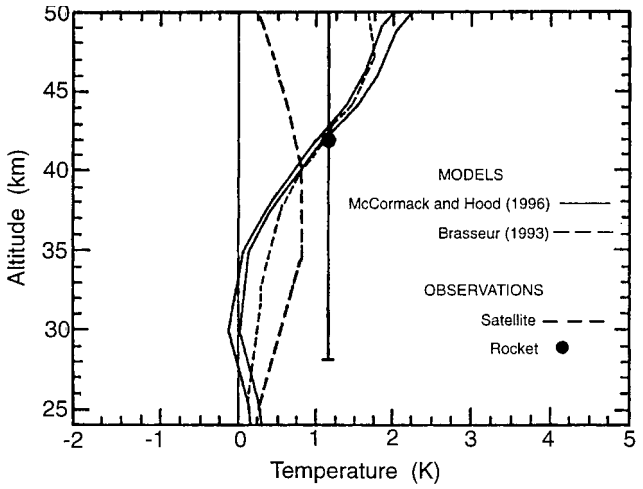

Figure 29. Comparison of model-computed, low-latitude (5°N) temperature response due to solar cycle variation with SSU satellite observations (bold dashed curve) and rocket data [*Dunkerton et al*., 1998]. *McCormack and Hood* [1996] perform two FDH calculations using the range of the observed ozone values; their model results (solid curves) are quite similar to those of *Brasseur* [1993] (thin dashed curve). The altitude extent of the rocket data analyzed (28–55 km) is indicated by the vertical bar, while the dot represents the corresponding height-mean value of the solar cycle signature. Adapted from *McCormack and Hood* [1996].

upper tropospheric easterly winds. *Haigh* [1998] further suggests that this easterly acceleration can come about as a result of a lowering of the tropopause and deceleration of the poleward meridional winds in the upper portions of the Hadley cells. More observational diagnostics work and model investigations are needed to confirm these hypotheses. A recent model investigation [*Shindell et al*., 1999b], accounting for the ozone changes, is able to produce an intensified subtropical ridge in connection with the phenomenon.

4. CHANGES IN TRACE SPECIES AND OBSERVED TEMPERATURE TRENDS

4.1. Lower Stratosphere

The importance of lower stratospheric ozone depletion relative to that due to changes in other greenhouse gases that are well mixed (CO_2, CH_4, N_2O, CFCs) has been evaluated by several studies with various types of models (1-D to 3-D). *Miller et al*. [1992] and *Hansen et al*. [1995] demonstrate that the global-mean lower stratospheric temperature change in the 1980s can be explained when only ozone changes are considered (Figure 25). *Ramaswamy et al*. [1996] show that the global, annual-mean GCM temperature change due to the decadal ozone losses in the ~50- to 100-hPa (~16–21 km) lower stratospheric region is much greater than that due to increases in CO_2 only and all well-mixed greenhouse gases combined (Figure 20). It is encouraging that all modeling studies, ranging from FDH and RCMs to GCMs, yield similar findings (see section 3.3.1). The global-mean decadal cooling in the 1980s due to ozone is estimated to be ~0.5–0.6 K, which is comparable to the reported decadal trends from observations (see section 2.3.2 and Figure 25). The effect of well-mixed gases is less than one fourth that due to ozone depletion. While the increase in CO_2 alone since 1765 yields a cooling of ~0.3 K, inclusion of the other well-mixed gases, which together tend to warm the tropopause region, yields ~0.15 K. It is clear that the computed 1979–1990 ozone effect on lower stratospheric temperature outweighs the effects of changes in other gases, not only over the last 10–30 years but also over the past 2 centuries. On the basis of model-observation comparisons and the current evidence regarding changes in the global concentrations of the radiative species, it can be concluded that the observed ozone depletion is the major cause of the observed global- and annual-mean cooling of the lower stratosphere over the 1980s. *WMO* [1999, chapter 7] indicates the theoretical basis for how a long-term global, annual-mean trend in the stratosphere must necessarily be associated with radiative perturbations. A factor that could potentially rival the importance of ozone is water vapor changes in the stratosphere [*Forster and Shine*, 1999]. Unfortunately, observational basis and evidence of global trends in stratospheric water vapor during the 1980s are rather weak (section 3.5) so that its role over this period may never be fully resolved.

Uncertainties arise in the simulations owing to incomplete observational knowledge of the vertical profile of global ozone loss near the tropopause, including that in the tropical areas. More thorough altitudinal measurements of ozone loss near the tropopause would lead to more precise simulation of temperature change. Nonetheless, the lower stratosphere, taken as a whole, can be expected to cool notably irrespective of the exact details of the profile, given the large ozone losses taking place in that region. A principal conclusion from all investigations thus far, whether ozone changes are prescribed or determined self-consistently within a model, is that the global lower stratospheric region, especially in the middle to high latitudes, cools substantially in simulations for the decades of the 1980s and 1990s.

In addition to the above, a principal feature, especially from the GCM studies, is the reasonably good correspondence of the zonal-mean lower stratospheric cooling trends since ~1979 with satellite and radiosonde records [e.g., *Hansen et al*., 1993]. It is concluded that the reasonable consistency of the simulated cooling pattern and magnitudes with that observed, including the regimes of statistically significant changes, coupled with the high correlations noted between observed temperature changes and ozone losses (section 3.3.1), confirm the notion that ozone depletion has caused a substantial spatially and seasonally dependent effect in the lower stratosphere over the past decade. For example, Figure 27 highlights the model-observation consistency with

regard to magnitude and statistical significance in the midlatitudes of both hemispheres during the first half of the year and during the Antarctic springtime. Note, though, that the existence of a high correlation in the patterns of ozone depletion and temperature change does not, by itself, confirm the quantitative aspects of such relationships at a specific location and time. Although the attribution of the observed temperature trends to the observed ozone depletion in the lower stratosphere is strong in the global, annual-mean sense, the spatial and temporal aspects demand more circumspection. *Forster and Shine* [1999] note that water vapor increases in the stratosphere could also yield somewhat similar spatial temperature change patterns; however, information on global trends in water vapor, especially during the 1980s, is either poor or not available (section 3.5). Among the species whose changes are well documented, it is significant that ozone losses yield a latitude-month fingerprint of temperature change that compares reasonably with the observations (Figure 27b). Thus, in the zonal-mean, seasonal sense, it can be stated that ozone is identifiable as an important causal factor of lower stratospheric temperature change.

Possible secular changes in other radiatively active species are estimated to contribute smaller decadal effects than the stratospheric ozone loss. Information on decadal changes in global water vapor (section 3.5) and clouds is insufficient to estimate their influence precisely; however, there is little information at present to suggest that their decadal-scale trends have been as strong as those due to the stratospheric ozone loss. Although volcanic aerosols can have a substantial impact over the 1–2 years that they are present in the lower stratosphere, their effect on the past decade's temperature trend has probably been small compared with the effect of ozone (sections 2.6.1 and 3.4). There is little evidence to suggest that forcings from the troposphere (e.g., sea surface temperature changes; see section 2.6.5) or natural climate variability or solar cycle (see sections 2.6.2 and 3.6) have significantly influenced the global lower stratospheric temperature change over the past 1.5 decades, although in the absence of rigorous long-term observations, a precise estimate of their contributions cannot be obtained. It is noted that some ozone loss has been reported for the 1970s [*Lacis et al*., 1990] which would have contributed to the small observed cooling during that decade (e.g., Figures 3a and 4). However, this contribution is not likely to have been as much as in the 1980s and 1990s, since the ozone losses for the earlier decades are not thought to have been as high as recently [*Bojkov and Fioletov*, 1995].

There is a scarcity of information on the low-frequency variability of the stratosphere and its causes, from either observations or models. Unlike surface temperature measurements which span multiple decades, those for the stratosphere are available only from about the late 1950s, with the continuous record available only at a few locations in the NH. This makes it difficult to assess accurately the low-frequency variability. While global coverage has become possible with the MSU and SSU satellites since 1979, the time period available to date is too short to assess anything beyond interannual variability. Unfortunately, rigorous decadal-scale variability analysis will not be possible until data for a few more decades become available. The model simulations to date suggest an interannual variability in some features that bears resemblance to that observed, but there are also features that the existing models cannot reproduce or fail to mimic [e.g., *Hamilton et al*., 1995]. A prominent uncertainty arises due to the lack of a proper simulation of the polar wintertime and winter-to-spring transitional temperatures (including sudden warmings) from first principles' modeling. The usual method to reproduce observations is to "tune" the model in some manner, for example, by gravity-wave drag. The quantitative effect that this has on the fidelity of the simulation of trends and variability remains to be determined.

The cold winters and springs occurring in the lower stratosphere of the Arctic in recent times (section 2.4) have drawn considerable attention, including a search for the possible causes. The Arctic temperatures can vary substantially in magnitude on interannual timescales (see Figure 12a), thus demanding caution in the inference and attribution of long-term trends there. *Baldwin et al*. [1994] and *Perlwitz and Graf* [1995] document the existence of a coupling between the winter polar vortex and middle troposphere, which builds upon the studies of *Kodera* [1994]. *Thompson and Wallace* [1998] show coherence between hemispheric wintertime surface air temperature and pressure and 50-hPa temperatures. The studies of *Manney et al*. [1996] and *Coy et al*. [1997] indicate that extreme low temperatures in spring are associated with record low planetary wave activity and an intense vortex. The above studies suggest a possible shift in Arctic meteorological conditions in the early to middle 1990s, one that is linked to tropospheric circulation and variability in planetary wave forcing. The notion that this could be related in some manner to greenhouse gas–induced warming of the lower atmosphere [*WMO*, 1999; *Shindell et al*., 1999a] is a plausible one and requires further exploration.

Indeed, the effect of tropospheric climate change due to changes in trace gases and aerosols, equator-to-pole tropospheric temperature gradient, waves propagating into the stratosphere, and the resulting radiative-dynamical-chemical stratospheric state are not quantitatively well understood. For example, different GCMs suggest substantially different changes in the characteristics of the planetary wave activity due to an increase of CO_2, which would, in turn, impact the radiative-dynamical interactions and the magnitude of stratospheric temperature changes [*Fels et al*., 1980; *Fels*, 1985; *Rind et al*., 1990; *Mahlman*, 1992; *Graf et al*., 1995; *Shindell et al*., 1998; *Rind et al*., 1998].

4.2. Middle and Upper Stratosphere

Unlike the case for the lower stratosphere, the trends and significance estimated from the different observational platforms for the middle and upper stratosphere are not as robustly consistent across the different data sets. The satellite, lidar, and rocket data, although having a consistency in terms of the cooling in the middle and upper stratosphere (above ~50 hPa, e.g., Figures 7 and 10), do not exhibit the same degree of coherency that exists with respect to both magnitude and statistical significance for the different data sets of the lower stratosphere (Plates 1 and 2).

In the middle and upper stratosphere, model results suggest that the increases in the well-mixed greenhouse gases and changes in ozone will contribute to temperature changes. The overall picture from the annual-mean model simulations is one of cooling from the lower to the upper stratosphere (Figures 21 and 22). This cooling in the middle stratosphere due to the well-mixed gases can be expected to be enhanced in FDH calculations that also consider ozone losses in the middle stratosphere; the latter is estimated to yield about a 0.3 K/decade cooling using the SAGE depletion for the 1980s period (section 3.3.2). The computed vertical profile (Figure 22) bears a qualitative similarity to the observations (e.g., Figures 5 and 7) with regard to the cooling of the entire stratosphere. This reaffirms the secular cooling trend due to greenhouse gas increases inferred for the stratosphere from shorter records [*WMO*, 1990a, 1990b].

However, at altitudes above the lower stratosphere, there are major quantitative differences between the modeled and observed cooling. The FDH-simulated cooling increases with height when only the well-mixed gases are considered (Figure 22), whereas the observations indicate a rather uniform trend between 20 and 35 km (with perhaps even a slight reduction at ~30–35 km; see Figures 5–10). It must be noted that the GCM's simulation of the effects due to ozone loss involves a dynamical change (not evident in FDH) that causes some warming above the location of the cooling in the lower stratosphere (section 3.3.1 and Figure 26). This GCM-simulated warming, which may not be statistically significant, occurs mainly in winter/spring and is qualitatively consistent with observations during that season (Figures 13 and 14). Consideration of this warming could retard somewhat the rapid increase of the well-mixed greenhouse gas–induced cooling with height (Figure 22), for example, above 25 km, and enable a full radiative-dynamical (i.e., GCM) computation to become more consistent with observations than the FDH results.

Additionally, the magnitude of the modeled cooling in the upper stratosphere is less than that observed; for example, at ~45 km the modeled cooling is about 1 K/decade due to the well-mixed greenhouse gases and about 0.3 K/decade due to ozone, while the observed cooling is greater than 1.5 K/decade (e.g., at 45 km in Figures 7 and 10). Some of this bias could be due to water vapor, whose global trend in the 1980s is not reliably known (section 3.5). Satellite data for the early to middle 1990s period suggest an upward trend, which would add to the cooling trend computed for the upper stratosphere (section 3.5) and reduce the present discrepancy.

The vertical and latitudinal magnitude of the cooling, and the location of the warming region above the cooling in the lower stratosphere, are very sensitive to the vertical profile of ozone depletion imposed in the model. The models invariably locate the cooling at exactly the region of the imposed ozone loss, with a warming immediately above it at the higher latitudes. Thus any shift of the altitude extent of ozone depletion in the model has the potential to shift the peak cooling and thus alter the vertical profile of the computed cooling trend. In turn, this affects the quantitative inferences about the consistency between computed and observed temperature trends in the middle and upper stratosphere.

4.3. Upper Troposphere

The cooling of the lower stratosphere in response to ozone losses also leads to a cooling below the ozone loss region in the global upper troposphere (~10–14 km), due in part to reduced infrared emission from the stratosphere [*Ramanathan and Dickinson*, 1979]. The cooling of the lower stratosphere also impacts the forcing of the troposphere [*WMO*, 1992, 1995, 1999]. Specifically, an ozone-induced cooling of the lower stratosphere implies a reduction in the longwave radiative emission from the stratosphere into the troposphere. This leads to a negative radiative forcing of the surface-troposphere system [*Hansen et al*., 1997a]. In general, GCMs simulating the effects of stratospheric ozone loss indicate a cooling of the upper troposphere (see Figures 23, 25, and 26).

All modeling efforts that have considered appropriate changes in trace gases yield a cooling of the tropopause region [e.g., *Hansen et al*., 1995; *Vinnikov et al*., 1996; *Santer et al*., 1996; *Hansen et al*., 1997a] (see also Figure 25). Here, again, the lower stratospheric ozone depletion effects dominate all other gases including CO_2. Further, the vertical profile of changes in ozone critically determines the profile of the temperature change in the upper troposphere.

A difficulty arises in comparing simulated upper tropospheric temperature changes due to ozone losses with observations over the past decade, as the "signal" from models (see Figures 25 and 26) is quite small, less so than that in the lower stratosphere (at 50 hPa or ~20 km). It is difficult at present to interpret the small change in the upper troposphere temperatures inferred from observations in terms of a change originating primarily from the stratosphere (e.g., lower stratospheric ozone loss) or one arising in the troposphere (e.g., tropospheric ozone chemistry). Further, the halocarbon-induced depletion of ozone in the lower stratosphere can also be expected to affect upper tropospheric ozone through a downward transport of the anomalies, thereby

contributing a cooling tendency in the upper troposphere.

In general, the temperature changes near the tropopause have the potential for affecting the water vapor distribution and cloudiness, especially cirrus clouds, which in turn can affect the radiative energy balance and thus the climate system [*IPCC*, 1996]. One example, available from observations of the effects in the upper troposphere due to a stratospheric perturbation, concerns the aftermath of the Pinatubo eruption. Lidar and other observations [*Sassen et al*., 1995] suggest that the aerosols from this volcanic eruption affected the occurrence of cirrus (ice) cloud formation near the tropopause. Another potential cause is a large increase in the aircraft fleet flying in the upper tropospheric regimes, which could affect the water vapor and upper level cloud distributions [*IPCC*, 1999].

The interactions between trace species' changes and the associated chemistry, microphysics, radiation, and dynamics remain to be more thoroughly explored, both from modeling and observational perspectives and bearing in mind the three-dimensional nature of the problem [*Holton et al*., 1995]. Meteorological parameters such as tropopause location [*Schubert and Munteanu*, 1988; *Hoinka*, 1999], temperature, and geopotential height [*Ohring and Muench*, 1960; *Spankuch and Schulz*, 1995] tend to be highly correlated to total ozone. They can therefore be expected to exhibit changes due to trends in ozone. At this time, such changes are not well documented (section 2.7). There is growing evidence of a connection between stratospheric variability and trends with those in the troposphere [e.g., *Kodera*, 1994; *Perlwitz and Graf*, 1995; *Kitoh et al*., 1996; *Shindell et al*., 1999a]. As noted earlier, *Thompson and Wallace* [1998] show a connection between the trend in winter-mean NH surface temperature and pressure and the trend in polar vortex strength. Such linkages inferred from observations emphasize that the radiative-chemical-dynamical interactions, which couple the stratospheric and tropospheric processes, need to be fully accounted for in order to attribute the observed temperature variations and trends to well-defined mechanisms that include changes in trace species.

5. SUMMARY

5.1. Observations

1. Data sets available for analyzing stratospheric temperature trends comprise measurements by radiosonde (1940s to present), satellite (1979 to present), lidar (1979 to present) and rocketsonde (periods varying with location, but most terminating by approximately the mid-1990s), meteorological analyses based on radiosonde and/or satellite data, and products based on assimilating observations using a general circulation model. Each of these contains varying degrees of uncertainty that influence the interpretation and statistical significance of the resulting temperature trends.

2. The temporary global annual-mean lower stratospheric (~50–100 hPa) warming (peak value ~1.5 K) associated with the aerosols from the 1991 Pinatubo volcanic eruption [see *WMO*, 1992, 1995], which lasted up to about 1993, has now given way to a relatively colder stratosphere.

3. Radiosonde and satellite data indicate a cooling trend of the global, annual-mean lower stratosphere since ~1980. Over the period 1979–1994 the trend is ~0.6 K/decade. For the period prior to 1980 the radiosonde data exhibit a substantially weaker long-term cooling trend.

4. Over the period 1979–1994, there is an annual-mean cooling of the Northern Hemisphere midlatitude lower stratosphere (~0.75 K/decade at 30°–60°N). This trend is coherent among the various data sets with regard to the magnitude and statistical significance. Over the longer period 1966–1994, the available data sets indicate an annual-mean cooling at 30°–60°N of ~0.3 K/decade.

5. In the ~15°–45° latitude belt of the Southern Hemisphere the radiosonde record indicates an annual-mean cooling of the lower stratosphere of up to ~0.5–1 K/decade over the period 1979–1994. The satellite record also indicates a cooling of the lower stratosphere in this latitude belt, but this is statistically significant only between about November and April.

6. Substantial cooling (~3–4 K/decade) is observed in the polar lower stratosphere during late winter/springtime in both hemispheres. An approximate decadal-scale cooling trend is evident in the Antarctic since about the early 1980s and in the Arctic since the early 1990s. However, the dynamical variability is large in these regions, particularly in the Arctic, and this introduces difficulties in establishing a high statistical significance of the trends.

7. A cooling of the upper stratosphere (pressure $<$ 3 hPa; height $>$40 km) is apparent over the 60°N–60°S region from the annual-mean SSU satellite data over the 1979–1994 period (up to ~3 K/decade near 50 km). There is a hint of a slight minimum in cooling in the middle stratosphere (~30–40 km), occurring between the slightly larger values below and the substantially larger values in the upper stratosphere.

8. Lidar and rocket data available from specific sites generally show a cooling over most of the middle and upper stratosphere (~30–50 km) of 1–2 K/decade since ~1970, with the magnitude increasing with altitude. The influence of the 11-year solar cycle is relatively large ($>$1 K) at these altitudes ($>$30 km).

9. The vertical profile of the annual-mean stratospheric temperature change observed in the Northern Hemisphere midlatitude (45°N) over the 1979–1994 period is robust among the different data sets (Figure 30). The mean trend consists of a ~0.75 K/decade cooling of the ~20- to 35-km region, with the cooling trend increas-

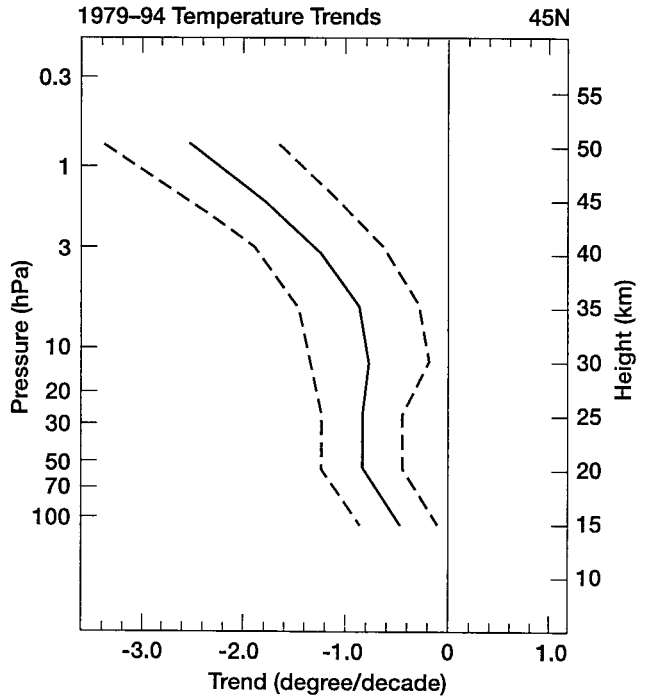

Figure 30. Mean vertical profile of temperature trend over the 1979–1994 period in the stratosphere at 45°N, as compiled using radiosonde, satellite, and analyzed data sets (section 2.3.3). The vertical profile of the averaged trend estimate was computed as a weighted mean of the individual system trends shown in Figure 7, with the weighting being inversely proportional to the individual uncertainty. The solid curve indicates the weighted trend estimate, while the dashed curves denote the uncertainty at the 2-σ level. The numerical values of trends at various altitudes and the uncertainty at the 1-σ level are listed in Table 6. (Data courtesy of SPARC Stratospheric Temperature Trends Assessment project.)

ing with height above (~2.5 K/decade at 50 km). The vertical profile of cooling, and especially the large upper stratospheric cooling, is consistent with the global plots of *WMO* [e.g., 1990a, Figure 6.17; 1990b, Figure 2.4-5] constructed from shorter data records.

In an overall sense, a more precise evaluation of the variability and trends in stratospheric temperatures is limited by a host of factors, including better consistency checks of the available data sets, the differences in altitude range spanned by the various observational platforms and differences in their respective sampling techniques, the different periods of measurements intrinsic to the various observational data sets, incomplete knowledge of natural variations and forcings, and the assumption of linearity in formulating the trend estimates.

5.2. Model Results and Model-Observation Comparisons

1. Model simulations based on the known changes in the stratospheric concentrations of various radiatively active species indicate that the depletion of lower stratospheric ozone is the major factor in the explanation of the observed global-mean lower stratospheric cooling trend (~0.5–0.6 K/decade) for the period 1979–1990. The contribution to this trend from increases in well-mixed greenhouse gases is estimated to be less than one fourth that due to ozone loss.

2. Model simulations indicate that ozone depletion is an important causal factor in the latitude-month pattern of the decadal (1979–1990) lower stratosphere cooling. The simulated lower stratosphere cooling trend in Northern and Southern Hemisphere midlatitudes (up to ~1 K), and in the Antarctic springtime (2 K or more), is statistically significant over this period and generally consistent with observations. The magnitude and the vertical extent of the simulated cooling in the lower stratosphere are subject to the uncertainties in the altitude profile of ozone loss.

3. The fixed dynamical heating, or FDH (equivalently, the pure radiative response), calculations yield a middle- to high-latitude annual-mean cooling that is approximately consistent with a general circulation model's radiative-dynamical response (Figure 26); however, changes in circulation simulated by the GCM cause an additional cooling in the tropics, besides affecting the meridional pattern of the temperature decrease.

4. FDH model results indicate that both well-mixed greenhouse gases and ozone changes are important contributors to the cooling in the middle and upper stratosphere; however, the computed upper stratospheric cooling is smaller than the observed decadal trend.

5. Increased water vapor in the lower to upper stratosphere domain could also be an important contributor to the cooling; however, decadal-scale stratospheric water vapor changes have not yet been determined with the same degree of certainty associated with the well-mixed greenhouse gas and ozone changes. Water vapor trends in the global stratosphere over the decade of the 1980s are not known, with the exception of measurements at a single location (Boulder). However, satellite measurements in the early to middle 1990s indicate increases in water vapor globally that if sustained for a decade or more like the ozone change, could impact the stratospheric temperatures measurably and become as important in the cooling of the stratosphere as inferred in the case of the lower stratospheric ozone losses.

6. Model simulations of the response to the observed global lower stratospheric ozone loss in middle to high latitudes suggest a radiative-dynamical feedback leading to a warming of the middle and upper stratospheric regions, especially during springtime; however, while the modeled warming is large and can be statistically significant during the Antarctic spring, it is not statistically significant during the Arctic spring. Antarctic radiosonde observations indicate a statistically significant warming trend in spring at ~30 hPa (24 km) and extending possibly to even higher altitudes; this region lies above a domain of strong cooling that is approximately colocated with the altitude of observed ozone depletion.

7. There is little evidence to suggest that tropospheric climate changes (e.g., those induced by greenhouse gas increases in the troposphere) and sea surface temperature variations have been dominant factors in the global-mean stratospheric temperature trend over the 1979–1994 period. The effect of potential shifts in atmospheric circulation patterns upon decadal-scale trends in global (i.e., localized regions and during specific seasons) stratospheric temperatures remains to be determined.

Although the well-mixed greenhouse gas and ozone change effects are undoubtedly manifest to a substantial extent in the global-mean lower stratospheric temperature changes over the past 2–3 decades, the uncertainties in the causal attribution of the long-term trend are larger on the zonal-mean spatial scales. In a general sense, a more rigorous observation-model comparison and detailed inferences thereof for the global stratosphere are limited by an incomplete knowledge of the (1) "natural" dynamical variations of the climate system and (2) distribution and magnitude of all of the applicable forcings over the time period considered.

6. FUTURE RESEARCH

There is a strong need for a continuous temperature trend assessment, based on updates of existing measurements, as well as new ones to be conducted at numerous locations, with research reports made available at frequent intervals (e.g., every 5 years). These should include updates and quality control of data sets, model-observation comparisons, detection and attribution analyses of the trends and causes, and improved estimates for the future based on scenarios of potential changes in atmospheric composition. Broadly speaking, this calls for systematic analyses of the quality and accuracy of all of the instrumental data; quantitative analyses of the spatial and temporal variations manifest in the observational data; improvements in model simulations and the understanding of "natural" or unforced variability; model responses to changes in composition that occur within the stratosphere and also in the troposphere (to the extent that they affect the stratosphere); and careful diagnoses of the trends and their attribution using observations and model simulations. Since the scope of the subject is necessarily large and global in nature, it would be beneficial for the overall monitoring and research to be performed in close coordination with appropriate international scientific bodies (e.g., WCRP/SPARC, WMO, etc.). It is also vital to sustain a linkage between temperature trend activities and the monitoring of the concentrations of radiatively active species, especially those that are temporally and spatially variable (e.g., ozone, water vapor, and aerosols). Specific points to be considered are listed below.

1. A critical component feeding into stratospheric temperature trend assessment is the availability of accurate and globally extensive temperature-time series. A high accuracy is needed for determining the trends and their statistical significance. A concern about the ground-based observations is the lack of adequate radiosonde coverage over oceanic regions, tropical belts, and the Southern Hemisphere, which poses limitations in inferring global trends. The rocketsonde data have been underutilized for trends partially because of the different periods of operation of the instruments at different locations. While rocketsonde observations of the middle stratospheric regions and above could be supplanted by lidar stations, a concern arises about the viability of their long-term monitoring operation and the adequacy of funding levels to maintain them. In this regard, the continuous operation of the OHP station in France should be considered a role model. With respect to satellite data, there are plans already under way (e.g., EOS, Envisat, National Polar-Orbiting Operational Environmental Satellite System (NPOESS)) for deploying new instruments which include the Advanced Microwave Sounding Unit (AMSU); this should ensure the continuity of the time series obtained from MSU and SSU. A concern with satellite monitoring is the requirement of continuous information on the accuracy and stability of the instrument. Yet another concern is the extent to which the data from successive generations of satellites can be appropriately combined and be interpreted correctly for purposes of estimating the variability and trends and their statistical significance. A potential for long-term surveillance of temperatures with a high spatial resolution and accuracy is offered by the Global Positioning System (GPS). It is recommended that the principle of the GPS operation and its deployment in a practical sense for inferring stratospheric temperatures be seriously considered.

2. With the availability and now assemblage of time series from several sources, it is necessary to maintain an appropriate "data archive," such that all of the existing data (plus future data) can be easily accessed and utilized by individual researchers and institutions. Provisions should also be made so that data available in the future from newer instrumentation and/or observing platforms can be added to the archive with relative ease.

3. It is important to analyze the discrepancies prevailing between the different sources of the instrumental data and ascertain their causes. It is also important to analyze the causes of differences in the temperature trend results derived from data sets that assimilate observations in some form, as well as in those that combine observations from more than one type of instrument. Corrections to the radiosonde data (being currently performed at some institutions) should be incorporated, and trend estimates should be revised, if necessary. The rocket data for the middle and upper stratosphere have been underexploited, and there should be more comparisons with the recently available lidar and satellite data. Issues related to all of the above are the examination of time series from the various data sources and the deter-

mination of the trends at individual geographical locations (as opposed to, say, zonal means only).

4. The variability on different scales, ranging from monthly to seasonal to annual to interannual to decadal, and spatial scales ranging from individual locations to regional areas to zonal belts to planetary dimensions, needs to be fully documented. In this regard, further work is needed on understanding and modeling the effects of variations due to solar irradiance changes, volcanic eruptions, and QBO in order to improve upon the estimates of natural variability, such that trends detection and in particular their attribution to anthropogenic causes, can be improved.

5. GCM experiments are needed to explore further the dynamical effects (whether originating from within the stratosphere or from the troposphere) influencing the temperature structure of the stratosphere (e.g., responses to greenhouse gas increases which lead to a change in the tropospheric equator-to-pole heating gradient and planetary wave propagation) and to what extent they can alter the stratospheric circulation. Such studies should continue to make comparisons with appropriate diagnostics of up-to-date observations so that the influences on circulation can be accurately quantified.

6. An important requirement for accurate evaluation of model-observation comparisons is high-precision monitoring of the quantitative changes occurring in various radiatively active species. This need exists in particular for ozone, water vapor, and aerosols in the lower stratosphere and upper troposphere regions. The importance of ascertaining accurately the ozone changes in the vicinity of the tropopause cannot be overemphasized. For water vapor, too, monitoring strategies need to improve considerably in order to provide information on trends in the upper troposphere and lower stratosphere.

7. Detailed model simulations and analyses are needed to confirm whether the changes observed in the upper and middle stratosphere and mesosphere from recent data sets are consistent with the known changes in species (primarily, the well-mixed greenhouse gases) and present radiative-dynamical-chemical knowledge. This situation is somewhat different from that prevailing for the lower stratosphere, where, despite some quantitative uncertainties, there is unambiguous identification of the cooling being attributable to ozone losses, with a sizeable contribution due to water vapor increases also a distinct possibility.

8. Given the fact that the time series of stratospheric temperatures is now available from a variety of platforms (Tables 1 and 2), and continuously over the global domain from 1979 onward, with adequate spatial coverage back to ~1960s, it is of considerable interest to perform equilibrium and transient GCM simulations of the stratosphere with varied assumptions about forcings. This would enable a broadly based understanding of the sensitivity of the stratospheric-mesospheric system to various known factors. Considerations for the model simulations could include no forcing at all (i.e., the "unforced" state), forcing from entirely tropospheric variability (e.g., sea surface temperature), forcing due to changes in well-mixed greenhouse gases, forcing due to observed changes in ozone, forcing due to water vapor changes, forcing due to the known aerosol loadings from volcanic eruptions, and forcing due to natural factors (e.g., solar variations and QBO). The specification of the spatial and temporal evolution of the forcings would necessarily rely on the long-term monitoring efforts. Some of the forcings could also be obtained from explicit modeling of the interactions involving emissions of compounds and the subsequent chemical, transport, and removal processes. Results from a series of such simulations, performed using models of adequate horizontal and vertical resolution, could then be compared with the observed temperature time series. These comparisons would yield insights into the variability and changes in stratospheric and mesospheric temperatures on different spatial and temporal scales and thus pave the way for more robust attribution of the observed changes to specific causal factors. As an example of the usefulness, GCM studies conducted over the past 6–7 years have begun yielding extremely useful insights into the likely causes of changes in the lower stratosphere and troposphere. This type of modeling activity will also lead to increased confidence in the detection and attribution of anthropogenic influences on the vertical profile of temperature change in the atmosphere. Another modeling venture of interest would be the predicted evolution of temperatures over the next few decades for specific scenarios (e.g., increases in the nonozone greenhouse gases and the anticipated slowdown of the ozone losses and turnaround in their concentrations). Comparisons of the model-predicted temperature evolution with that observed would provide a test of the models and the ability to predict future states of the climate system.

9. Since the temperature changes in the stratosphere can be a significant factor in the forcing of the surface-troposphere system [*WMO*, 1995], the temperature variability and trend analyses can be used to determine the surface-troposphere radiative forcing. This could be done using either models or observations by themselves or some relevant combination of both. Of particular interest is the future forcings due to radiatively active species in the stratosphere that have a spatial and temporal variation. A follow-up to this would be an investigation of the response of the surface-troposphere climate system to the forcings originating particularly near the tropopause (e.g., ozone and water vapor).

ACKNOWLEDGMENTS. Numerous persons have contributed in different ways to the compilation of this work. The pioneering works of R. Dickinson, S. Fels, J. Hansen, J. Mahlman, S. Manabe, and V. Ramanathan on the modeling and description of the general response of the stratosphere to changes in radiatively active species have been the inspiration for the present trends investigation. We acknowledge the ob-

servational and theoretical scientific knowledge imparted by various scientists in the successive WMO assessments of the state of stratospheric ozone over the past one and a half decades; these have provided the underpinnings for the current analyses. We are grateful to several individuals, notably J. Christy, L. Coy, H. Komuro, and D. Parker, for making their data available to us. Data and figures from the investigations of P. Forster, G. Kokin, J. Hansen, E. Lysenko, and J. McCormack provided key information for this study. The work conducted by the SPARC projects has contributed to some of the inferences drawn here, and we thank the individuals associated with that organization, in particular, M. Geller, for facilitating and being supportive of this work. P. Forster and M. D. Schwarzkopf are thanked for clarifying some issues regarding the scientific content. We are grateful to K. Hamilton and J. Mahlman for sharing many valuable insights and providing excellent comments. Substantive technical input and suggestions from a number of scientists, first in the context of the *WMO* [1999] report, then the SPARC implementation document, and now the present manuscript, are duly acknowledged; such persons number too many to be listed here. Finally, a careful and thorough review of the manuscript was provided by J. Christy, D. Rind, and one other anonymous reviewer; their constructive suggestions have strengthened the manuscript considerably and are appreciated.

Michael Coffey was the Editor responsible for this paper. He thanks David Rind and an anonymous reviewer for technical reviews and Barbara Dutrow for the cross-disciplinary review.

REFERENCES

Angell, J. K., The close relation between Antarctic total-ozone depletion and cooling of the Antarctic low stratosphere, *Geophys. Res. Lett*., *13*, 1240–1243, 1986.

Angell, J. K., Variations and trends in tropospheric and stratospheric global temperatures, *J. Clim*., *1*, 1296–1313, 1988.

Angell, J. K., Changes in tropospheric and stratospheric global temperatures, 1958–1988, in *Greenhouse-Gas-Induced Climatic Change: A Critical Appraisal of Simulations and Observations*, edited by M. E. Schlesinger, pp. 231–247, Elsevier Sci., New York, 1991a.

Angell, J. K., Stratospheric temperature change as a function of height and sunspot number during 1972–1989 based on rocketsonde and radiosonde data, *J. Clim*., *4*, 1170–1180, 1991b.

Angell, J. K., Comparisons of stratospheric warming following Agung, El Chichon, and Pinatubo volcanic eruptions, *Geophys. Res. Lett*., *20*, 715–718, 1993.

Angell, J. K., Stratospheric warming due to Agung, El Chichon, and Pinatubo taking into account the quasi-biennial oscillation, *J. Geophys. Res*., *102*, 9479–9485, 1997.

Austin, J., N. Butchart, and K. P. Shine, Probability of an Arctic ozone hole in a doubled CO_2 climate, *Nature*, *360*, 221–225, 1992.

Bailey, M. J., A. O'Neill, and V. D. Pope, Stratospheric analyses produced by the United Kingdom Meteorological Office, *J. Appl. Meteorol*., *32*(9), 1472–1483, 1993.

Balachandran, N. K., and D. Rind, Modeling the effects of solar variability and the QBO on the troposphere/stratosphere system, part I, The middle atmosphere, *J. Clim*., *8*, 2058–2079, 1995.

Baldwin, M. P., and T. J. Dunkerton, Biennial, quasi-biennial, and decadal oscillations of potential vorticity in the northern stratosphere, *J. Geophys. Res*., *103*, 3919–3928, 1998a.

Baldwin, M. P., and T. J. Dunkerton, Quasi-biennial modulation of the Southern Hemisphere stratospheric polar vortex, *Geophys. Res. Lett*., *25*, 3343–3346, 1998b.

Baldwin, M. P., and D. O'Sullivan, Stratospheric effects of ENSO-related tropospheric circulation anomalies, *J. Clim*., *8*, 649–667, 1995.

Baldwin, M. P., X. Cheng, and T. J. Dunkerton, Observed correlation between winter-mean tropospheric and stratospheric anomalies, *Geophys. Res. Lett*., *21*, 1141–1144, 1994.

Berntsen, T., I. S. A. Isaksen, G. Myrhe, J. S. Fuglestvedt, F. Stordahl, T. A. Larsen, R. S. Freckleton, and K. P. Shine, Effects of anthropogenic emissions on tropospheric ozone and its radiative forcing, *J. Geophys. Res*., *102*, 28,101–28,126, 1997.

Bojkov, R., and V. E. Fioletov, Estimating the global ozone characteristics during the last 30 years, *J. Geophys. Res*., *100*, 16,537–16,551, 1995.

Bojkov, R., and V. E. Fioletov, Changes of the lower stratospheric ozone over Europe and Canada, *J. Geophys. Res*., *102*, 1337–1347, 1997.

Brasseur, G., The response of the middle atmosphere to long-term and short-term solar variability: A two-dimensional model, *J. Geophys. Res*., *98*, 23,079–23,090, 1993.

Brasseur, G., and C. Granier, Mount Pinatubo aerosols, chlorofluorocarbons and ozone depletion, *Science*, *258*, 1239–1242, 1992.

Bruhl, C., and P. Crutzen, Scenarios of possible changes in atmospheric temperatures and ozone concentrations due to man's activities, estimated with a one-dimensional coupled photochemical climate model, *Clim. Dyn*., *2*, 173–203, 1988.

Butchart, N., and J. Austin, On the relationship between the quasi-biennial oscillation, total chlorine and the severity of the Antarctic ozone hole, *Q. J. R. Meteorol. Soc*., *122*, 183–217, 1996.

Cariolle, D., A. Lasserre-Bigorry, J.-F. Royer, and J. F. Geleyn, A GCM simulation of the springtime Antarctic decrease and its impact on midlatitudes, *J. Geophys. Res*., *95*, 1883–1898, 1990.

Chanin, M.-L., Long-term trend in the middle atmosphere temperature, in *The Role of the Stratosphere in Global Change*, edited by M.-L. Chanin, *NATO ASI Ser*., *8*, 301–317, 1993.

Chanin, M.-L., and P. Keckhut, Influence on the middle atmosphere of the 27-day and 11-year solar cycles: Radiative and/or dynamical forcing?, *J. Geomagn. Geoelectr*., *43*, 647–655, 1991.

Chipperfield, M. P., and J. A. Pyle, Two-dimensional modeling of the Antarctic lower stratosphere, *Geophys. Res. Lett*., *15*, 875–878, 1988.

Christiansen, B., A. Guldberg, A. W. Hansen, and L. P. Riishojgaard, On the response of a three-dimensional general circulation model to imposed changes in the ozone distribution, *J. Geophys. Res*., *102*, 13,051–13,077, 1997.

Christy, J. R., Temperature above the surface layer, *Clim. Change*, *31*, 455–474, 1995.

Christy, J., and S. Drouilhet, Variability in daily, zonal-mean lower stratospheric temperatures, *J. Clim*., *7*, 106–120, 1994.

Christy, J. R., R. W. Spencer, and R. T. McNider, Reducing noise in the daily MSU lower tropospheric temperature data set, *J. Clim*., *8*, 888–896, 1995.

Chubachi, S., On the cooling of stratospheric temperatures at Syowa, Antarctica, *Geophys. Res. Lett*., *13*, 1221–1223, 1986.

Coy, L., E. R. Nash, and P. A. Newman, Meteorology of the polar vortex: Spring 1997, *Geophys. Res. Lett*., *24*, 2693–2696, 1997.

Cunnold, D. M., H. Wang, W. Chu, and L. Froidevaux, Comparisons between SAGE II and MLS ozone measurements

and aliasing of SAGE II ozone trends in the lower stratosphere, *J. Geophys. Res*., *101*, 10,061–10,075, 1996a.

Cunnold, D. M., L. Froidevaux, J. Russell, B. Connor, and A. Roche, An overview of UARS ozone validation based primarily on intercomparisons among UARS and SAGE II measurements, *J. Geophys. Res*., *101*, 10,335–10,350, 1996b.

Donnelly, R. F., H. E. Hinterreger, and D. F. Heath, Temporal variation of solar EUV, UV, and 10830-Å radiations, *J. Geophys. Res*., *91*, 5567–5578, 1986.

Dunkerton, T. J., and M. P. Baldwin, Modes of interannual variability in the stratosphere, *Geophys. Res. Lett*., *19*, 49–52, 1992.

Dunkerton, T. J., and D. P. Delisi, Climatology of the equatorial lower stratosphere: An observational study, *J. Atmos. Sci*., *42*, 376–396, 1985.

Dunkerton, T., D. Delisi, and M. Baldwin, Middle atmosphere cooling trend in historical rocketsonde data, *Geophys. Res. Lett*., *25*, 3371–3374, 1998.

Efron, B., *The Jacknife, The Bootstrap, and Other Resampling Plans*, Soc. for Ind. and Appl. Math., Philadelphia Pa., 1982.

Elliott, W. P., and D. J. Gaffen, On the utility of radiosonde humidity archives for climate studies, *Bull. Am. Meteorol. Soc*., *72*, 1507–1520, 1991.

Elliott, W. P., D. J. Gaffen, J. D. Kahl, and J. K. Angell, The effect of moisture on layer thicknesses used to monitor global temperatures, *J. Clim*., *7*, 304–308, 1994.

Eluszkiewicz, J., D. Crisp, R. G. Grainger, A. Lambert, A. E. Roche, J. B. Kumer, and J. L. Mergenthaler, Sensitivity of the residual circulation diagnosed from UARS data to the uncertainties in the input fields and to the inclusion of aerosols, *J. Atmos. Sci*., *54*, 1739–1757, 1997.

Fels, S. B., A parameterization of scale-dependent radiative damping rates in the middle atmosphere, *J. Atmos. Sci*., *39*, 1141–1152, 1982.

Fels, S. B., Radiative-dynamical interactions in the middle atmosphere, *Adv. Geophys*., *28A*, 277–300, 1985.

Fels, S. B., and L. D. Kaplan, A test of the role of longwave radiative transfer in a general circulation model, *J. Atmos. Sci*., *33*, 779–789, 1975.

Fels, S. B., J. D. Mahlman, M. D. Schwarzkopf, and R. W. Sinclair, Stratospheric sensitivity to perturbations in ozone and carbon dioxide: Radiative and dynamical response, *J. Atmos. Sci*., *37*, 2265–2297, 1980.

Finger, F. G., M. E. Gelman, J. D. Wild, M. L. Chanin, A. Hauchecorne, and A. J. Miller, Evaluation of NMC upper-stratospheric temperature analyses using rocketsonde and lidar data, *Bull. Am. Meteorol. Soc*., *74*, 789–799, 1993.

Fleming, E., S. Chandra, C. H. Jackman, D. B. Considine, and A. R. Douglass, The middle atmosphere response to short- and long-term solar UV variations: Analysis of observations and 2-D model results, *J. Atmos. Terr. Phys*., *57*, 333–365, 1995.

Folland, C. K., D. M. H. Sexton, D. J. Karoly, C. E. Johnson, D. P. Rowell, and D. E. Parker, Influence of anthropogenic and oceanic forcing on recent climate change, *Geophys. Res. Lett*., *25*, 353–356, 1998.

Forster, P., and K. P. Shine, Radiative forcing and temperature trends from stratospheric ozone changes, *J. Geophys. Res*., *102*, 10,841–10,855, 1997.

Forster, P., and K. P. Shine, Stratospheric water vapor changes as a possible contributor to observed stratospheric cooling, *Geophys. Res. Lett*., *26*, 3309–3312, 1999.

Forster, P., R. S. Freckleton, and K. P. Shine, On aspects of the concept of radiative forcing, *Clim. Dyn*., *13*, 547–560, 1997.

Fortuin, J. P. F., and H. Kelder, Possible links between ozone and temperature profiles, *Geophys. Res. Lett*., *23*, 1517–1520, 1996.

Gaffen, D. J., Temporal inhomogeneities in radiosonde temperature records, *J. Geophys. Res*., *99*, 3667–3676, 1994.

Gaffen, D. J., A digitized metadata set of global upper-air station histories, *NOAA Tech. Memo. ERL-ARL 211*, 38 pp., 1996.

Gaffen, D. J., M. A. Sargent, R. E. Habermann, and J. R. Lanzante, Sensitivity of tropospheric and stratospheric temperature trends to radiosonde data quality, *J. Clim*., *13*, 1776–1796, 2000.

Garcia, R. R., S. Solomon, R. G. Roble, and D. W. Rusch, A numerical study of the response of the middle atmosphere to the 11-year solar cycle, *Planet. Space Sci*., *32*, 411–423, 1984.

Gelman, M. E., A. J. Miller, K. W. Johnson, and R. M. Nagatani, Detection of long-term trends in global stratospheric temperature from NMC analyses derived from NOAA satellite data, *Adv. Space Res*., *6*(10), 17–26, 1986.

Gelman, M. E., A. J. Miller, R. N. Nagatani, and C. S. Long, Use of UARS data in the NOAA stratospheric monitoring program, *Adv. Space Res*., *14*(9), 21–31, 1994.

Gille, S. T., A. Hauchecorne, and M.-L. Chanin, Semidiurnal and diurnal tide effects in the middle atmosphere as seen by Rayleigh lidar, *J. Geophys. Res*., *96*, 7579–7587, 1991.

Golitsyn, G. S., A. I. Semenov, N. N. Shefov, L. M. Fishkova, E. V. Lysenko, and S. P. Perov, Long-term temperature trends in the middle and upper atmosphere, *Geophys. Res. Lett*., *23*, 1741–1744, 1996.

Goody, R., and Y. Yung, *Atmospheric Radiation*, chap. 9, pp. 388–425, Oxford Univ. Press, New York, 1989.

Graf, H.-F., I. Kirchner, A. Robock, and I. Schult, Pinatubo eruption winter climate effects: Models versus observations, *Clim. Dyn*., *9*, 81–93, 1993.

Graf, H.-F., J. Perlwitz, I. Kirchner, and I. Schult, Recent northern winter climate trends, ozone changes and increased greenhouse gas forcing, *Contrib. Atmos. Phys*., *68*, 233–248, 1995.

Graham, N. E., Simulation of recent global temperature trends, *Science*, *267*, 666–671, 1995.

Haigh, J., The impact of solar variability on climate, *Science*, *272*, 981–984, 1996.

Haigh, J., A GCM study of climate change in response to the 11-year solar cycle, *Q. J. R. Meteorol. Soc*., *125*, 871–892, 1998.

Halpert, M. S., and G. D. Bell, Climate assessment for 1996, *Bull. Am. Meteorol. Soc*., *78*, S1–S49, 1997.

Hamilton, K., An example of observed Southern Oscillation effects in the Northern Hemisphere stratosphere, *J. Atmos. Sci*., *50*, 3468–3473, 1993.

Hamilton, K., R. J. Wilson, J. D. Mahlman, and L. J. Umscheid, Climatology of the GFDL SKYHI troposphere-stratosphere-mesosphere general circulation model, *J. Atmos. Sci*., *52*, 5–43, 1995.

Hansen, J., and H. Wilson, Commentary on the significance of global temperature records, *Clim. Change*, *25*, 185–191, 1993.

Hansen, J. E., W.-C. Wang, and A. A. Lacis, Mount Agung provides test of a global climate perturbation, *Science*, *199*, 1065–1068, 1978.

Hansen, J., A. Lacis, R. Ruedy, M. Sato, and H. Wilson, How sensitive is the world's climate?, *Natl. Geogr. Res. Explor*., *9*, 142–158, 1993.

Hansen, J. E., H. Wilson, M. Sato, R. Ruedy, K. Shah, and E. Hansen, Satellite and surface temperature data at odds?, *Clim. Change*, *30*, 103–117, 1995.

Hansen, J. E., M. Sato, and R. Ruedy, Radiative forcing and climate response, *J. Geophys. Res*., *102*, 6831–6864, 1997a.

Hansen, J., et al., Forcings and chaos in interannual to decadal climate change, *J. Geophys. Res*., *102*, 25,679–25,720, 1997b.

Hansen, J., M. Sato, R. Ruedy, A. Lacis, and J. Glascoe,

Global climate data and models: A reconciliation, *Science*, *281*, 930–932, 1998.

Harshvardhan, Perturbation of the zonal radiation balance by a stratospheric aerosol layer, *J. Atmos. Sci*., *36*, 1274–1285, 1979.

Hauchecorne, A., M.-L. Chanin, and P. Keckhut, Climatology and trends of the middle atmospheric temperature (33–87 km) as seen by Rayleigh lidar over the south of France, *J. Geophys. Res*., *96*, 15,297–15,309, 1991.

Hoinka, K. P., Statistics of the global tropopause pressure, *Mon. Weather Rev*., *126*, 3303–3325, 1998.

Hoinka, K. P., Temperature, humidity and wind at the global tropopause, *Mon. Weather Rev*., *127*, 2248–2265, 1999.

Holton, J. R., and H.-C. Tan, The influence of the equatorial quasi-biennial oscillation on the global circulation at 50 mb, *J. Atmos. Sci*., *37*, 2200–2208, 1980.

Holton, J. R., and H.-C. Tan, The quasi-biennial oscillation in the Northern Hemisphere lower stratosphere, *J. Meteorol. Soc. Jpn*., *60*, 140–148, 1982.

Holton, J. R., P. H. Haynes, M. E. McIntyre, A. R. Douglass, R. B. Rood, and L. Pfister, Stratosphere-troposphere exchange, *Rev. Geophys*., *33*, 403–439, 1995.

Hood, L. L., J. L. Jirikowic, and J. P. McCormack, Quasi-decadal variability of the stratosphere: Influence of long-term solar ultraviolet variations, *J. Atmos. Sci*., *50*, 3941–3958, 1993.

Huovila, S., and A. Tuominen, On the influence of radiosonde lag error on upper-air climatological data in Finland 1951–1988, *Meteorol. Publ. 14*, 29 pp., Finn. Meteorol. Inst., Helsinki, 1990.

Intergovernmental Panel on Climate Change, 1994, *Radiative Forcing of Climate Change and an Evaluation of the IPCC IS92 Emission Scenarios*, edited by J. T. Houghton et al., 339 pp., Cambridge Univ. Press, New York, 1995.

Intergovernmental Panel on Climate Change, 1995, *The Science of Climate Change*, edited by J. T. Houghton et al., 572 pp., Cambridge Univ. Press, New York, 1996.

Intergovernmental Panel on Climate Change, *Aviation and the Global Atmosphere*, edited by J. Penner et al., 370 pp., Cambridge Univ. Press, New York, 1999.

Jones, A. E., and J. D. Shanklin, Continued decline of total ozone over Halley, Antarctica, since 1985, *Nature*, *376*, 409–411, 1995.

Jones, P. D., Recent warming in global temperature series, *Geophys. Res. Lett*., *21*, 1149–1152, 1994.

Kalnay, E., et al., The NCEP/NCAR 40-year reanalysis project, *Bull. Am. Meteorol. Soc*., *77*, 437–471, 1996.

Karl, T. R., V. E. Derr, D. R. Easterling, C. K. Folland, D. J. Hofmann, S. Levitus, N. Nicholls, D. E. Parker, and G. W. Withee, Critical issues for long-term climate monitoring, *Clim. Change*, *31*, 185–221, 1995.

Keckhut, P., A. Hauchecorne, and M. L. Chanin, Midlatitude long-term variability of the middle atmosphere: Trends and cyclic and episodic changes, *J. Geophys. Res*., *100*, 18,887–18,897, 1995.

Keckhut, P., et al., Semidiurnal and diurnal temperature tides (30–55 km): Climatology and effect on UARS lidar data comparisons, *J. Geophys. Res*., *101*, 10,299–10,310, 1996.

Keckhut, P., F. J. Schmidlin, A. Hauchecorne, and M.-L. Chanin, Trend estimates from rocketsondes at low latitude station (8S–34N), taking into account instrumental changes and natural variability, *J. Atmos. Sol. Terr. Phys*., *61*, 447–459, 1999.

Kiehl, J. T., and B. A. Boville, The radiative-dynamical response of a stratospheric-tropospheric general circulation model to changes in ozone, *J. Atmos. Sci*., *45*, 1798–1817, 1988.

Kiehl, J. T., and S. Solomon, On the radiative balance of the stratosphere, *J. Atmos. Sci*., *43*, 1525–1534, 1986.

Kiehl, J. T., B. A. Boville, and B. P. Briegleb, Response of a general circulation model to a prescribed Antarctic ozone hole, *Nature*, *332*, 501–504, 1988.

Kirchner, I., G. Stenchikov, H.-F. Graf, A. Robock, and J. Antuna, Climate model simulation of winter warming and summer cooling following the 1991 Mount Pinatubo eruption, *J. Geophys. Res*., *104*, 19,039–19,055, 1999.

Kitoh, A., H. Koide, K. Kodera, S. Yukimoto, and A. Noda, Interannual variability in the stratospheric-tropospheric circulation in a coupled ocean-atmosphere general circulation model, *Geophys. Res. Lett*., *23*, 543–546, 1996.

Kodera, K., Influence of volcanic eruptions on the troposphere through stratospheric dynamical processes in the Northern Hemisphere winter, *J. Geophys. Res*., *99*, 1273–1282, 1994.

Kodera, K., and K. Yamazaki, Long-term variation of upper stratospheric circulation in the Northern Hemisphere in December, *J. Meteorol. Soc. Jpn*., *68*, 101–105, 1990.

Kodera, K., and K. Yamazaki, A possible influence of recent polar stratospheric coolings on the troposphere in the Northern Hemisphere winter, *Geophys. Res. Lett*., *21*, 809–812, 1994.

Kokin, G., and E. Lysenko, On temperature trends of the atmosphere from rocket and radiosonde data, *J. Atmos. Terr. Phys*., *56*, 1035–1044, 1994.

Kokin, G., Y. Lysenko, and S. Rozenfeld, Temperature changes in the stratosphere and mesosphere in 1964–1988 based on rocket sounding data, *Izv. Atmos. Oceanic Phys*., *26*(6), 518–523, 1990.

Komuro, H., Long-term cooling in the stratosphere observed by aerological rockets at Ryori, Japan, *J. Meteorol. Soc. Jpn*., *67*, 1081–1082, 1989.

Koshelkov, Y. P., and G. R. Zakharov, On temperature trends in the Arctic lower stratosphere, *Meteorol. Gidrol*., *5*, 45–54, 1998.

Labitzke, K., and M. P. McCormick, Stratospheric temperature increases due to Pinatubo aerosols, *Geophys. Res. Lett*., *19*, 207–210, 1992.

Labitzke, K., and H. van Loon, Association between the 11-year solar cycle, the QBO and the atmosphere, part I, The troposphere and stratosphere in the Northern Hemisphere in winter, *J. Atmos. Terr. Phys*., *50*, 197–206, 1988.

Labitzke, K., and H. van Loon, The 11-year solar cycle in the stratosphere in the northern summer, *Ann. Geophys*., *7*, 595–598, 1989.

Labitzke, K., and H. van Loon, On the association between the QBO and the extratropical stratosphere, *J. Atmos. Terr. Phys*., *54*, 1453–1463, 1992.

Labitzke, K., and H. van Loon, Trends of temperature and geopotential height between 100 and 10 hPa in the Northern Hemisphere, *J. Meteorol. Soc. Jpn*., *72*, 643–652, 1994.

Labitzke, K., and H. van Loon, A note on the distribution of trends below 10 hPa: The extratropical Northern Hemisphere, *J. Meteorol. Soc. Jpn*., *73*, 883–889, 1995.

Labitzke, K., and H. van Loon, The signal of the 11-year sunspot cycle in the upper troposphere–lower stratosphere, *Space Sci. Rev*., *80*, 393–410, 1997.

Lacis, A. A., D. J. Wuebbles, and J. A. Logan, Radiative forcing of climate by changes in the vertical distribution of ozone, *J. Geophys. Res*., *95*, 9971–9981, 1990.

Lait, L. R., M. R. Schoeberl, and P. A. Newman, Quasi-biennial modulation of Antarctic ozone depletion, *J. Geophys. Res*., *94*, 11,559–11,571, 1989.

Luers, J. K., Estimating the temperature error of the radiosonde rod thermistor under different environments, *J. Atmos. Oceanic Technol*., *7*, 882–895, 1990.

Lysenko, E. V., G. Nelidova, and A. Prostova, Changes in the stratospheric and mesospheric thermal conditions during the last 3 decades, 1, The evolution of a temperature trend, *Izv. Atmos. Oceanic Phys*., *33*(2), 218–225, 1997.

Mahlman, J. D., A looming Arctic ozone hole?, *Nature*, *360*, 209, 1992.

Mahlman, J. D., J. P. Pinto, and L. J. Umscheid, Transport, radiative, and dynamical effects of the Antarctic ozone hole: A GFDL "SKYHI" model experiment, *J. Atmos. Sci*., *51*, 489–508, 1994.

Manabe, S., and R. T. Wetherald, Thermal equilibrium of the atmosphere with a given distribution of relative humidity, *J. Atmos. Sci*., *24*, 241–259, 1967.

Manney, G. L., R. Swinbank, S. T. Massie, M. E. Gelman, A. J. Miller, R. Nagatani, A. O'Neill, and R. W. Zurek, Comparison of U.K. Meteorological Office and U.S. National Meteorological Center stratospheric analyses during northern and southern winter, *J. Geophys. Res*., *101*, 10,311–10,334, 1996.

McCormack, J. P., and L. L. Hood, Relationship between ozone and temperature trends in the lower stratosphere: Latitude and seasonal dependences, *Geophys. Res. Lett*., *21*, 1615–1618, 1994.

McCormack, J. P., and L. L. Hood, Apparent solar cycle variations of upper stratospheric ozone and temperature: Latitudinal and seasonal dependences, *J. Geophys. Res*., *101*, 20,933–20,944, 1996.

McCormick, M. P., L. W. Thomason, and C. R. Trepte, Atmospheric effects of the Mount Pinatubo eruption, *Nature*, *373*, 399–404, 1995.

Miller, A. J., R. M. Nagatani, G. C. Tiao, X. F. Niu, G. C. Reinsel, D. Wuebbles, and K. Grant, Comparisons of observed ozone and temperature trends in the lower stratosphere, *Geophys. Res. Lett*., *19*, 929–932, 1992.

Mohanakumar, K., Solar activity forcing of the middle atmosphere, *Ann. Geophys*., *13*, 879–885, 1995.

Nash, J., and G. F. Forrester, Long-term monitoring of stratospheric temperature trends using radiance measurements obtained by the TIROS-N series of NOAA spacecraft, *Adv. Space Res*., *6*(10), 37–44, 1986.

Naujokat, B., An update of the observed quasi-biennial oscillation of the stratospheric winds over the tropics, *J. Atmos. Sci*., *43*, 1873–1877, 1986.

Naujokat, B., and S. Pawson, The cold stratospheric winters 1994–1995 and 1995–1996, *Geophys. Res. Lett*., *23*, 3703–3706, 1996.

Nedoluha, G. E., R. M. Bevilacqua, R. M. Gomez, D. E. Siskind, and B. C. Hicks, Increases in middle atmospheric water vapor as observed by the Halogen Occultation Experiment and the ground-based water vapor millimeter-wave spectrometer from 1991 to 1997, *J. Geophys. Res*., *103*, 3531–3543, 1998.

Newman, P. A., and W. J. Randel, Coherent, ozone-dynamical changes during the Southern Hemisphere spring, 1979–1986, *J. Geophys. Res*., *93*, 12,585–12,606, 1988.

Newman, P., J. Gleason, R. D. McPeters, and R. Stolarski, Anomalous low ozone over the Arctic, *Geophys. Res. Lett*., *24*, 2689–2692, 1997.

Ohring, G., and H. S. Muench, Relationship between ozone and meteorological parameters in the lower stratosphere, *J. Meteorol*., *17*, 195–206, 1960.

Oltmans, S., and D. Hoffman, Increase in lower stratospheric water vapor at midlatitude Northern Hemisphere, *Nature*, *374*, 146–149, 1995.

Oort, A. H., and H. Liu, Upper-air temperature trends over the globe, 1956–1989, *J. Clim*., *6*, 292–307, 1993.

Pan, Y. H., and A. H. Oort, Global climate variations connected with sea surface temperature anomalies in the eastern equatorial Pacific Ocean for the 1958–1973 period, *Mon. Weather Rev*., *111*, 1244–1258, 1983.

Parker, D. E., On the detection of temperature changes induced by increasing atmospheric carbon dioxide, *Q. J. R. Meteorol. Soc*., *111*, 587–601, 1985.

Parker, D. E., and D. I. Cox, Towards a consistent global climatological rawindsonde database, *Int. J. Climatol*., *15*, 473–496, 1995.

Parker, D. E., M. Gordon, D. P. N. Cullum, D. M. H. Sexton, C. K. Folland, and N. Rayner, A new global gridded radiosonde temperature database and recalculated temperature trends, *Geophys. Res. Lett*., *24*, 1499–1502, 1997.

Pawson, S., and B. Naujokat, Trends in daily wintertime temperatures in the northern stratosphere, *Geophys. Res. Lett*., *24*, 575–578, 1997.

Perlwitz, J., and H. F. Graf, The statistical connection between tropospheric and stratospheric circulation of the Northern Hemisphere in winter, *J. Clim*., *8*, 2281–2295, 1995.

Pinnock, S., M. D. Hurley, K. P. Shine, T. J. Wallington, and T. J. Smyth, Radiative forcing of climate by hydrochlorofluorocarbons and hydrofluorocarbons, *J. Geophys. Res*., *100*, 23,227–23,238, 1995.

Pitari, G., M. Verdecchia, and G. Visconti, A transformed Eulerian model to study possible effects of the El Chichon eruption on stratospheric circulation, *J. Geophys. Res*., *92*, 10,961–10,975, 1987.

Pollack, J., and T. Ackerman, Possible effects of the El Chichon cloud on the radiation budget of the northern tropics, *Geophys. Res. Lett*., *10*, 1057–1060, 1983.

Prather, M. J., M. M. Garcia, R. Suozzo, and D. Rind, Global impact of the Antarctic ozone hole: Dynamical dilution with a three-dimensional chemical transport model, *J. Geophys. Res*., *95*, 3449–3471, 1990.

Ramanathan, V., The role of ocean-atmosphere interactions in the CO_2 climate problem, *J. Atmos. Sci*., *38*, 918–930, 1981.

Ramanathan, V., and R. E. Dickinson, The role of stratospheric ozone in the zonal and seasonal radiative energy balance of the Earth-troposphere system, *J. Atmos. Sci*., *36*, 1084–1104, 1979.

Ramanathan, V., R. J. Cicerone, H. B. Singh, and J. T. Kiehl, Trace gas trends and their potential role in climate change, *J. Geophys. Res*., *90*, 5547–5566, 1985.

Ramaswamy, V., and M. M. Bowen, Effect of changes in radiatively active species upon the lower stratospheric temperatures, *J. Geophys. Res*., *99*, 18,909–18,921, 1994.

Ramaswamy, V., M. D. Schwarzkopf, and K. P. Shine, Radiative forcing of climate from halocarbon-induced global stratospheric ozone loss, *Nature*, *355*, 810–812, 1992.

Ramaswamy, V., M. D. Schwarzkopf, and W. Randel, Fingerprint of ozone depletion in the spatial and temporal pattern of recent lower-stratospheric cooling, *Nature*, *382*, 616–618, 1996.

Randel, W. J., The anomalous circulation in the Southern Hemisphere stratosphere during spring 1987, *Geophys. Res. Lett*., *15*, 911–914, 1988.

Randel, W. J., and J. B. Cobb, Coherent variations of monthly mean total ozone and lower stratospheric temperature, *J. Geophys. Res*., *99*, 5433–5447, 1994.

Randel, W. J., and F. Wu, Cooling of the Arctic and Antarctic polar stratosphere due to ozone depletion, *J. Clim*., *12*, 1467–1479, 1999.

Randel, W. J., F. Wu, J. M. Russell III, J. W. Waters, and L. Froidevaux, Ozone and temperature changes in the stratosphere following the eruption of Mount Pinatubo, *J. Geophys. Res*., *100*, 16,753–16,764, 1995.

Randel, W. J., F. Wu, R. Swinbank, J. Nash, and A. O'Neill, Global QBO circulation derived from UKMO stratospheric analyses, *J. Atmos. Sci*., *56*, 457–474, 1999.

Reid, G. C., Seasonal and interannual temperature variations in the tropical stratosphere, *J. Geophys. Res*., *99*, 18,923–18,932, 1994.

Reid, G. C., K. S. Gage, and J. R. McAfee, The thermal response of the tropical atmosphere to variations in equa-

torial Pacific sea surface temperature, *J. Geophys. Res*., *94*, 14,705–14,716, 1989.

Rind, D., and P. Lonergan, Modeled impacts of stratospheric O_3 and H_2O perturbations with implications for high-speed civil transport aircraft, *J. Geophys. Res*., *100*, 7381–7396, 1995.

Rind, D., R. Suozzo, N. Balachandran, and M. Prather, Climate change and the middle atmosphere, part I, The doubled CO_2 climate, *J. Atmos. Sci*., *47*, 475–494, 1990.

Rind, D., N. Balachandran, and R. Suozzo, Climate change and the middle atmosphere, part II, The impact of volcanic aerosols, *J. Clim*., *5*, 189–207, 1992.

Rind, D., D. Shindell, P. Lonergan, and N. K. Balachandran, Climate change and the middle atmosphere, part III, The doubled CO_2 climate revisited, *J. Clim*., *11*, 876–894, 1998.

Rosenfield, J., D. B. Considine, P. E. Meade, J. T. Bacmeister, C. H. Jackman, and M. R. Schoeberl, Stratospheric effects of Mount Pinatubo aerosol studied with a coupled two-dimensional model, *J. Geophys. Res*., *102*, 3649–3670, 1997.

Salby, M., P. Callaghan, and D. Shea, Interdependence of the tropical and extratropical QBO: Relationship to the solar cycle versus a biennial oscillation of the stratosphere, *J. Geophys. Res*., *102*, 789–798, 1997.

Santer, B. D., et al., A search for human influences on the thermal structure of the atmosphere, *Nature*, *382*, 39–46, 1996.

Santer, B. D., J. J. Hnilo, T. M. L. Wigley, J. S. Boyle, C. Doutriaux, M. Fiorino, D. E. Parker, and K. E. Taylor, Uncertainties in observationally based estimates of temperature change in the free atmosphere, *J. Geophys. Res*., *104*, 6305–6333, 1999.

Sassen, K., D. O'C. Starr, G. G. Mace, M. R. Poellot, S. H. Melfi, W. L. Eberhard, J. D. Spinhirne, E. W. Eloranta, D. E. Hagen, and J. Hallett, The 5–6 December 1991 FIRE IFO II jet stream cirrus case study: Possible influences of volcanic aerosols, *J. Atmos. Sci*., *52*, 97–123, 1995.

Schubert, S., and M. Munteanu, An analysis of tropopause pressure and total ozone, *Mon. Weather Rev*., *116*, 569–582, 1988.

Schubert, S. R., R. Rood, and J. Pfaendtner, An assimilated data set for Earth science applications, *Bull. Am. Meteorol. Soc*., *74*, 2331–2342, 1993.

Schwarzkopf, M. D., and V. Ramaswamy, Radiative forcing due to ozone in the 1980s: Dependence on altitude of ozone change, *Geophys. Res. Lett*., *20*, 205–208, 1993.

Scrase, F. J., Application of radiation and lag corrections to temperatures measured with Meteorological Office radiosonde, *Meteorol. Mag*., *1005*(85), 65–78, 1956.

Shindell, D. T., D. Rind, and P. Lonergan, Increased polar stratospheric ozone losses and delayed eventual recovery owing to increasing greenhouse-gas concentrations, *Nature*, *392*, 592–598, 1998.

Shindell, D. T., R. Miller, A. Schmidt, and L. Pandolfo, Simulation of recent northern winter climate trends by greenhouse gases, *Nature*, *399*, 452–455, 1999a.

Shindell, D. T., D. Rind, N. Balachandran, J. Lean, and P. Lonergan, Solar cycle variability, ozone and climate, *Science*, *284*, 305–308, 1999b.

Shine, K. P., On the modeled thermal response of the Antarctic stratosphere to a depletion of ozone, *Geophys. Res. Lett*., *13*, 1331–1334, 1986.

Shine, K. P., The greenhouse effect and stratospheric change, in *The Role of the Stratosphere in Global Change*, edited by M.-L. Chanin, *NATO ASI Ser*., *8*, 285–300, 1993.

Sinha, A., and K. P. Shine, A one-dimensional study of possible cirrus cloud feedbacks, *J. Clim*., *7*, 158–175, 1994.

Solomon, S., R. W. Portmann, R. R. Garcia, L. W. Thomason, L. R. Poole, and M. P. McCormick, The role of aerosol variations in anthropogenic ozone depletion at northern midlatitudes, *J. Geophys. Res*., *101*, 6713–6727, 1996.

Spankuch, D., and E. Schulz, Diagnosing and forecasting total column ozone by statistical relations, *J. Geophys. Res*., *100*, 873–885, 1995.

Spencer, R. W., and J. R. Christy, Precision lower stratospheric temperature monitoring with the MSU technique: Validation and results, 1979–1991, *J. Clim*., *6*, 1194–1204, 1993.

Steinbrecht, W., H. Claude, U. Koehler, and K. Hoinka, Correlations between tropopause height and total ozone: Implications for long-term changes, *J. Geophys. Res*., *103*, 19,183–19,192, 1998.

Sun, D.-Z., and A. H. Oort, Humidity-temperature relationships in the tropical troposphere, *J. Clim*., *8*, 1974–1987, 1995.

Suzuki, S., and M. Asahi, Influence of solar radiation on the temperature measurement before and after the change of the length of suspension used for the Japanese radiosonde observation, *J. Meteorol. Soc. Jpn*., *56*, 61–64, 1978.

Swinbank, R., and A. O'Neill, A stratosphere-troposphere data assimilation system, *Mon. Weather Rev*., *122*, 686–702, 1994.

Taalas, P., and E. Kyrö, 1987–1989 total ozone sounding observations in northern Scandinavia and Antarctica, and the climatology of the lower stratosphere during 1965–1988 in northern Finland, *J. Atmos. Terr. Phys*., *54*, 1089–1099, 1992.

Taalas, P., and E. Kyrö, The stratospheric winter of 1991–1992 at Sodankylä in the European Arctic as compared with 1965–1992 meteorological and 1988–1991 ozone sounding statistics, *Geophys. Res. Lett*., *21*, 1207–1210, 1994.

Tett, S. F. B., J. F. B. Mitchell, D. E. Parker, and M. R. Allen, Human influence on the atmospheric vertical temperature structure: Detection and observations, *Science*, *274*, 1170–1173, 1996.

Teweles, S., and F. G. Finger, Reduction of diurnal variation in the reported temperatures and heights of stratospheric constant pressure surfaces, *J. Meteorol*., *17*, 177–194, 1960.

Thompson, D. W. J., and J. M. Wallace, The Arctic Oscillation signature in the wintertime geopotential height, and the stratospheric and temperature fields, *Geophys. Res. Lett*., *25*, 1297–1300, 1998.

Tie, X. X., G. P. Brasseur, B. Briegleb, and C. Granier, Two-dimensional simulation of Pinatubo aerosol and its effect on stratospheric ozone, *J. Geophys. Res*., *99*, 20,545–20,562, 1994.

Trenberth, K. E., and J. G. Olson, Temperature trends at the South Pole and McMurdo Sound, *J. Clim*., *2*, 1196–1206, 1989.

van Loon, H., and K. Labitzke, Association between the 11-year solar cycle, the QBO, and the atmosphere, part IV, The stratosphere, not grouped by the phase of the QBO, *J. Clim*., *3*, 827–837, 1990.

van Loon, H., and K. Labitzke, The global range of the stratospheric decadal wave, part I, Its association with the sunspot cycle and its annual mean, and with the troposphere, *J. Clim*., *11*, 1529–1537, 1998.

Vinnikov, K. Y., A. Robock, R. J. Stouffer, and S. Manabe, Vertical patterns of free and forced climate variations, *Geophys. Res. Lett*., *23*, 1801–1804, 1996.

Wang, W.-C., M. P. Dudek, X.-Z. Liang, and J. T. Kiehl, Inadequacy of effective CO_2 as a proxy in simulating the greenhouse effect of other radiatively active gases, *Nature*, *350*, 573–577, 1991.

World Meteorological Organization, Atmospheric ozone: 1985, Global Ozone Res. and Monit. Proj., *Rep. 16*, chap. 15, pp. 821–893, Geneva, 1986.

World Meteorological Organization, Report of the Interna-

tional Ozone Trends Panel: 1988, Global Ozone Res. and Monit. Proj., *Rep. 18*, chap. 6, pp. 443–498, Geneva, 1990a.

World Meteorological Organization, Scientific assessment of stratospheric ozone: 1989, Global Ozone Res. and Monit. Proj., *Rep. 20*, chapters 1 and 2, pp. 1–281, Geneva, 1990b.

World Meteorological Organization, Scientific assessment of ozone depletion: 1991, Global Ozone Res. and Monit. Proj., *Rep. 25*, chapters 2 and 7, pp. 2.1–2.33 and 7.1–7.28, Geneva, 1992.

World Meteorological Organization, Scientific assessment of ozone depletion: 1994, Global Ozone Res. and Monit. Proj., *Rep. 37*, chap. 8, pp. 8.1–8.26, Geneva, 1995.

World Meteorological Organization, Scientific assessment of ozone depletion: 1998, Global Ozone Res. and Monit. Proj., *Rep. 44*, 546 pp., Geneva, 1999.

Zalcik, M. S., Western Canada noctilucent cloud incidence map, *Climatol. Bull*., *27*, 165–169, 1993.

Zhai, P., and R. E. Eskridge, Analyses of inhomogeneities in radiosonde temperature and humidity time series, *J. Clim*., *9*, 676–705, 1996.

J. Angell and D. Gaffen, NOAA Air Resources Laboratory, Silver Spring, MD 20910.

J. Barnett, Department of Atmospheric Physics, Oxford University, Oxford OX1 3PU, England.

M.-L. Chanin, P. Keckhut, and Y. Koshelkov, Service d'Aéronomie du CNRS, 91 371 Verrieres-le-Buisson Cedex, France.

M. Gelman and J.-J. R. Lin, NCEP Climate Prediction Center, Washington, DC 20233.

K. Labitzke, Institut für Meteorologie, Frei Universitat Berlin, D-1000, Berlin 41, Germany.

J. Nash and R. Swinbank, U. K. Meteorological Office, Bracknell, Berkshire RG12 2SZ, England.

A. O'Neill and K. Shine, Department of Meteorology, University of Reading, Reading RG6 6BB, England.

V. Ramaswamy, NOAA Geophysical Fluid Dynamics Laboratory, Princeton University, P.O. Box 308, Princeton, NJ 08452. (vr@gfdl.gov)

W. Randel, National Center for Atmospheric Research, P.O. Box 3000, Boulder, CO 80307.

R. Rood, NASA Goddard Space Flight Center, Greenbelt, MD 20771.

M. Shiotani, Division of Ocean and Atmospheric Science, Hokkaido University, Sapporo 060, Japan.